NAWCWPNS TP 8316

Superconducting Spiral With Integrated Coplanar Balun

by
Michael M. Neel
Guidance and Control Division

SEPTEMBER 1996

NAVAL AIR WARFARE CENTER WEAPONS DIVISION
CHINA LAKE, CA 93555-6100

Naval Air Warfare Center Weapons Division

FOREWORD

This report presents the design, construction and testing of a high temperature superconductive spiral with integrated coplanar balun. This work was performed at the Naval Air Warfare Center Weapons Division, China Lake, Calif., during fiscal year 1995 in support of Accelerated Technology Initiative Investigating High-Temperature Superconducting Antennas sponsored by the Office of Naval Research, Information, Electronics, and Surveillance Science and Technology Department (ONR 31). This work was monitored initially by Dr. Don Liebenberg and subsequently by Dr. Deborah Van Vechten under funding document N0001494WX35177.

This report is a working document subject to change and was reviewed for technical accuracy by Donald R. Bowling and Robert Joy.

Approved by
K. L. HIGGINS, *Head*
Guidance and Control Systems Division
4 September 1996

Under authority of
J. V. CHENEVEY
Capt., U.S. Navy
Commander

Released for publication by
S. HAALAND
Director for Research and Engineering

NAWCWPNS Technical Publication 8316

Published by . . . . Technical Information Division
Collation . . . . Cover, 44 leaves
First printing . . . . 55 copies

REPORT DOCUMENTATION PAGE

Form Approved
OMB No. 0704-0188

1. AGENCY USE ONLY *(Leave blank)*

2. REPORT DATE
September 1996

3. REPORT TYPE AND DATES COVERED
Final—October 1993-January 1995

4. TITLE AND SUBTITLE
SUPERCONDUCTING SPRIAL WITH INTEGRATED COPLANAR BALUN

5. FUNDING NUMBERS
N0001495WX20154

6. AUTHOR(S)
Michael M. Neel

7. PERFORMING ORGANIZATION NAME(S) AND ADDRESS(ES)
Naval Air Warfare Center Weapons Division
China Lake, CA 93555-6100

8. PERFORMING ORGANIZATION REPORT NUMBER
NAWCWPNS TP 8316

9. SPONSORING/MONITORING AGENCY NAME(S) AND ADDRESS(ES)
Dr. Deborah Von Vechten
Code 312
Office of Naval Research
Washington, D.C.

10. SPONSORING/MONITORING AGENCY REPORT NUMBER

11. SUPPLEMENTARY NOTES

12A. DISTRIBUTION/AVAILABILITY STATEMENT
A Statement: distribution unlimited

12B. DISTRIBUTION CODE

13. ABSTRACT *(Maximum 200 words)*

(U) This report presents the design and construction of high-temperature superconducting (HTS) spiral antenna with an integrated coplanar waveguide feed. Test results are shown to compare a HTS spiral with a normal metal spiral, indicating a large increase in gain at lower than usual frequencies.

14. SUBJECT TERMS
Superconducting Antenna
Sprial
Coplanar Waveguide

15. NUMBER OF PAGES
86

16. PRICE CODE

17. SECURITY CLASSIFICATION OF REPORT	18. SECURITY CLASSIFICATION OF THIS PAGE	19. SECURITY CLASSIFICATION OF ABSTRACT	20. LIMITATION OF ABSTRACT
UNCLASSIFIED	UNCLASSIFIED	UNCLASSIFIED	UL

CONTENTS

INTRODUCTION

During fiscal year 1994, work began on the design and fabrication of a superconducting spiral antenna in conjunction with a parallel effort by contractors to fabricate a superconducting spiral. The NAWCWPNS design incorporates a coplanar waveguide (CPW) feedline, which coexists with one of the spiral arms, serving as the balanced feedline needed for the two-arm spiral design. This approach provides a completely planar circuit for the antenna and balun, eliminating the troublesome substrate holes used to accommodate conventional coaxial or other perpendicular feedlines into the center of the spiral. One edge connector at the antenna perimeter is all that is required to obtain the Mode 1 spiral output.

This technical publication will address the approach used to design and fabricate the antenna, and the final test results of the different configurations tested. These test results are compared to results for a conventional spiral design, which also uses superconducting metal for the spiral arms.

DESIGN OF INTEGRATED FEEDLINE WITH SPIRAL ARMS

The idea of integrating the feedline with the arms of a two-arm spiral antenna began in the early days of spiral work in the 1950's. In those early designs, the spiral arm widths and diameters investigated were quite large. Because all that was necessary to excite a two arm spiral was to feed the arms out of phase with each other, the problem was fairly simple. A coaxial line was placed in the center of one arm and brought down to the center feed point, where its center conductor was connected to the opposite spiral arm. This approach worked fairly well for these applications if mismatch was not a large concern. In later years, attempts at refining this approach by using a microstrip line in conjunction with the spiral arm to provide the balanced feed and match the feed-point impedance were used. Results of these efforts yielded inconsistent results. Some designs worked well, but appeared to be quite sensitive to the immediate surroundings close to the microstrip line.

The idea conceived for this effort was to place a CPW line in the center of one of the spiral arms and bring it in to the spiral center, where the middle line is connected to the opposite spiral arm. This approach is illustrated in simple fashion in Figure 1.

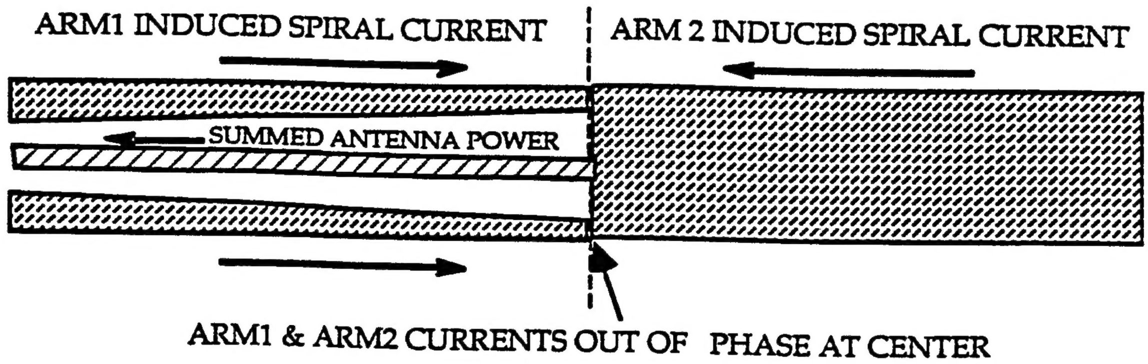

FIGURE 1. Coplanar Waveguide Integrated Spiral Balun Feed (Simplified Illustration).

The spiral currents are concentrated on the outside edges, and the CPW currents are concentrated on the outside edges of the centerline and inside edges of the outer "ground" lines. All the circuit lines are on one side of the substrate, making this structure mechanically simple. At the same time, the feedline has plenty of length to taper the impedance from the 50-ohm input to the 90-ohm-per-arm equivalent at the spiral's center.

Because of the difficulty of cutting holes in the brittle substrates needed for the superconducting metal, this idea held promise for simplifying the design of the antenna.

DESIGN OF COPLANAR WAVEGUIDE FEEDLINE

The design of the CPW line had several constraints on the dimensions of the lines used. Because it had to coexist with the spiral arm, the overall width had to be kept to a minimum to avoid a large spiral arm width. This approach was necessary to maximize the total spiral arm length for best operation at low frequencies. Other practical considerations had to be taken into account for use in an antenna application.

COPLANAR WAVEGUIDE LINE GEOMETRY

The overall width (W2, as shown in Figure 2), is the distance across the centerline, gaps, and outer lines. The centerline width is denoted by W and the gap width(s) by S. For the case studied, there is no bottom ground plane, but the substrate thickness T and the dielectric constant Er is taken into account in the calculations.

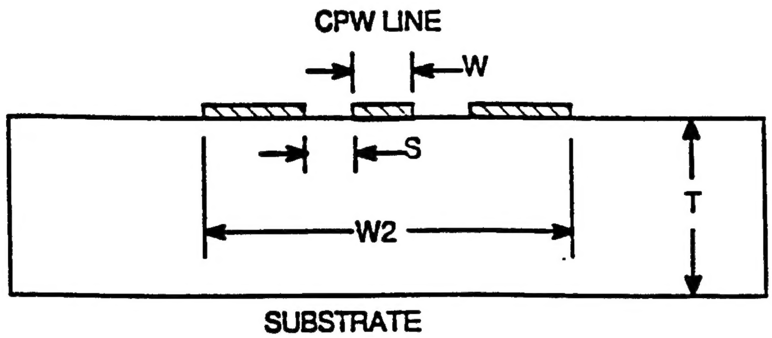

FIGURE 2. Basic Geometry Parameter of the CPW Line.

In general, the impedance of the line is affected most by changes in the gaps, or, correspondingly, by changes in W. Changes in the outer-line widths affect the impedance less, except where the ratio of outer- to inner-line widths become < 2:1. An example of a parametric study of W versus S is illustrated in Figure 3. (The values calculated were obtained using the CPW Line code (Reference 1, Appendix A).)

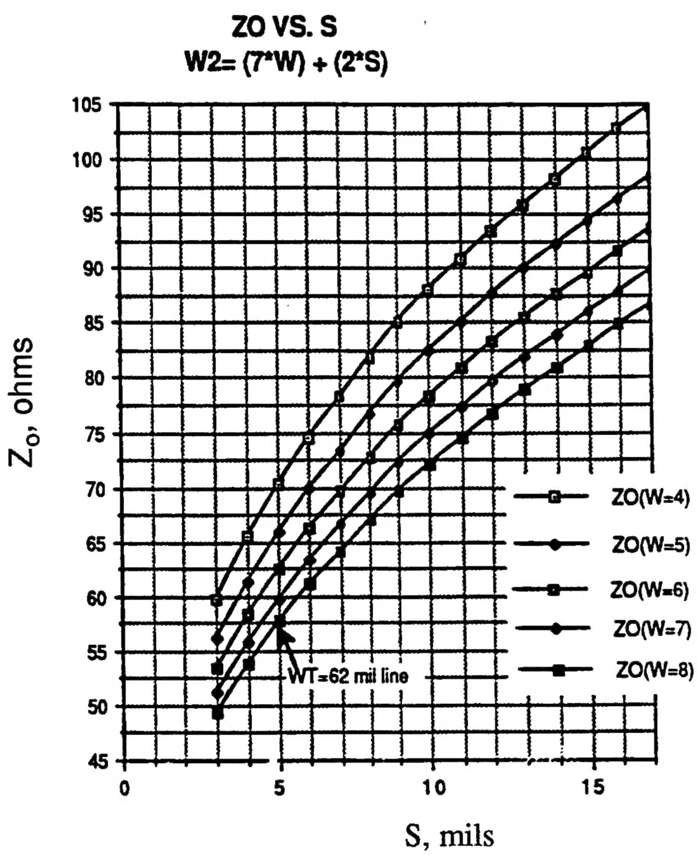

FIGURE 3. Coplanar Waveguide (T = 0.025 inch, ER = 10).

This case is where the substrate Er is equal to 10.0 and is 0.025 inch thick. The outer- to inner-line-width ratio is kept at a constant 3:1. The impedance is seen to change rapidly as S changes for a fixed centerline width W. Correspondingly, the impedance changes rapidly as W changes with a fixed gap (S). For the case of the antenna feedline application, parametric studies were done using the substrate dielectric constant and thickness as fixed constants. The impedance versus S and W were calculated and plotted similarly to Figure 3. The impedance was affected drastically whenever the outer-to-inner-line-width ratio was below 2:1; therefore a ratio of 3:1 was used as the lowest bound. This approach should keep any radiation from the feedline suppressed. To incorporate impedance matching along with the CPW line, parametric curves could be used to find S and W values that allowed a constant W2 width and gave the needed impedance taper. An example of this approach is illustrated in Figure 4.

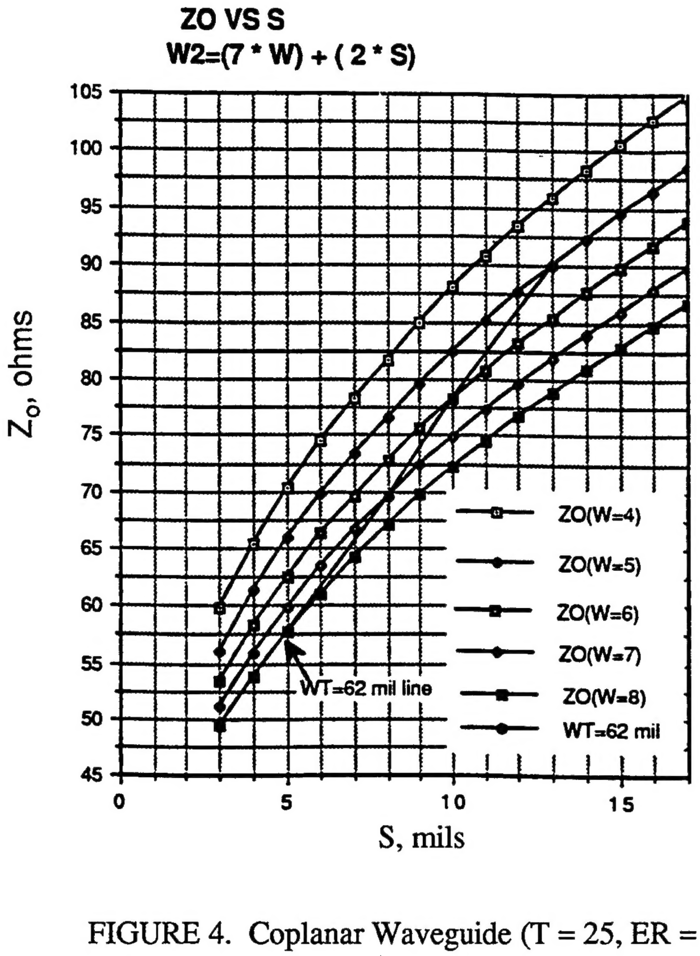

FIGURE 4. Coplanar Waveguide (T = 25, ER = 10).

The line for the WT is equal to 62 mils is plotted over the other curves. By using these data, a curve fit can be applied to get an equation for the line, which will be a constant 62 mils overall width, with the corresponding W and S values for the impedance needed at any point. The curve and equation for the case illustrated are shown in Figure 5.

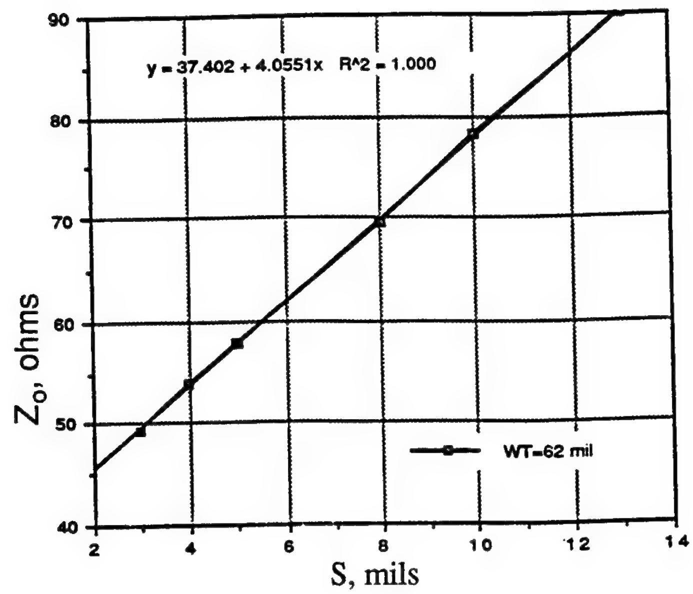

FIGURE 5. W2 = 62 Mil CPW Line.

Thus, the gap for the line is $\frac{Z_o}{37.4} - 4.055$, and because the line is held to a constant W2, W2=2*S+7*W, W=(62-(2*S))/7. A spreadsheet was set up to calculate the line length versus Z_o for the spiral feedline impedance taper and the corresponding S and W for the CPW line. Using these equations, the complete spiral arm design was completed.

The first unit was built on Roger's Corporation 6010 material, which has a dielectric constant of 10.0, overlaid with 0.7-mil-thick copper. The initial antenna was built and tested without a cavity. The assembly drawing for the antenna and a picture of the unit are shown in Appendix B.

The first set of tests were done with the antenna in a "free-space" mounting (i.e., on top of a Styrofoam tower with no metal or absorbers surrounding it. The first set of patterns at 2 to 8 GHz were disappointing. After several attempts at improving the patterns no improvement was gained possibly because of radiation from the CPW line itself.

A test method was devised to check for feedline radiation. By using the same CPW spiral arm as a back-to-back delay line, the feedline radiation should be directly observable. A test unit was constructed as a delay line and tested for transmission loss and phase. A non-linear response or highly increasing loss would indicate radiation. Accordingly, the delay line showed erratic loss between 2 to 4 GHz, and highly erratic phase changes in this range.

The unit was taken to our Microelectronics Lab, where 10-mil copper ribbons were bonded across the outer lines at positions that would be approximately every 90 degrees of transmission phase at 4 GHz. These bonds force the outer lines to remain in phase with each other, creating a nonradiating transmission line with equal and opposite currents on the through and on both ground lines.

This unit was then tested for the same parameters as before. The linearity and amount of transmission loss improved up to 4 GHz. The phase variations improved markedly. This indicated the previous existence of a radiating feedline, and the design correction needed.

Ribbon bonds were added to the antenna, and the antenna was retested. These patterns were improved up to 4 GHz, which is the upper frequency limit of improvement for the ribbon bonds used. These patterns and the delay line tests are shown in Appendix C.

HIGH-TEMPERATURE SUPERCONDUCTING SPIRAL DESIGN

The basic design approach for the High-Temperature Superconducting (HTS) spiral was now defined. The feedline radiation problem is improved by using wire/ribbon bonds across the outer CPW lines, and can also be further improved by keeping the electrostatic coupling of the centerline and outer lines as high as possible. This step is done by keeping the characteristic impedance low. Therefore, for the HTS design, the feedline was not tapered to 90 ohms. A 50-ohm geometry was used for the entire length. The substrate used was lanthanum aluminate, which is compatible with the HTS material. Lanthanum aluminate has a dielectric constant of 23.5. The thickness was chosen to be 0.020 inches. The CPW line cross-section dimensions for the 50 ohm feedline were

W = 0.005 inch
S = 0.0078 inch
W2 = 0.046 inch

This provides for an outer ground line width of 0.0127 inch, which is 2.5 times the center line width. This ratio should keep the CPW center and outer lines closely coupled to prevent radiation due to loose coupling.

Since this spiral design required a cavity, a low frequency cavity absorber configuration was needed to attenuate the back radiated energy. The cavity/absorber design is shown Figure 6.

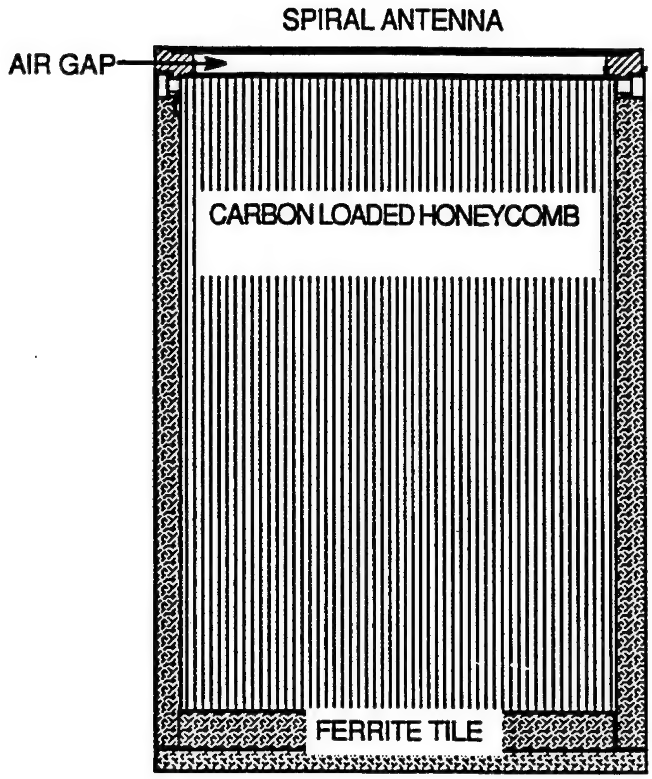

FIGURE 6. Spiral Cavity Assembly.

The honeycomb absorber was four-inch long material with tapered carbon loading designed to provide a well matched load down to 1.5 GHz, with the ferrite tile serving as the load from 1.5 GHz down to 0.5 GHz. (Honeycomb absorber from Keene Corp. Mass., custom design; ferrite tile from Fair Rite, Wazicill, NY, Type 47 tile.)

The connection to the antenna is done at the top surface of the substrate. A coaxial cable fed through a stainless steel block was mounted at the perimeter of the antenna. The center conductor comes out just above the substrate and is connected to the CPW center line with a ribbon bond. The ground contact is made by ribbon bonds from the connector block to the two outer CPW lines. This is illustrated in Figure 7.

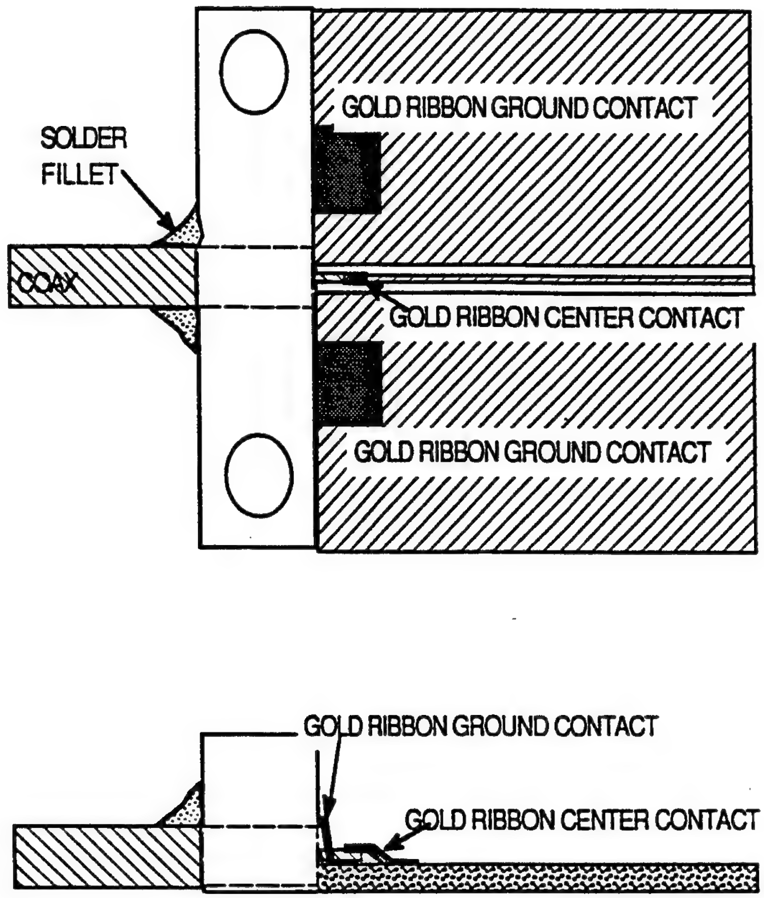

FIGURE 7. Coplanar Waveguide to Connector Block Transition.

Pictures of the HTS spiral on the mounting ring and the complete assembly are illustrated in Appendix D.

For the purpose of performance comparison, one spiral of this design was made out of 6-micron-thick gold, and one out of TBBCO HTS material. These antennae were fabricated at Superconducting Technologies, Santa Barbara, Calif. The spirals were then mounted on the cavity assembly and tested.

HTS SPIRAL TESTS

The spiral tests were conducted in the Naval Air Warfare Center's Code 472300D large anechoic chamber. The tests were defined to investigate the frequency range from 0.5 to 2.0 GHz. Antenna patterns were taken over this range with a rotating linear transmit horn to illustrate the antenna's axial ratio, pattern shape, and gain. The antennae were cooled by a simple method of placing them in a foam box filled with liquid nitrogen. This box was placed on a shelf mounted on the antenna rotation tower, with 4-inch-thick absorber behind

2.0 GHz. Antenna patterns were taken over this range with a rotating linear transmit horn to illustrate the antenna's axial ratio, pattern shape and gain. The antennae were cooled by a simple method of placing them in a foam box filled with liquid nitrogen. This box was placed on a shelf mounted on the antenna rotation tower, with four-inch thick absorber behind it. The patterns for the gold and HTS spirals over the loaded cavity are illustrated in Appendix E.

The results for the gold spiral at room temperature and the HTS spiral are illustrated in Figure 8.

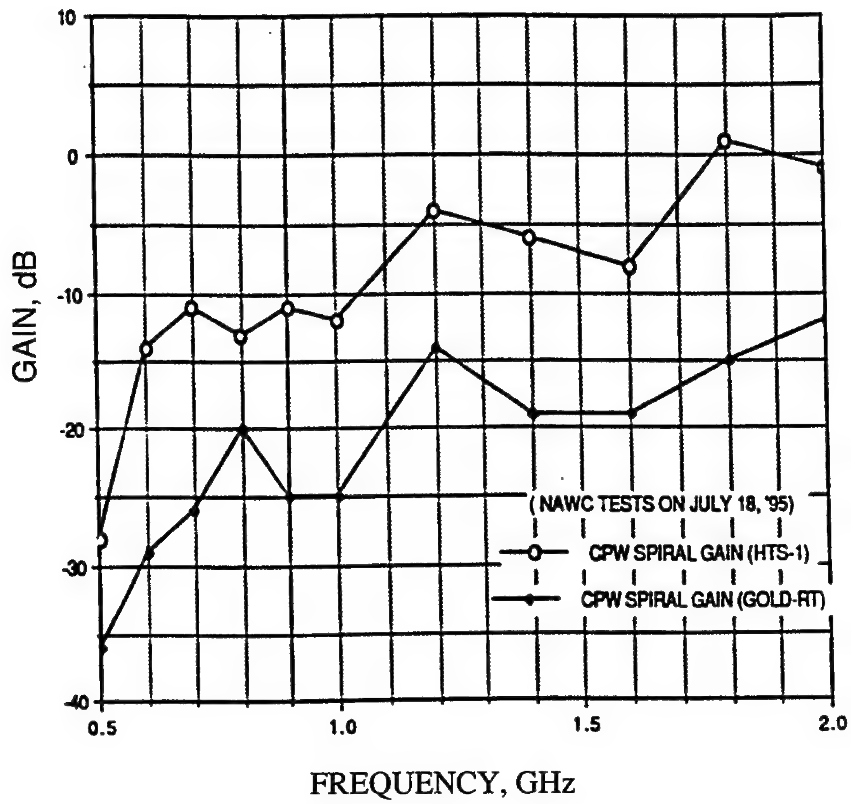

FIGURE 8. Gain of CPW HTS Spiral Versus Gold Spiral at Room Temperature.

These results are similar to those gotten with the HTS spirals built by AEL Industries, Lansdale, Penn. during the same time and tested at NAWCWPNS (Reference 2). The gain increase of the HTS over the normal metal spiral is a nominal 10 to 15 dB. The axial ratio of each spiral is the same.

The question of whether this design is better or worse than the traditional balun center-fed spiral design has to be answered by a comparison of the gain, axial ratio, and pattern shape. The gain comparison of the two designs is illustrated in Figure 9.

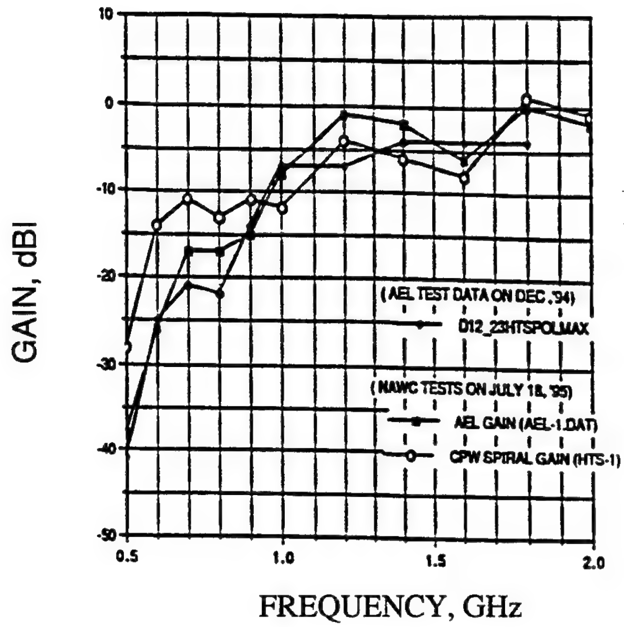

FIGURE 9. Gain of CPW-Fed Spiral Versus AEL Balun-Fed Spiral.

From these data, it can be seen that the gains are similar down to 0.9 GHz. Below that, the gain of the CPW-fed spiral is 5 to 10 dB higher.

The axial ratio of the two designs is illustrated in Figure 10.

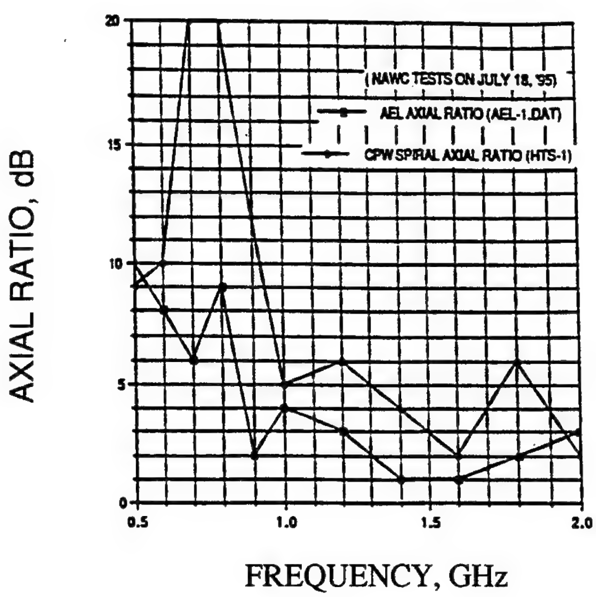

FIGURE 10. Axial Ratio of CPW-Fed Spiral Versus AEL Balun-Fed Spiral.

From these data, it appears that the traditional balun center-fed design has better circular polarization performance. (These data are shown in Appendix E.)

One factor of the design of the CPW-fed spiral, which was limited by the material available for the substrate, is the axial ratio. The initial design of the copper spiral indicated that a lower dielectric substrate worked better. Its substrate had a dielectric constant of 10.0, as compared to the HTS substrate with 23.5. The patterns on these antennae at 2 to 4 GHz indicate a lower axial ratio for the spiral on a lower dielectric constant substrate. The fabrication of a HTS spiral on a lower dielectric constant material such as sapphire could bring a substantial improvement in axial ratio.

SPIRAL MODE MICROSTRIP (SMM) CONFIGURATION

Because of the planar construction of this spiral design, it is easy to change the cavity behind the antenna. The spiral can be removed and mounted to a different cavity to investigate other designs without making additional, expensive antennae substrates. One possible cavity design for this spiral is a derivation of the Wang-Tripp design, which was developed under work for the Air Force. This design places the spiral electrically close to a ground plane, while still attaining most of the characteristics of the cavity-loaded spiral. Because of the relative ease of changing the spiral cavity and potential advantages of an absorberless cavity, the spiral was removed from the original loaded cavity and placed on a similar cavity with a 1.50-inch gap between the spiral and ground plane. This is equivalent to 0.06 wavelengths at 0.5 GHz and 0.25 wavelengths at 2 GHz. This configuration is illustrated in Figure 11.

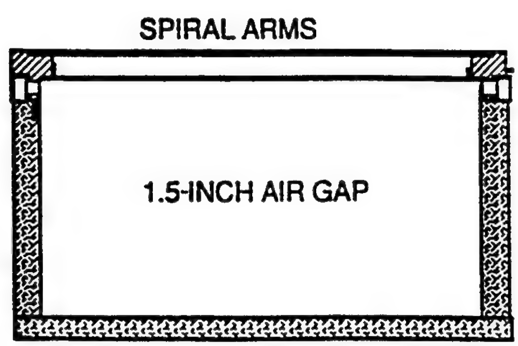

LENGTH REDUCTION OF 2.5 OVER
LOADED CAVITY.

OVERALL VOLUME REDUCTION OF
10:1 OVER CONVENTIONAL SPIRAL.

FIGURE 11. Microstrip Mode Spiral Assembly.

The same set of tests that were performed on the loaded cavity were done on this configuration. The patterns are illustrated in Appendix F.

The gain and axial ratio versus frequency results are shown in Figures 12 and 13.

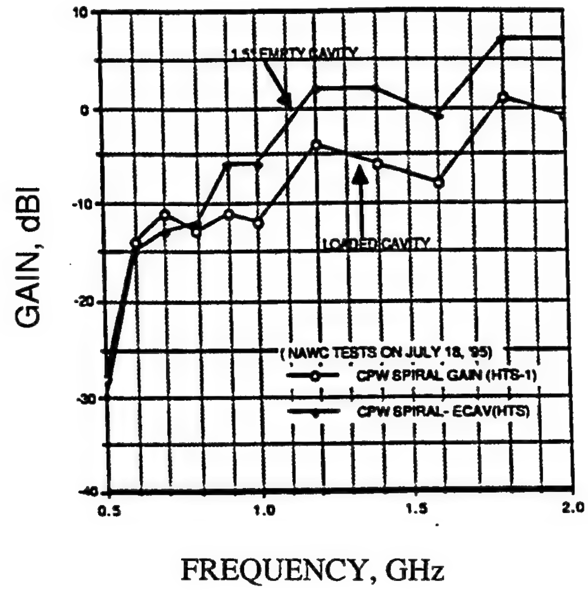

FIGURE 12. Gain of CPW-Fed HTS Spiral Versus CPW-Fed Empty Cavity Spiral.

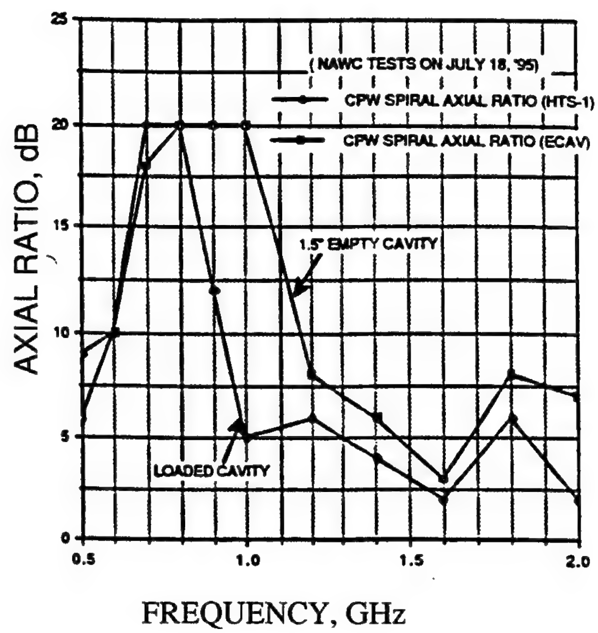

FIGURE 13. Axial Ratio of CPW-Fed HTS Spiral Versus CPW-Fed Empty Cavity Spiral.

These data show an increased gain from the 0.9- to 2.0-GHz range, with a worse axial ratio over the lower frequency range from 0.8 to 1.2 GHz. This result indicates a higher degree of linear polarization in the E-field of the antenna. The increased gain that was hoped for was gained over about half of the frequency band. This cavity length was one of three attempted, and was the best attained in this set of trials.

The SMM mode for a electrically small spiral antenna is demonstrated here to produce a much simpler configuration, with some performance increases.

CONCLUSION

A new CPW-fed HTS spiral has been demonstrated to provide performance similar to a conventional feed design. The assembly is simpler and more robust. The optional cavity configurations available allow the designer to optimize the overall antenna to his needs. The design limitations of higher axial ratio may be improved with the use of lower dielectric substrate materials. These materials are being investigated in the HTS materials community and should become available in the future. The need for a practical cryogenic cooling system remains the major design problem to overcome before a fieldable antenna system is available.

The small size and tremendous antenna gain improvements available with the HTS spiral make design options possible that have not previously been a consideration. Systems that need to go further down in frequency without increasing the antenna size can now explore this possibility.

REFERENCES

1. Barry Spielman. "Computer Aided Analysis of Dissipation Losses in Isolated and Coupled Transmission Lines for Microwave and Millimeter-Wave Integrated-Circuit Applications," NRL Report 8009, July 1976.

2. Naval Air Warfare Center Weapons Division. *Data Analysis of High Temperature Superconductive Spiral Antenna Chamber Patterns*, by Michael Neel. China Lake, Calif., NAWCWPNS, December 1995. (NAWCWPNS TP 8270, publication UNCLASSIFIED.)

Appendix A

COPLANAR WAVEGUIDE CODE

```
C SINGLE STRIP COPLANAR WAVEGUIDE ANALYSIS AFTER SPIELMAN
C
C   NRL Report 8009 , "Computer-Aided Analysis of Dissipation Losses in
C   Isolated and Coupled Transmission Lines for Microwave and Millimeter
C     -Wave Integrated-Circuit Applications," July 1976
C
C
C      COPLANAR WAVEGUIDE , SUBSTRATE SUSPENDED IN AIR
      REAL L
      PRINT *,' ENTER NUMBER OF DATA SETS TO BE ANALYZED'
      PRINT *
      READ *,NSETS
      DO 2 MN=1,NSETS
       PRINT *,' ENTER W,S,H(MILS),L(INS),ER,TAND1(X10**4),SIGMA(X10**-07
     . MHO)'
      PRINT *
       READ *,W,S,H,L,ER,TAND1,SIGMA
      TAND1=TAND1*1.E-04
      SIGMA=SIGMA*1.E+07
      WRITE(*,8)
8      FORMAT(1H ,///' STRIP METALIZATION THICKNESS=250 MICROINCHES')
       WRITE(*,4)W,S,H,L,ER,TAND1,SIGMA
4        FORMAT(1H ,' W=',F5.1,3X,' S=',F5.1,3X,' H=',F5.1,3X,' L=',
      .F10.6,3X,' ER=',F10.6,3X,' TAND1=',E10.3,3X,' SIGMA=',E10.3)
      FACTOR=(1.E-05)*(1./0.393700)
      W=W*FACTOR
      S=S*FACTOR
      H=H*FACTOR
      L=L*FACTOR*(1.E+03)
      E1=ER
      E2=ER+.01*ER
       CALL CPWF(W,S,H,L,E1,SIGMA,C,PDDSQ)
C     PDDSQF=PDDSQ
C       CALL CPWF(W,S,H,L,E2,SIGMA,CP,PDDSQ)
      CALL CPWE(W,S,H,L,CE)
      A=C*CE
C     B=CE/C
      Z0=1./((3.E+08)*SQRT(A))
C     V=3.E+08*SQRT(B)
C     ARG1=B
C     ARG2=CE/CP
```

```
C     ER1=1./ARG1
C     ER2=1./ARG2
C     FACTC=10./2.3
C     FACTD=27.3/3.E+08
C     AC=FACTC*PDDSQF*ER1*Z0
C     AD=FACTD*(E1/SQRT(ER1))*((ER2-ER1)/(E2-E1))*TAND1
      WRITE(*,5)
C5      FORMAT(1H ,1X,' Z0(OHMS)',5X,' V(M/SEC)',5X,
C     .' ALPHAC(DB/M)/SQRT(F)',5X,' ALPHAD(DB/M)/F')
5     FORMAT(1H ,1X,' Z0(OHMS)')
      WRITE(*,6)Z0
6     FORMAT(1H ,2X,F6.2)
2     CONTINUE
        pause
      STOP
      END
C USED BY CPW: COPLANAR WAVEGUIDE ANALYSIS
      SUBROUTINE CPWE(W,S,H,L,CH1)
      DIMENSION N(3),X(70,3),Y(70,3),ALPHA(70,3),BETA1(70,3)
     .,BETA2(70,3),GAMMA(70,3),CH(70,3),SCH(3),TSCD(70,3,4)
      COMMON/HELP/A(252,252)
      REAL L
      NO=3
      N(1)=41
      N(2)=70
      N(3)=70
      E0=1./(4.*3.14159*2.99776*2.9976E+09)
      FACTOR=(1.0E-05)*(1./0.393700)
      DELW=W/40.
      DELG=(L/2.-W/2.-S)/69
      X(1,1)=-W/2.
      Y(1,1)=0.
      DO 26 I=1,40
      IP1=I+1
      X(IP1,1)=X(I,1)+DELW
      Y(IP1,1)=Y(I,1)
      ALPHA(I,1)=1.
      BETA1(I,1)=0.
      BETA2(I,1)=0.
26    GAMMA(I,1)=1.
      X(1,2)=-L/2.
      Y(1,2)=0.
      X(1,3)=L/2.
      Y(1,3)=0.
      DO 27 I=1,69
      IP1=I+1
      X(IP1,2)=X(I,2)+DELG
      Y(IP1,2)=Y(I,2)
      X(IP1,3)=X(I,3)-DELG
      Y(IP1,3)=Y(I,3)
      ALPHA(I,2)=1.
```

```
      BETA1(I,2)=0.
      BETA2(I,2)=0.
      GAMMA(I,2)=0.
      ALPHA(I,3)=1.
      BETA1(I,3)=0.
      BETA2(I,3)=0.
27    GAMMA(I,3)=0.
      XMIN=0.
      XMAX=0.
      YMIN=0.
      YMAX=0.
      NX=0
      NY=0
      IDIM=70
      R=1.0E+05
      NAXDIM=252
      NAYDIM=252
      CALL
LPLACE(NO,N,X,Y,ALPHA,BETA1,BETA2,GAMMA,CH,SCH,IDIM,R,TSCD,
     .XMIN,XMAX,NX,YMIN,YMAX,NY,NAXDIM,NAYDIM)
      CH1=SCH(1)*6.2831852*E0
      RETURN
      END
      SUBROUTINE CPWF(W,S,H,L,ER,SIGMA,CHRG,PDDSQF)
      DIMENSION N(6),X(59,6),Y(59,6),ALPHA(59,6),BETA1(59,6),
     .BETA2(59,6),GAMMA(59,6),CH(59,6),SCH(6),TSCD(59,6,4)
      COMMON/HELP/A(252,252)
      REAL L
      NO=6
      N(1)=41
      N(2)=59
      N(3)=59
      N(4)=21
      N(5)=21
      N(6)=51
      E0=1./(4.*3.14159*2.99776*2.99776E+09)
      AAA=3.14159*4.E-07*3.14159/SIGMA
      RDSQF=SQRT(AAA)
      FACTN=4.*3.14159*3.14159*RDSQF*8.85E-12
      FACTD=4.*3.14159*1.E-07
      FACTL=FACTN/FACTD
      FACTOR=(1.0E-05)*(1./0.393700)
      DELW=W/19.
      E=ER*E0
      X(1,1)=-W/2.
      Y(1,1)=-0.25*FACTOR
      DO 26 I=1,19
      IP1=I+1
      X(IP1,1)=X(I,1)+DELW
26    Y(IP1,1)=Y(1,1)
      X(21,1)=X(20,1)
```

```
      Y(21,1)=0.
      DO 27 I=21,39
      IP1=I+1
      X(IP1,1)=X(I,1)-DELW
27    Y(IP1,1)=Y(I,1)
      X(41,1)=X(1,1)
      Y(41,1)=Y(1,1)
      DELG=(L/2.-W/2.-S)/28.
      X(1,2)=-L/2.
      Y(1,2)=0.
      X(30,2)=-(W/2.)-S
      Y(30,2)=-0.25*FACTOR
      X(1,3)=L/2.
      Y(1,3)=0.
      X(30,3)=(W/2.)+S
      Y(30,3)=-0.25*FACTOR
      DO 28 I=1,28
      IP1=I+1
      IP30=I+30
      IP30M1=IP30-1
      X(IP1,2)=X(I,2)+DELG
      Y(IP1,2)=0.
      X(IP30,2)=X(IP30M1,2)-DELG
      Y(IP30,2)=Y(30,2)
      X(IP1,3)=X(I,3)-DELG
      Y(IP1,3)=0.
      X(IP30,3)=X(IP30M1,3)+DELG
28    Y(IP30,3)=Y(30,3)
      X(59,2)=X(1,2)
      Y(59,2)=Y(1,2)
      X(59,3)=X(1,3)
      Y(59,3)=Y(1,3)
      DELS=S/20.
      X(1,4)=-W/2.-S
      Y(1,4)=0.
      X(1,5)=W/2.+S
      Y(1,5)=0.
      DO 29 I=1,20
      IP1=I+1
      X(IP1,4)=X(I,4)+DELS
      Y(IP1,4)=0.
      X(IP1,5)=X(I,5)-DELS
29    Y(IP1,5)=0.
      DELH=H/2.
      DELL=L/46.
      X(1,6)=-L/2.
      Y(1,6)=0.
      X(49,6)=L/2.
      Y(49,6)=H
      DO 30 I=1,2
      IP1=I+1
```

```
      IP49=I+49
      IP49M1=IP49-1
      X(IP1,6)=X(I,6)
      Y(IP1,6)=Y(I,6)+DELH
      X(IP49,6)=X(IP49M1,6)
30    Y(IP49,6)=Y(IP49M1,6)-DELH
      DO 31 I=1,46
      IP3=I+3
      IP3M1=IP3-1
      X(IP3,6)=X(IP3M1,6)+DELL
31    Y(IP3,6)=H
      DO 60 I=1,40
      ALPHA(I,1)=1.
      BETA1(I,1)=0.
      BETA2(I,1)=0.
60    GAMMA(I,1)=1.
      DO 61I=1,58
      ALPHA(I,2)=1.
      ALPHA(I,3)=1.
      BETA1(I,2)=0.
      BETA1(I,3)=0.
      BETA2(I,2)=0.
      BETA2(I,3)=0.
      GAMMA(I,2)=0.
61    GAMMA(I,3)=0.
      DO 62 I=1,20
      ALPHA(I,4)=0.
      ALPHA(I,5)=0.
      BETA1(I,4)=E0
      BETA1(I,5)=E
      BETA2(I,4)=E
      BETA2(I,5)=E0
      GAMMA(I,4)=0.
62    GAMMA(I,5)=0.
      DO 63 I=1,50
      ALPHA(I,6)=0.
      BETA1(I,6)=E
      BETA2(I,6)=E0
63    GAMMA(I,6)=0.
      XMIN=0.
      XMAX=0.
      YMIN=0.
      YMAX=0.
      NX=0
      NY=0
      IDIM=59
      R=1.0E+05
      NAXDIM=252
      NAYDIM=252
      CALL
LPLACF(NO,N,X,Y,ALPHA,BETA1,BETA2,GAMMA,CH,SCH,IDIM,R,TSCD,
```

```
.XMIN,XMAX,NX,YMIN,YMAX,NY,NAXDIM,NAYDIM)
      DELF=W/19.
      DELE=0.25*FACTOR
      FF1=6.2831852*E*DELF
      FF2=6.2831852*E0*DELE
      FF4=6.2831852*E0*DELF
      CHRG=0.
      DO 50 I=1,19
50      CHRG=CHRG+FF4*CH(I,1)
      DO 51 I=21,39
51      CHRG=CHRG+FF1*CH(I,1)
      CHRG=CHRG+FF2*(CH(20,1)+CH(40,1))
      SUM=0.
      DO 64 J=1,NO
      IF(ALPHA(1,J).NE.1)GO TO 64
      NJ1=N(J)-1
      DO 65 I=1,NJ1
      IP1=I+1
      SEGX=X(IP1,J)-X(I,J)
      SEGY=Y(IP1,J)-Y(I,J)
      SEGARG=SEGX*SEGX+SEGY*SEGY
      SEGLEN=SQRT(SEGARG)
65      SUM=SUM+CH(I,J)*CH(I,J)*SEGLEN
64    CONTINUE
      PDDSQF=FACTL*SUM
54    CONTINUE
      RETURN
      END
      SUBROUTINE SIMQ(A,B,N,KS)
C  SUBROUTINE SIMQ FROM IBM SSP P 120
C  PURPOSE
C  OBTAIN SOLUTION OF A SET OF SIMULTANEOUS LINEAR EQUATIONS,
C  AX=B
C
C DESCRIPTION OF PARAMETERS
C  A - MATRIX OF COEFFICIENTS STORED COLUMNWISE.  THESE ARE
C DESTROYED IN THE COMPUTATION.  SIZE OF MATRIX A IS N X N.
C B - VECTOR OF ORIGINAL  CONSTANTS(LENGTH N).  THESE ARE REPLACED
BY
C FINAL SOLUTION VALUES,VECTOR X.
C N - NUMBER OF EQUATIONS AND VARIABLES. N MUST BE .GT. ONE.
C KS - OUTPUT DIGIT
C  0 FOR NORMAL SOLUTION
C  1 FOR SINGULAR SET OF EQUATIONS
C
C  REMARKS
C   MATRIX A MUST BE GENERAL.
C   IF MATRIX A IS SINGULAR, SOLUTION VALUES ARE MEANINGLESS.
C   AN ALTERNATIVE SOLUTION MAY BE OBTAINED BY USING MATRIX
C   INVERSION (MINV) AND MATRIX PRODUCT (GMPRD)
C  SUBROUTINES AND FUNCTION SUBPROGRAMS REQUIRED
```

```
C  NONE
C
C METHOD
C  METHOD OF SOLUTION IS BY ELIMINATION USING LARGEST PIVOTAL
C  DIVISOR. EACH STAGE OF ELIMINATION CONSISTS OF INTERCHANGING
C   ROWS WHEN NECESSARY TO AVOID DIVISION BY ZERO OR SMALL
ELEMENTS.
C  THE FORWARD SOLUTION TO OBTAIN VARIABLE N IS DONE IN N STAGES.
C   THE BACK SOLUTION FOR THE OTHER VARIABLES IS CALCULATED BY
SUCCESSIVE
C  SUBSTITUTIONS.
C     FINAL SOLUTION VALUES ARE DEVELOPED IN VECTOR B, WITH
VARIABLE 1 IN B(1),
C   VARIABLE 2 IN B(2)........., VARIABLE N IN B(N).
C   IF NO PIVOT CAN BE FOUND EXCEEDING A TOLERANCE OF 0.0, THE
MATRIX IS
C   CONSIDERED SINGULAR AND KS IS SET TO 1. THIS TOLERANCE CAN BE
C  MODIFIED BY REPLACING THE FIRST STATEMENT.
   DIMENSION A(1),B(1)
C
C FORWARD SOLUTION
C
   TOL=0.0
   KS=0
   JJ=-N
   DO 65 J=1,N
   JY=J+1
   JJ=JJ+N+1
   BIGA=0.
   IT=JJ-J
   DO 30 I=J,N
C
C  SEARCH FOR MAXIMUM COEFFICIENT IN COLUMN
C
   IJ=IT+I
C
C TEST FOR PIVOT LESS THAN TOLERANCE (SINGULAR MATRIX)
   IF(ABS(BIGA)-ABS(A(IJ)))20,30,30
20  BIGA=A(IJ)
   IMAX=I
30  CONTINUE
   IF(ABS(BIGA)-TOL)35,35,40
35  KS=1
   RETURN
C
C INTERCHANGE ROWS IF NECESSARY
C
40  I1=J+N*(J-2)
   IT=IMAX-J
   DO 50 K=J,N
   I1=I1+N
```

```
      I2=I1+IT
      SAVE=A(I1)
      A(I1)=A(I2)
      A(I2)=SAVE
C
C DIVIDE EQUATION BY LEADING COEFFICIENT
C
50    A(I1)=A(I1)/BIGA
      SAVE=B(IMAX)
      B(IMAX)=B(J)
      B(J)=SAVE/BIGA
C
C ELIMINATE NEXT VARIABLE
C
      IF(J-N)55,70,55
55    IQS=N*(J-1)
      DO 65 IX=JY,N
      IXJ=IQS+IX
      IT=J-IX
      DO 60 JX=JY,N
      IXJX=N*(JX-1)+IX
      JJX=IXJX+IT
60    A(IXJX)=A(IXJX)-(A(IXJ)*A(JJX))
65    B(IX)=B(IX)-(B(J)*A(IXJ))
C
C BACK SOLUTION
C
70    NY=N-1
      IT=N*N
      DO 80 J=1,NY
      IA=IT-J
      IB=N-J
      IC=N
      DO 80 K=1,J
      B(IB)=B(IB)-A(IA)*B(IC)
      IA=IA-N
80    IC=IC-1
      RETURN
      END
      SUBROUTINE
LPLACE(NO,N,X,Y,ALPHA,BETA1,BETA2,GAMMA,CH,SCH,IDIM,R,
     * TSCD,XMIN,XMAX,NX,YMIN,YMAX,NY,NAXDIM,NAYDIM)
      DIMENSION X(IDIM,NO),Y(IDIM,NO),ALPHA(IDIM,NO),BETA1(IDIM,NO),

*BETA2(IDIM,NO),GAMMA(IDIM,NO),CH(IDIM,NO),TSCD(IDIM,NO,4),N(NO),
     *A(252,252),SCH(NO),B(246)
      COMMON/HELP/A
      PI=3.1415926
      RR=R*R
      DO 1 L=1,NO
      NN=N(L)-1
```

```
      DO 1 I=1,NN
      XI=X(I+1,L)-X(I,L)
      YI=Y(I+1,L)-Y(I,L)
      TSCD(I,L,1)=ATAN2(YI,XI)
      TSCD(I,L,2)=SIN(TSCD(I,L,1))
      TSCD(I,L,3)=COS(TSCD(I,L,1))
    1 TSCD(I,L,4)=SQRT(XI*XI+YI*YI)
      JJJ=0
      DO 4 LJ=1,NO
      NJ=N(LJ)-1
      JAJ=JJJ
      JJJ=JJJ+NJ
      DO 4 J=1,NJ
      JJ=JAJ+J
      XJ=(X(J,LJ)+X(J+1,LJ))/2.
      YJ=(Y(J,LJ)+Y(J+1,LJ))/2.
      III=0
      DO 4 LI=1,NO
      NI=N(LI)-1
      III=III+NI
      IAI=III-NI
      DO 4 I=1,NI
      II=IAI+I
      IF(II.EQ.JJ)GO TO 3
      X1=XJ-X(I,LI)
      X2=XJ-X(I+1,LI)
      Y1=YJ-Y(I,LI)
      Y2=YJ-Y(I+1,LI)
      R1=X1*X1+Y1*Y1
      R2=X2*X2+Y2*Y2
      S1=0.
      S2=0.
      YT=Y(I,LI)*X2-Y(I+1,LI)*X1+YJ*(X(I+1,LI)-X(I,LI))
      XT=X1*X2+Y1*Y2
      TETA=ATAN2(YT,XT)
      IF(ALPHA(J,LJ).EQ.0.)GO TO 2
      S1=TSCD(I,LI,4)*(1.-0.5*ALOG(R2/RR))+0.5*ALOG(R2/R1)*(X1*TSCD(I,LI
     *,3)+Y1*TSCD(I,LI,2))+TETA*(X1*TSCD(I,LI,2)-Y1*TSCD(I,LI,3))
    2 TETA1=TSCD(J,LJ,1)-TSCD(I,LI,1)
      S2=0.5*SIN(TETA1)*ALOG(R2/R1)+COS(TETA1)*TETA
      S3=-S2
      GO TO 4
    3 S1=TSCD(I,LI,4)*(1.-ALOG(TSCD(I,LI,4)/2./R))
      S2=-PI
      S3=-PI
    4 A(JJ,II)=ALPHA(J,LJ)*S1+BETA1(J,LJ)*S2+BETA2(J,LJ)*S3
      M=0
      DO 5 L=1,NO
    5 M=M+N(L)-1
      JJJ=0
      DO 6 L=1,NO
```

```
      NN=N(L)-1
      JAJ=JJJ
      JJJ=JJJ+NN
      DO 6 J=1,NN
      JJ=JAJ+J
    6 B(JJ)=GAMMA(J,L)
      CALL ARRAY(2,M,M,NAXDIM,NAYDIM,A,A)
      CALL SIMQ(A,B,M,KS)
      IF(KS.NE.0) WRITE(6,100)
  100 FORMAT(1H0,18HSYSTEM IS SINGULAR)
      JJJ=0
      DO 7 L=1,NO
      NN=N(L)-1
      JAJ=JJJ
      JJJ=JJJ+NN
      DO 7 J=1,NN
      JJ=JAJ+J
    7 CH(J,L)=B(JJ)
      DO 8 L=1,NO
      NN=N(L)-1
      SCH(L)=0.
      DO 8 I=1,NN
    8 SCH(L)=SCH(L)+TSCD(I,L,4)*CH(I,L)
      IF(NX-1)17,9,10
    9 DX=0.
      GO TO 11
   10 DX=(XMAX-XMIN)/FLOAT(NX-1)
   11 IF(NY-1)17,12,13
   12 DY=0.
      GO TO 14
   13 DY=(YMAX-YMIN)/FLOAT(NY-1)
   14 DO 16 II=1,NX
      XJ=XMIN+FLOAT(II-1)*DX
      DO 16 JJ=1,NY
      YJ=YMIN+FLOAT(JJ-1)*DY
      A(II,JJ)=0.
      DO 16 LI=1,NO
      NN=N(LI)-1
      DO 16 I=1,NN
      X1=XJ-X(I,LI)
      X2=XJ-X(I+1,LI)
      Y1=YJ-Y(I,LI)
      Y2=YJ-Y(I+1,LI)
      R1=X1*X1+Y1*Y1
      R2=X2*X2+Y2*Y2
      IF((R1.EQ.0.).OR.(R2.EQ.0.)) GO TO 15
      YT=Y(I,LI)*X2-Y(I+1,LI)*X1+YJ*(X(I+1,LI)-X(I,LI))
      XT=X1*X2+Y1*Y2
      TETA=ATAN2(YT,XT)
      S1=TSCD(I,LI,4)*(1.-0.5*ALOG(R2/RR))+0.5*ALOG(R2/R1)*(X1*TSCD(I,LI
     *,3)+Y1*TSCD(I,LI,2))+TETA*(X1*TSCD(I,LI,2)-Y1*TSCD(I,LI,3))
```

```
   GO TO 16
  15 S1=TSCD(I,LI,4)*(1.-0.5*ALOG((R1+R2)/RR))
  16 A(II,JJ)=A(II,JJ)+S1*CH(I,LI)
  17 RETURN
   END
C
C
   SUBROUTINE ARRAY(MODE,I,J,N,M,S,D)
C
C SUBROUTINE ARRAY
C PURPOSE
C   CONVERT DATA ARRAY FROM SINGLE TO DOUBLE DIMENSION OR VICE
C   VERSA.  THIS SUBROUTINE IS USED TO LINK THE USER PROGRAM
C   WHICH HAS DOUBLE DIMENSION ARRAYS AND THE SSP SUBROUTINES
C   WHICH OPERATE ON ARRAYS OF DATA IN A VECTOR FASHION.
C
C USAGE
C  CALL ARRAY(MODE,I,J,N,M,S,D)
C    MODE - CODE INDICATING TYPE OF CONVERSION
C DESCRIPTION OF PARAMETERS
C          1 - FROM SINGLE TO DOUBLE DIMENSION
C          2 - FROM DOUBLE TO SINGLE DIMENSION
C    I - NUMBER OF ROWS IN ACTUAL DATA MATRIX
C     J - NUMBER OF COLUMNS IN ACTUAL DATA MATRIX
C     N - NUMBER OF ROWS SPECIFIED FOR THE MATRIX D IN
C        DIMENSION STATEMENT
C     M - NUMBER OF COLUMNS SPECIFIED FOR THE MATRIX D IN
C        DIMENSION STATEMENT
C     S - IF MODE=1,THIS VECTOR IS INPUT WHICH CONTAINS THE
C        ELEMENTS OF A DATA MATRIX OF SIZE I BY J. COLUMN I+1
C        OF DATA MATRIX FOLLOWS COLUMN I, ETC.  IF MODE=2,
C        THIS VECTOR IS OUTPUT REPRESENTNG A DATA MATRIX OF
C        SIZE I BY J CONTAINING ITS COLUMNS CONSECUTIVELY.
C         THE LENGTH OF S IS IJ, WHERE IJ=I*J..
C     D - IF MODE=1,THIS MATRIX OF SIZE N BY M IS OUTPUT,
C        CONTAINING A DATA MATRIX OF SIZE I BY J IN THE FIRST
C        I ROWS AND J COLUMNS. IF MODE=2, THIS N BY M MATRIX
C        IS INPUT CONTAINING A DATA MATRIX OF SIZE I BY J IN
C        THE FIRST I ROWS AND  J COLUMNS.
C   REMARKS
C     VECTOR S CAN BE IN THE SAME LOCATION AS MARIX D.  VECTOR S
C         IS REFERRED AS A MARIX IN OTHER SSP ROUTINES, SINCE IT
CONTAINS
C     A DATA MATRIX.
C         THIS SUBROUTINE CONVERTS ONLY GENERAL DATA MATRICES
(STORAGE
C     MODES OF 0).
C
C   SUBROUTINES AND FUNCTION SUBPROGRAMS REQUIRED:
C      NONE
C
```

```
C   METHOD
C    REFER TO THE DISCUSSION ON VARIABLE DATA SIZE IN THE SECTION
C    DESCRIBING OVERALL RULES FOR USAGE IN THIS MANUAL.
C
    REAL    S(1),D(1)
    NI=N-I
C
C TEST TYPE OF CONVERSION
C
    IF(MODE-1)100,100,120
C
C CONVERT FROM SINGLE TO DOUBLE DIMENSION
C
100  IJ=I*J+1
    NM=N*J+1
    DO 110 K=1,J
    NM=NM-NI
    DO 110 L=1,I
    IJ=IJ-1
    NM=NM-1
110  D(NM)=S(IJ)
    GO TO 140
C
C CONVERT FROM DOUBLE TO SINGLE DIMENSION
C
120  IJ=0
    NM=0
    DO 130 K=1,J
    DO 125 L=1,I
    IJ=IJ+1
    NM=NM+1
125  S(IJ)=D(NM)
130  NM=NM+NI
140  RETURN
    END
C
C
C
    SUBROUTINE
LPLACF(NO,N,X,Y,ALPHA,BETA1,BETA2,GAMMA,CH,SCH,IDIM,R,
   .TSCD,XMIN,XMAX,NX,YMIN,YMAX,NY,NAXDIM,NAYDIM)
    DIMENSIONX(IDIM,NO),Y(IDIM,NO),ALPHA(IDIM,NO),BETA1(IDIM,NO)

.,BETA2(IDIM,NO),GAMMA(IDIM,NO),CH(IDIM,NO),TSCD(IDIM,NO,4),N(NO),
   .SCH(NO),B(246),A(252,252)
    COMMON/HELP/A
    PI=3.1415926
    RR=R*R
    DO 1 L=1,NO
    NN=N(L)-1
    DO 1 I=1,NN
```

```
      XI=X(I+1,L)-X(I,L)
      YI=Y(I+1,L)-Y(I,L)
      TSCD(I,L,1)=ATAN2(YI,XI)
      TSCD(I,L,2)=SIN(TSCD(I,L,1))
      TSCD(I,L,3)=COS(TSCD(I,L,1))
1     TSCD(I,L,4)=SQRT(XI*XI+YI*YI)
      JJJ=0
      DO 4 LJ=1,NO
      NJ=N(LJ)-1
      JAJ=JJJ
      JJJ=JJJ+NJ
      DO 4 J=1,NJ
      JJ=JAJ+J
      XJ=(X(J,LJ)+X(J+1,LJ))/2.
      YJ=(Y(J,LJ)+Y(J+1,LJ))/2.
      III=0
      DO 4 LI=1,NO
      NI=N(LI)-1
      III=III+NI
      IAI=III-NI
      DO 4 I=1,NI
      II=IAI+I
      IF(II.EQ.JJ)GO TO 3
      X1=XJ-X(I,LI)
      X2=XJ-X(I+1,LI)
      Y1=YJ-Y(I,LI)
      Y2=YJ-Y(I+1,LI)
      R1=X1*X1+Y1*Y1
      R2=X2*X2+Y2*Y2
      S1=0.
      S2=0.
      YT=Y(I,LI)*X2-Y(I+1,LI)*X1+YJ*(X(I+1,LI)-X(I,LI))
      XT=X1*X2+Y1*Y2
      TETA=ATAN2(YT,XT)
      IF(ALPHA(J,LJ).EQ.0.)GO TO 2
      S1=TSCD(I,LI,4)*(1.-0.5*ALOG(R2/RR))+0.5*ALOG(R2/R1)*(X1*TSCD(I,LI
     .,3)+Y1*TSCD(I,LI,2))+TETA*(X1*TSCD(I,LI,2)-Y1*TSCD(I,LI,3))
2     TETA1=TSCD(J,LJ,1)-TSCD(I,LI,1)
      S2=0.5*SIN(TETA1)*ALOG(R2/R1)+COS(TETA1)*TETA
      S3=-S2
      GO TO 4
3     S1=TSCD(I,LI,4)*(1.-ALOG(TSCD(I,LI,4)/2./R))
      S2=-PI
      S3=-PI
4     A(JJ,II)=ALPHA(J,LJ)*S1+BETA1(J,LJ)*S2+BETA2(J,LJ)*S3
      M=0
      DO 5 L=1,NO
5     M=M+N(L)-1
      JJJ=0
      DO 6 L=1,NO
      NN=N(L)-1
```

```
      JAJ=JJJ
      JJJ=JJJ+NN
      DO 6 J=1,NN
      JJ=JAJ+J
6     B(JJ)=GAMMA(J,L)
      CALL ARRAY(2,M,M,NAXDIM,NAYDIM,A,A)
      CALL SIMQ(A,B,M,KS)

      IF(KS.NE.0)WRITE(*,100)
100   FORMAT(1H ,'SYSTEM IS SINGULAR')
      JJJ=0
      DO 7 L=1,NO
      NN=N(L)-1
      JAJ=JJJ
      JJJ=JJJ+NN
      DO 7 J=1,NN
      JJ=JAJ+J
7     CH(J,L)=B(JJ)
      DO 8 L=1,NO
      NN=N(L)-1
      SCH(L)=0.
      DO 8 I=1,NN
8     SCH(L)=SCH(L)+TSCD(I,L,4)*CH(I,L)
      IF(NX-1)17,9,10
9     DX=0.
      GO TO 11
10    DX=(XMAX-XMIN)/FLOAT(NX-1)
11    IF(NY-1)17,12,13
12    DY=0.
      GO TO 14
13    DY=(YMAX-YMIN)/FLOAT(NY-1)
14    DO 16 II=1,NX
      XJ=XMIN+FLOAT(II-1)*DX
      DO 16 JJ=1,NY
      YJ=YMIN+FLOAT(JJ-1)*DY
      A(II,JJ)=0.
      DO 16 LI=1,NO
      NN=N(LI)-1
      DO 16 I=1,NN
      X1=XJ-X(I,LI)
      X2=XJ-X(I+1,LI)
      Y1=YJ-Y(I,LI)
      Y2=YJ-Y(I+1,LI)
      R1=X1*X1+Y1*Y1
      R2=X2*X2+Y2*Y2
      IF((R1.EQ.0.).OR.(R2.EQ.0.))GO TO 15
      YT=Y(I,LI)*X2-Y(I+1,LI)*X1+YJ*(X(I+1,LI)-X(I,LI))
      XT=X1*X2+Y1*Y2
      TETA=ATAN2(YT,XT)
      S1=TSCD(I,LI,4)*(1.-0.5*ALOG(R2/RR))+0.5*ALOG(R2/R1)*(X1*TSCD(I,LI
     .,3)+Y1*TSCD(I,LI,2))+TETA*(X1*TSCD(I,LI,2)-Y1*TSCD(I,LI,3))
```

```
   GO TO 16
15  S1=TSCD(I,LI,4)*(1.-0.5*ALOG((R1+R2)/RR))
16  A(II,JJ)=A(II,JJ)+S1*CH(I,LI)
17  RETURN
   END
```

Appendix B

HTS SPIRAL ASSEMBLY

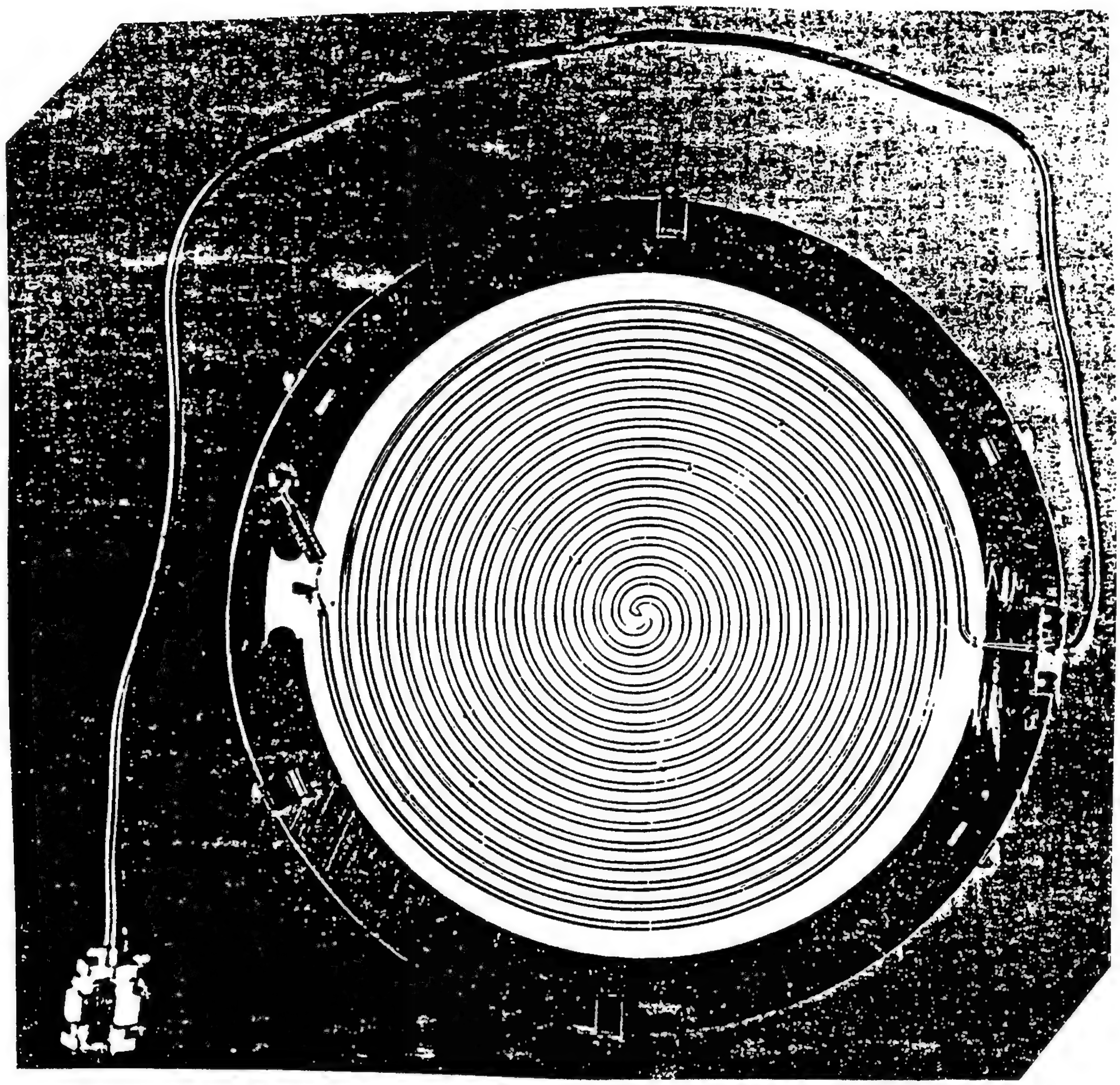

FIGURE B-1. Copper Spiral Assembly

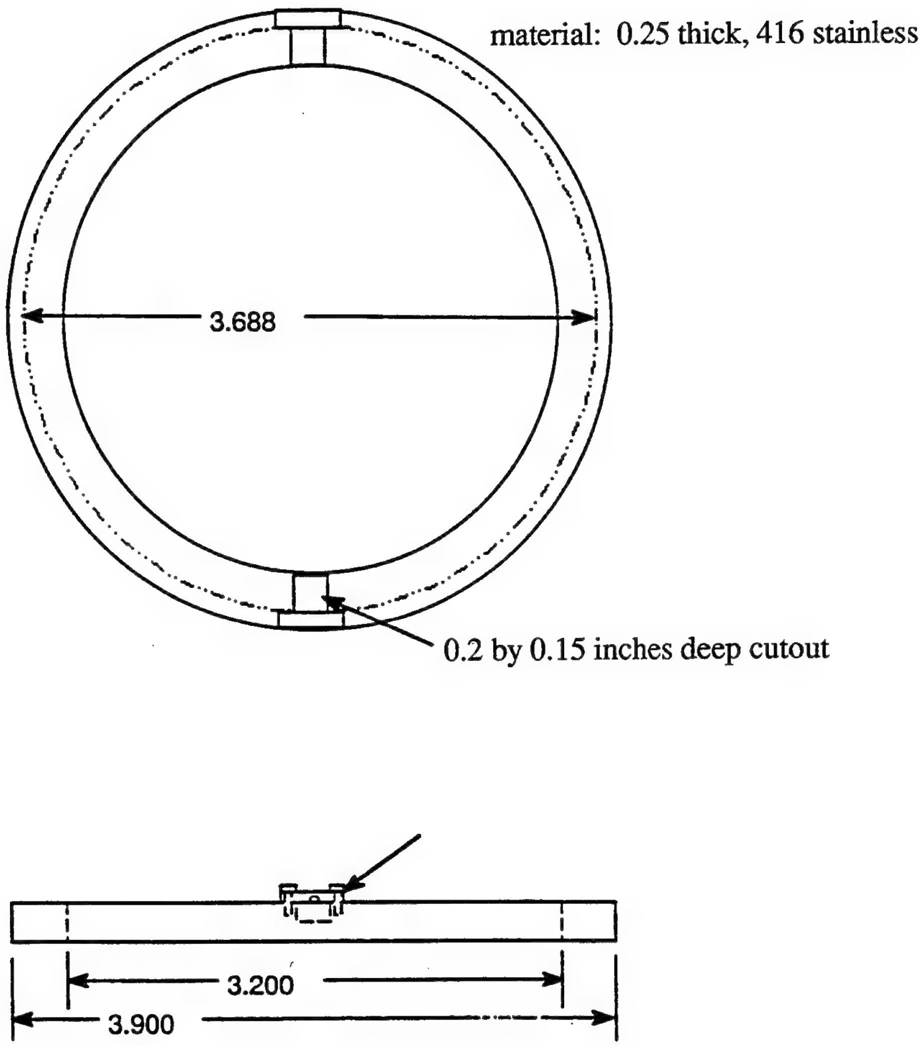

FIGURE B-2. Spiral Mount Ring.

Appendix C

CPW DELAY LINE TESTS AND COPPER SPIRAL PATTERNS

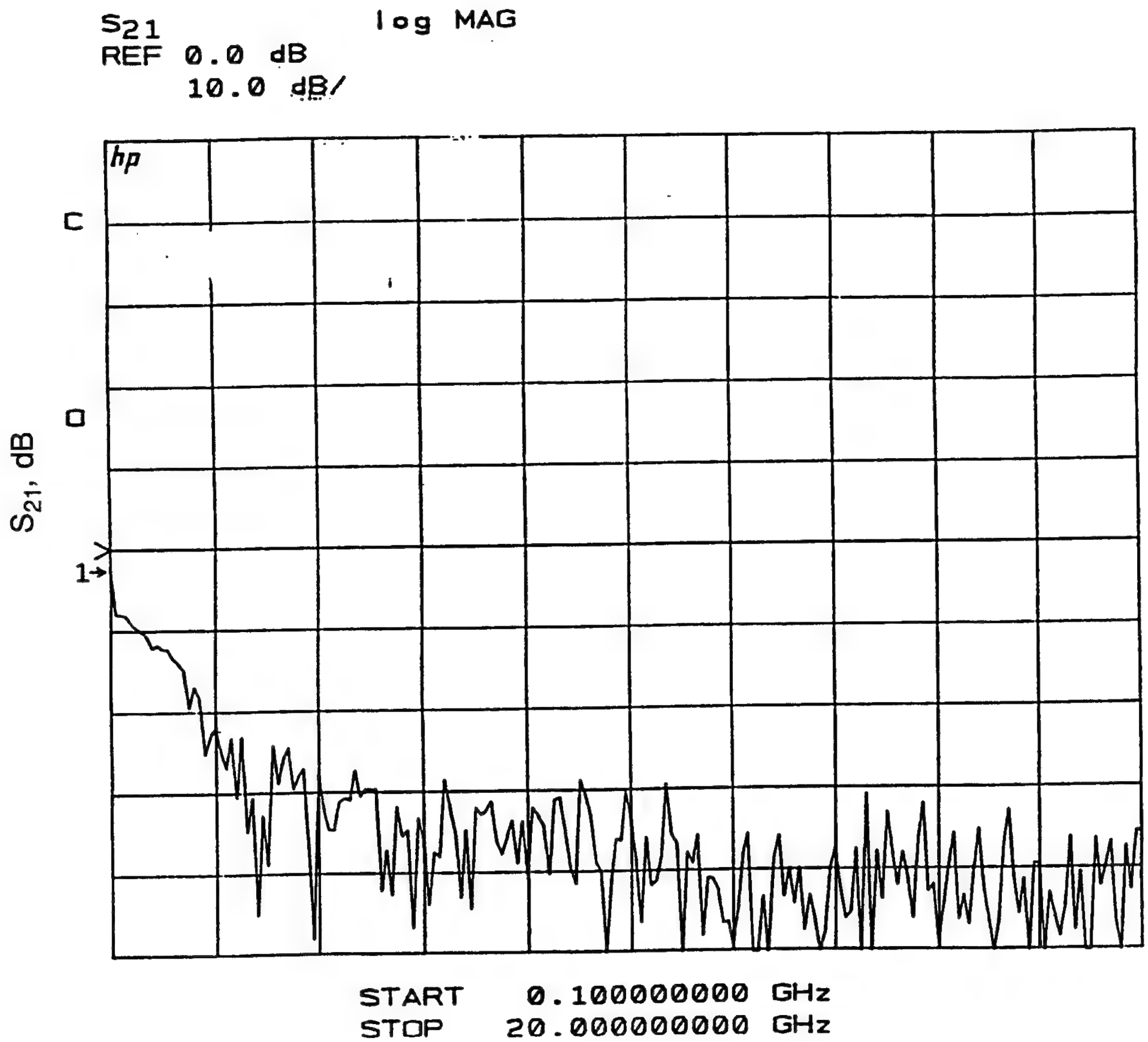

FIGURE C-1. CPW Spiral Delay Line—Without Ribbon Bridges Transmission Loss.

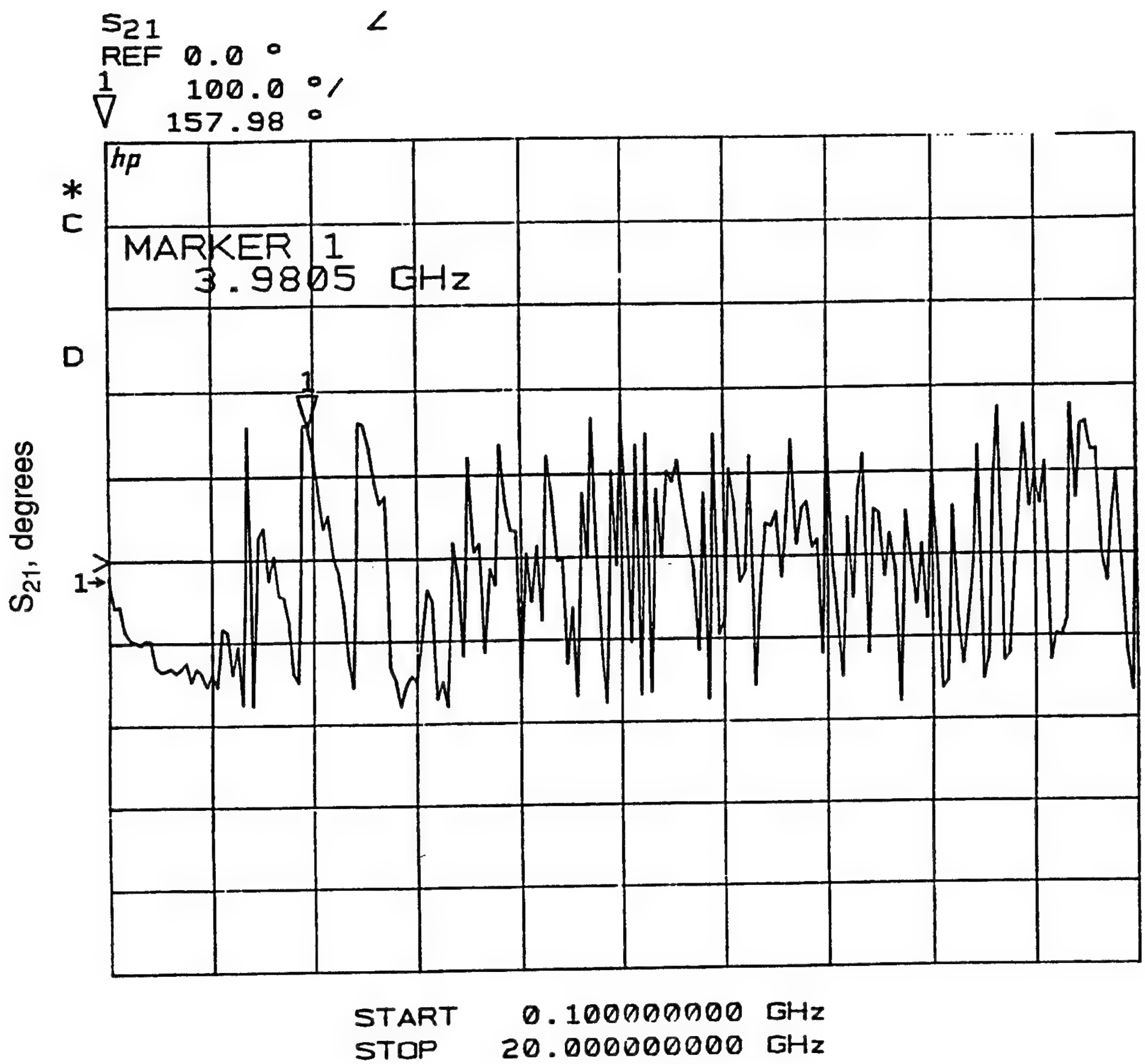

FIGURE C-2. CPW Spiral Delay Line—Withough Ribbon Bridges Transmission Phase.

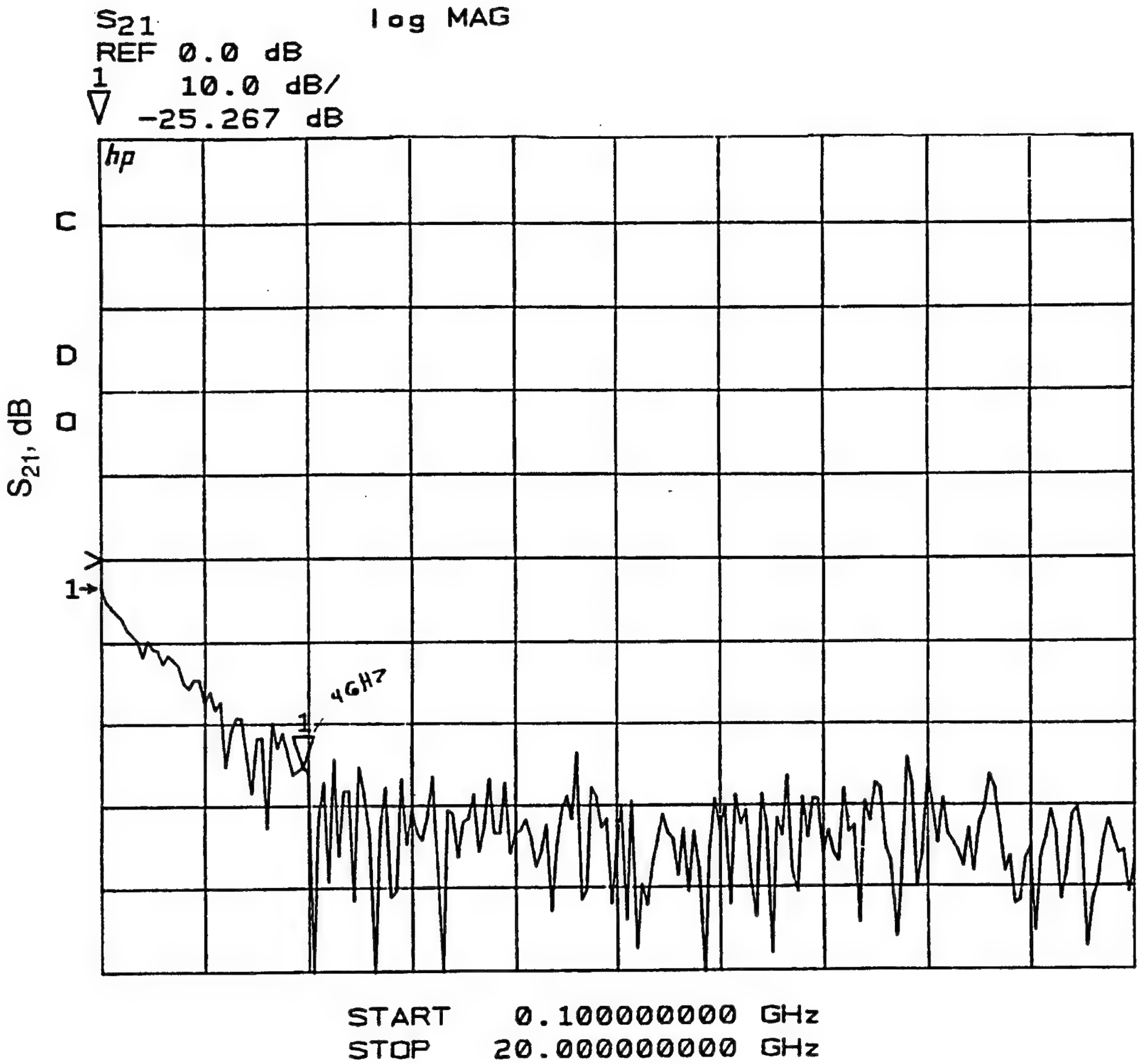

FIGURE C-3. CPW Spiral Delay Line—With Ribbon Bridges Transmission Loss.

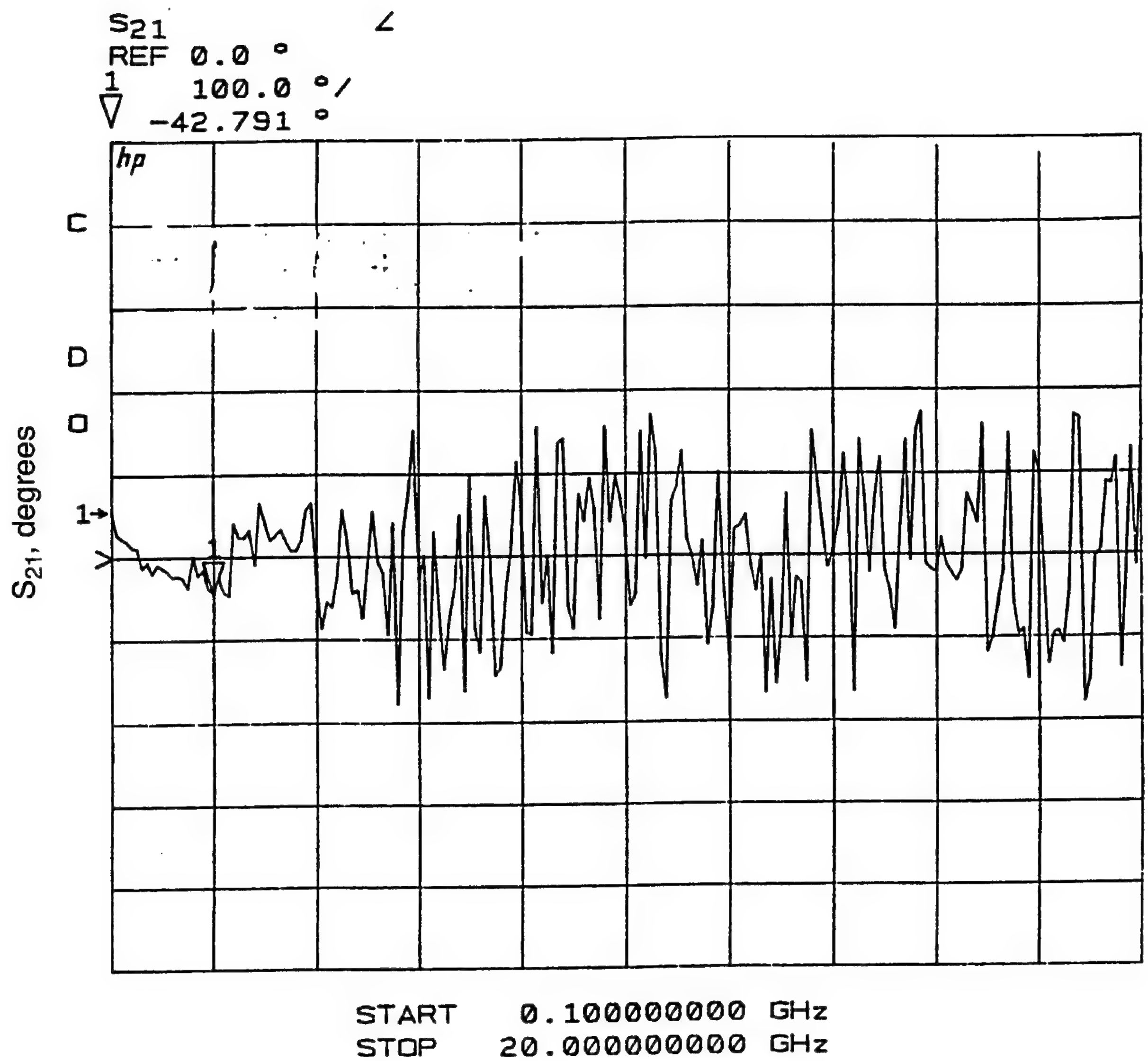

FIGURE C-4. CPW Spiral Delay Line—With Ribbon Bridges Transmission Phase.

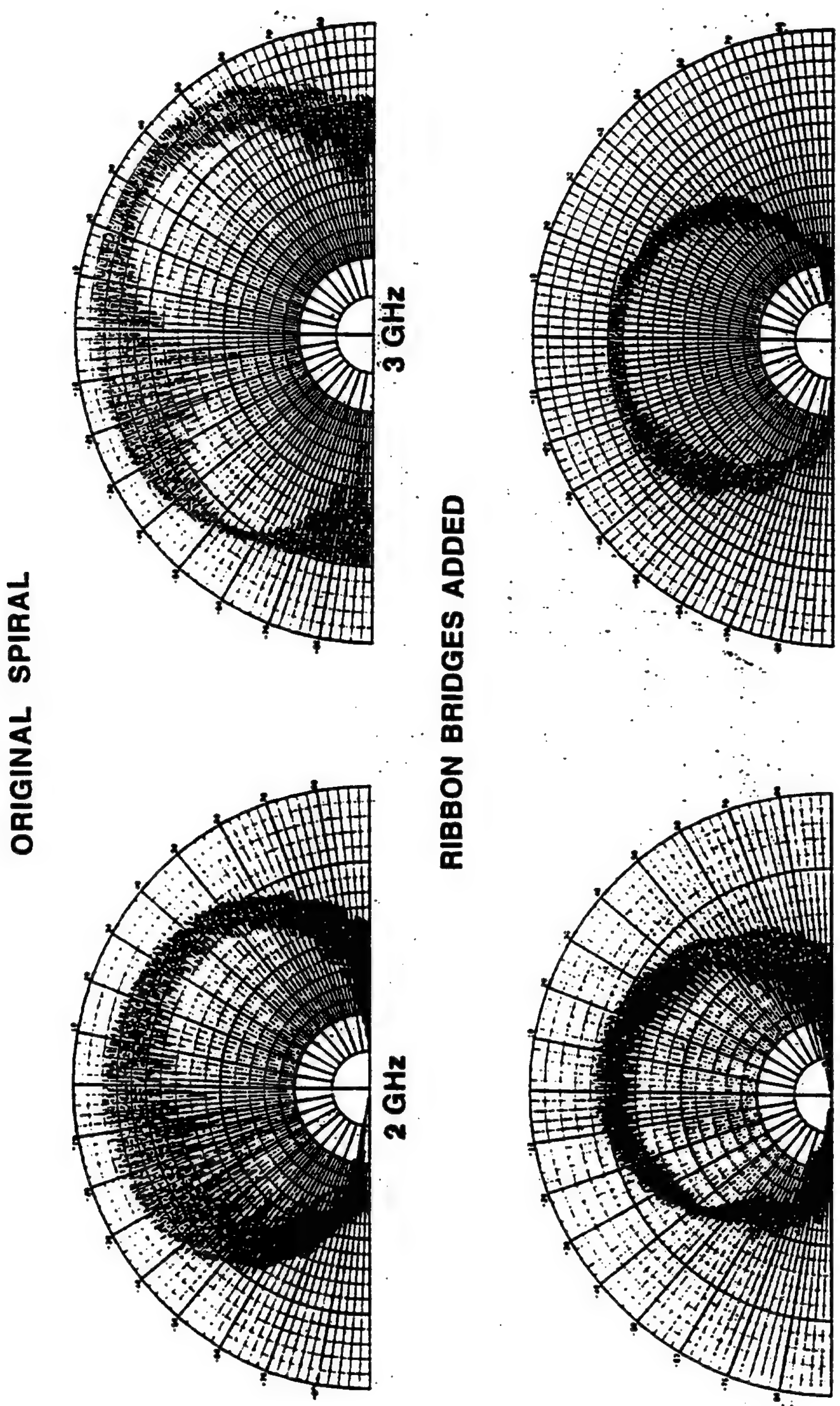

FIGURE C-5. Copper CPW-Fed Spiral.

Appendix D

HTS SPIRAL ASSEMBLY PICTURES

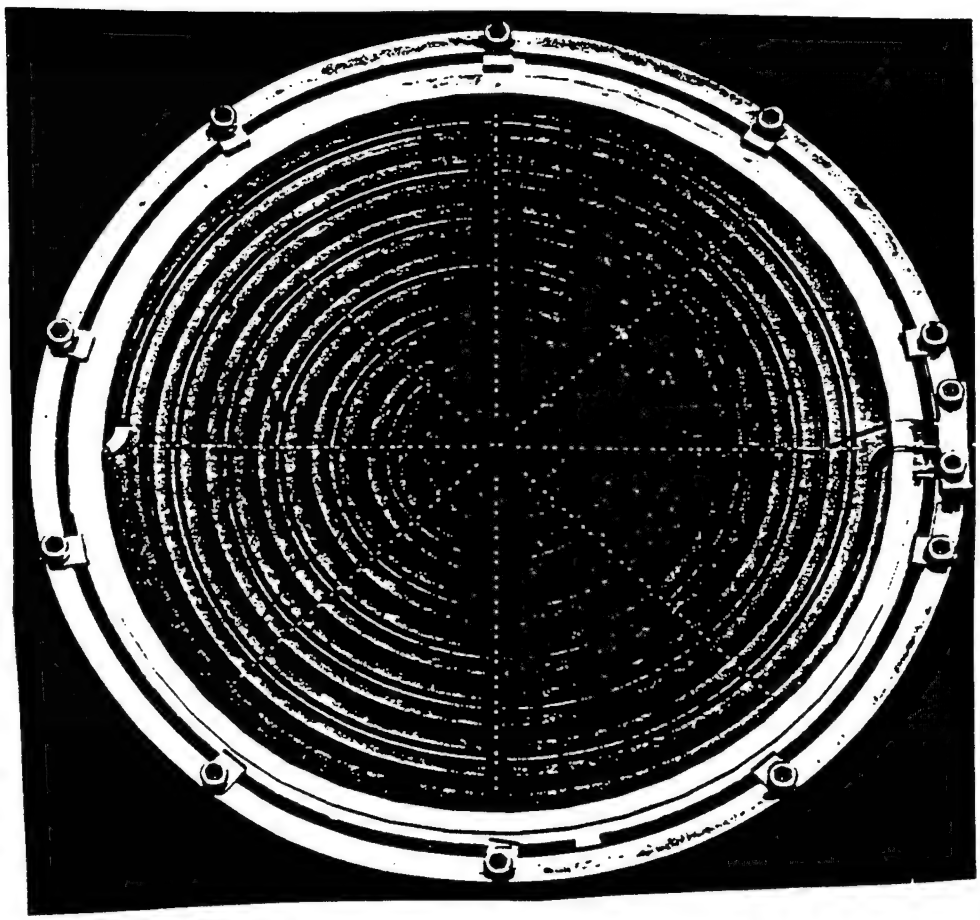

FIGURE D-1. Coplanar Waveguide Balun-Fed HTS Spiral

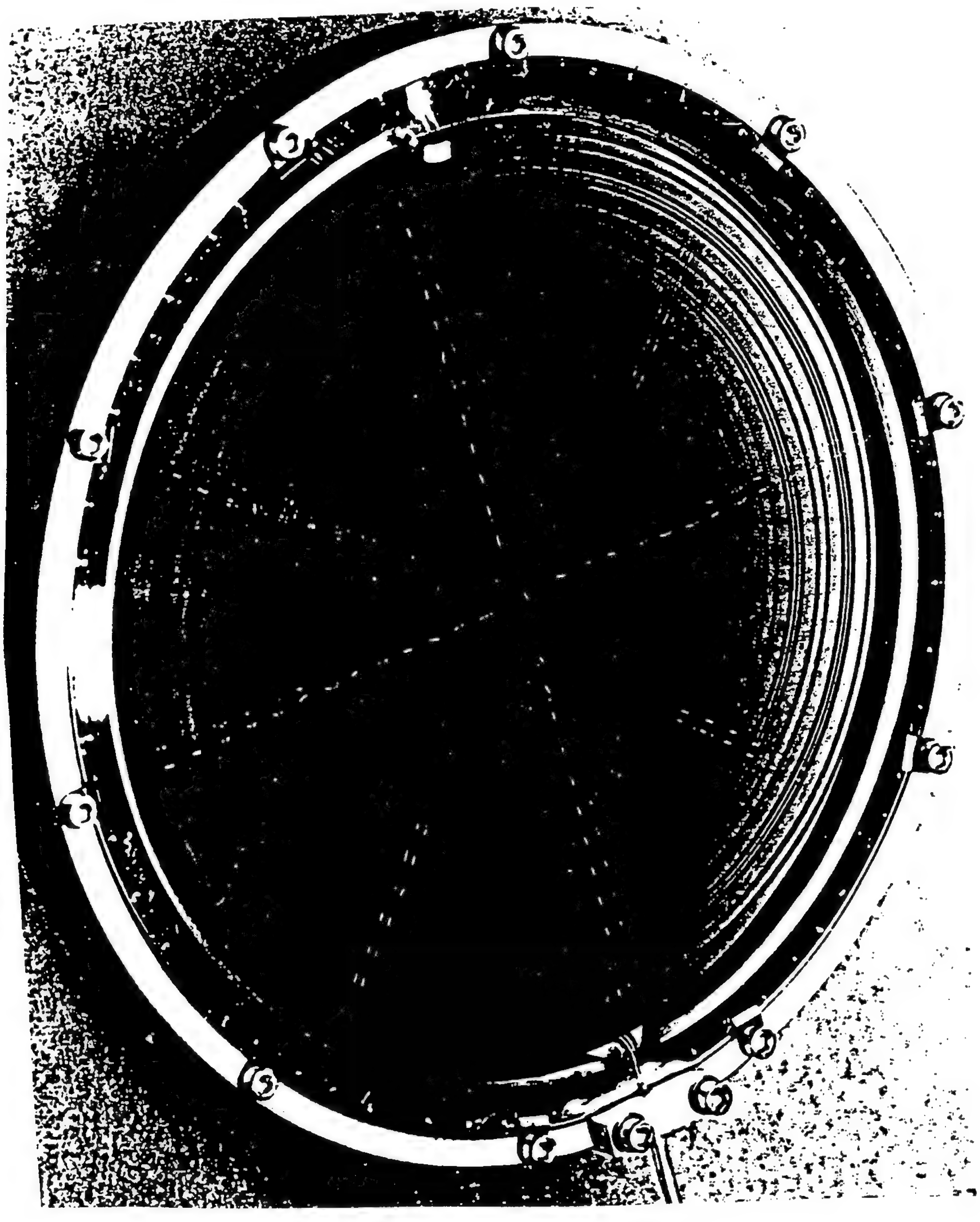

FIGURE D-2. Closeup of CPW HTS Spiral.

Appendix E

HTS SPIRAL TEST DATA

The data in this section illustrates the antenna chamber patterns taken on three spiral assemblies.

The data labeled "GOLD CPW SPIRAL-ROOM TEMP" is for the coplanar integrated balun design with absorber loaded cavity and gold metal on the spiral arms at room temperature.

The data labeled "HTS CPW-FED SPIRAL" is for the coplanar integrated balun design with absorber-loaded cavity and HTS metal on the spiral arms at 77° Kelvin.

The data labeled "AEL SN 1 SPIRAL" is for an Archimedean spiral design built by AEL Corporation in 1994 with absorber-loaded cavity and HTS metal on the spiral arms at 77° Kelvin.

File : GLD–RM9.DAT
Frequency : 0.500 GHz

Date: 25/10/94 16:52
Operator: Mike Neel

GOLD CPW SPIRAL– ROOM TEMP

uniform loaded honeycomb cavity

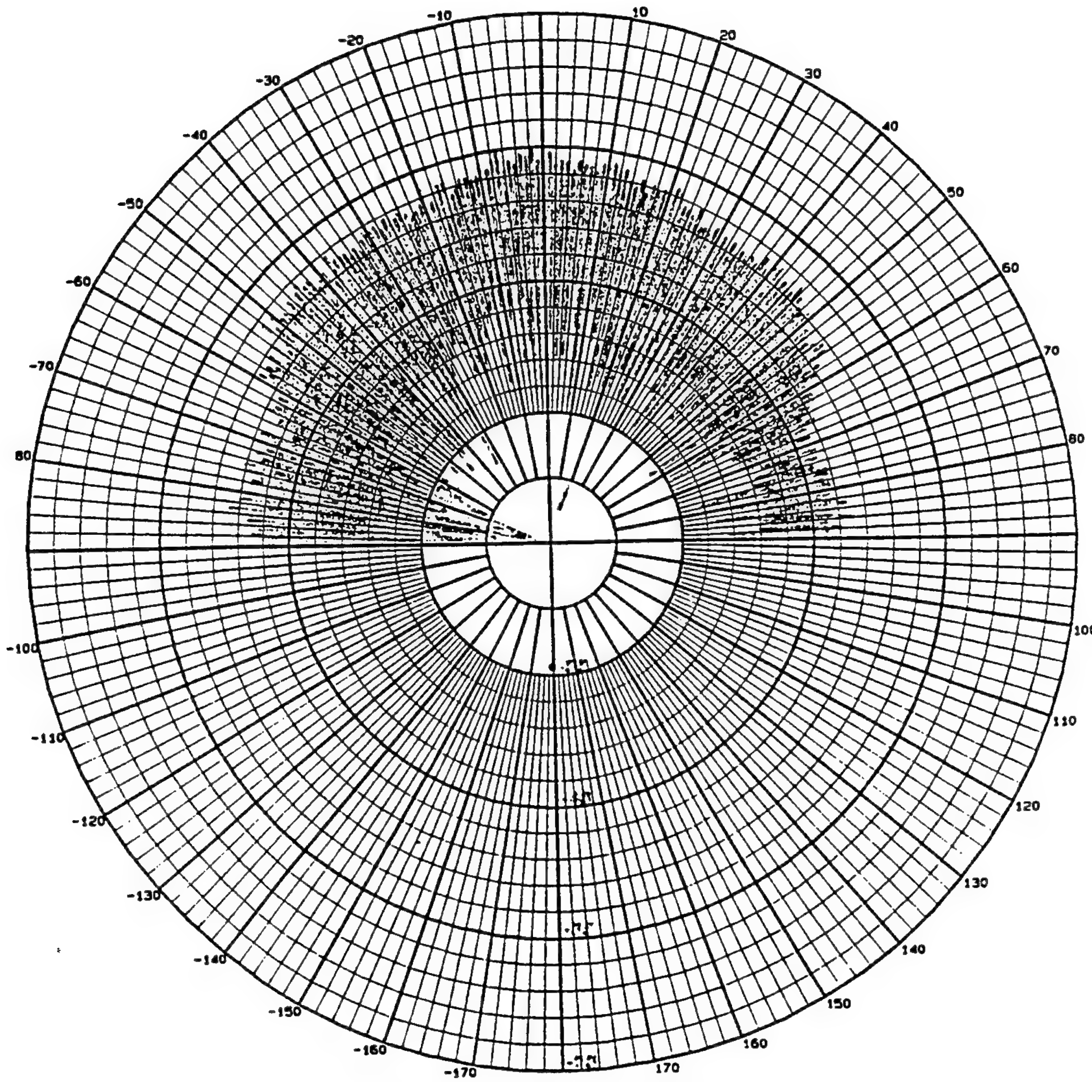

Az Vs. azamp

File : GLD-RM9.DAT
Frequency : 0.600 GHz

Date: 25/10/94 16:52
Operator: Mike Neel

GOLD CPW SPIRAL- ROOM TEMP

uniform loaded honeycomb cavity

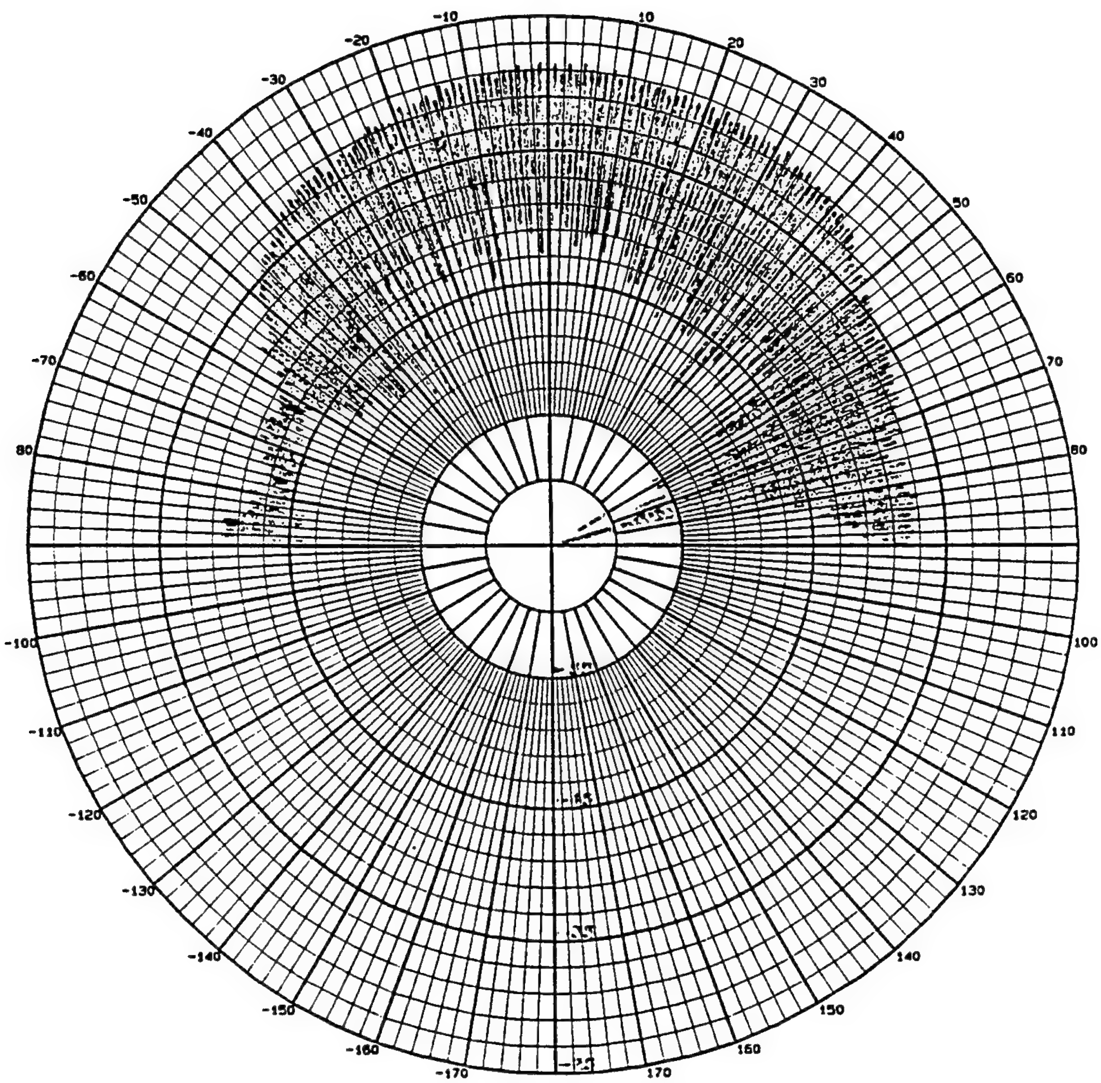

Az Vs. azamp

File : GLD–RM9.DAT
Frequency : 0.700 GHz

Date: 25/10/94 16:52
Operator: Mike Neel

GOLD CPW SPIRAL– ROOM TEM.

uniform loaded honeycomb cavity

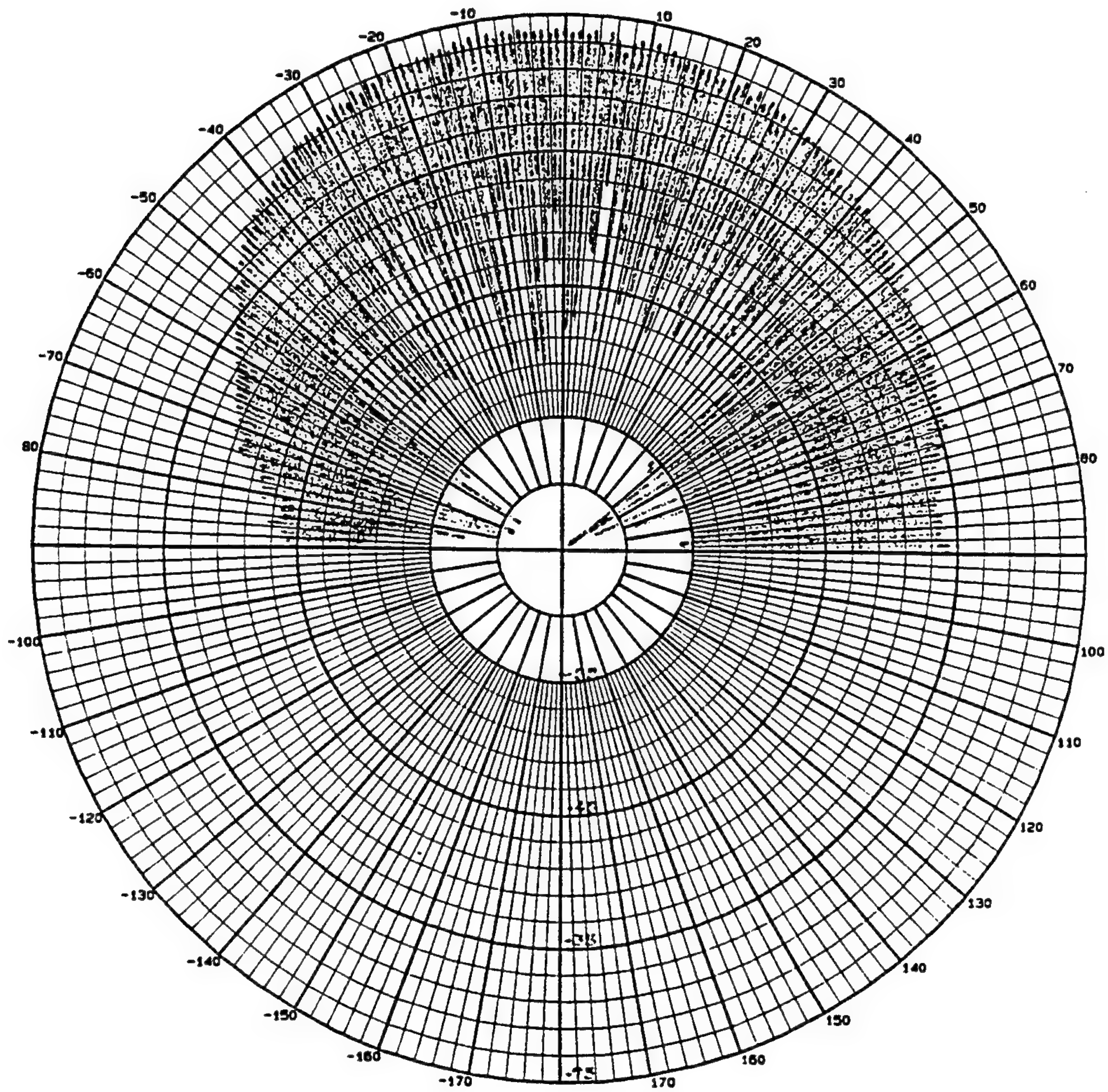

Az Vs. azamp

File : GLD-RM9.DAT
Frequency : 0.800 GHz

Date: 25/10/94 16:52
Operator: Mike Neel

GOLD CPW SPIRAL- ROOM TEMP

uniform loaded honeycomb cavity

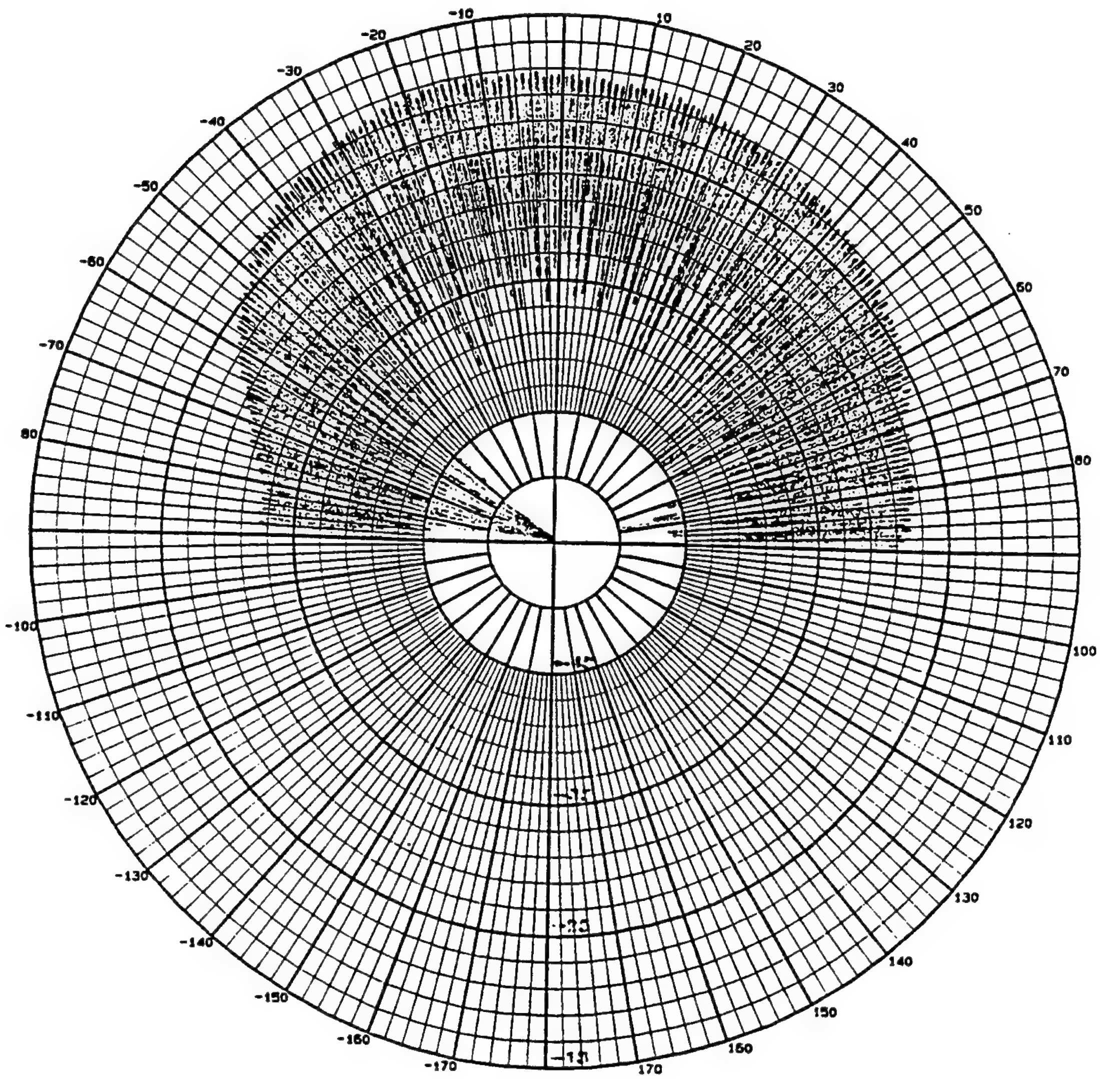

Az Vs. azamp

File : GLD–RM9.DAT
Frequency : 0.900 GHz

Date: 25/10/94 16:52
Operator: Mike Neel

GOLD CPW SPIRAL– ROOM TEMP

uniform loaded honeycomb cavity

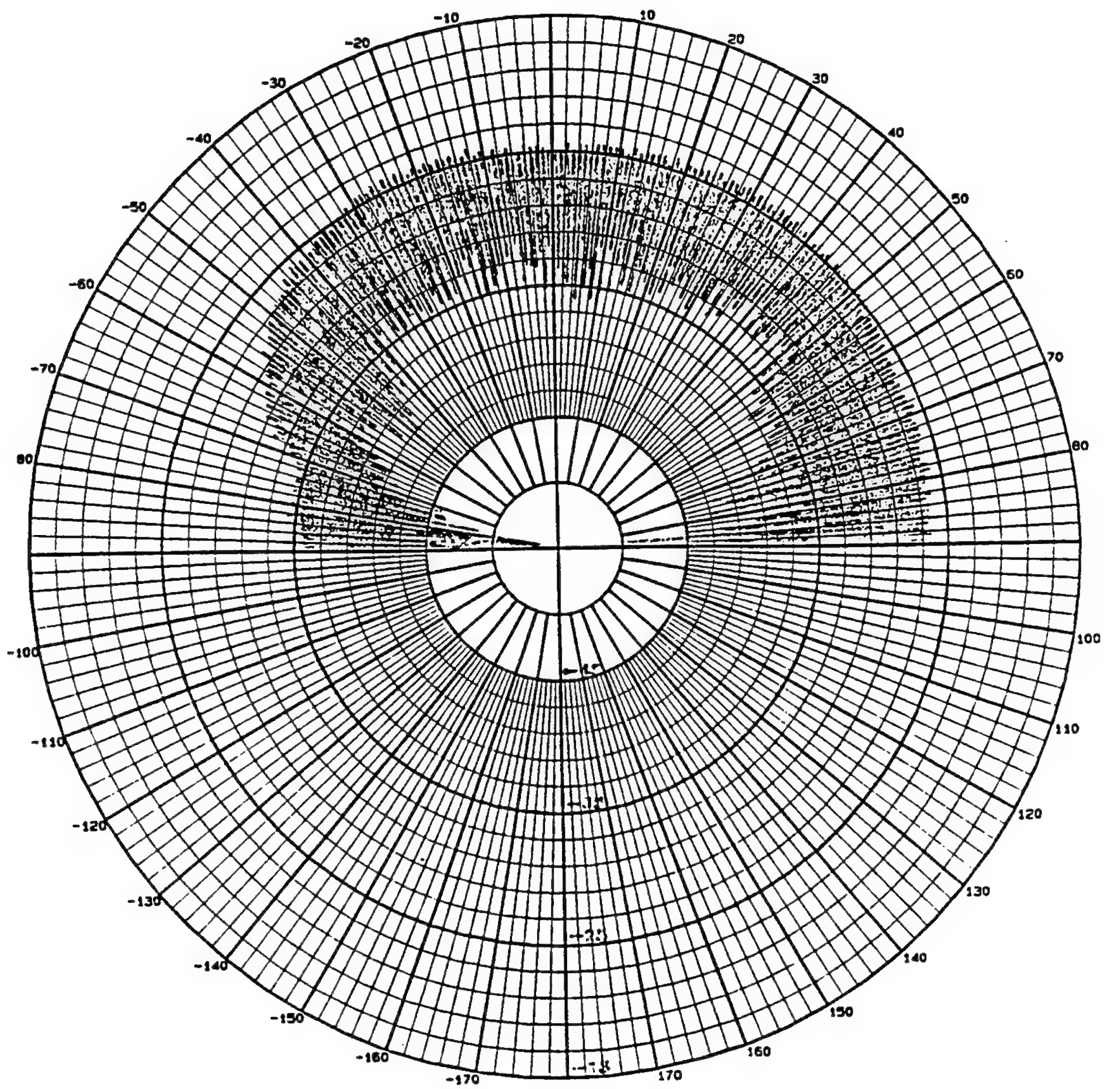

Az Vs. azamp

File : GLD–RM9.DAT
Frequency : 1.000 GHz

Date: 25/10/94 16:52
Operator: Mike Neel

GOLD CPW SPIRAL– ROOM TEMP

uniform loaded honeycomb cavity

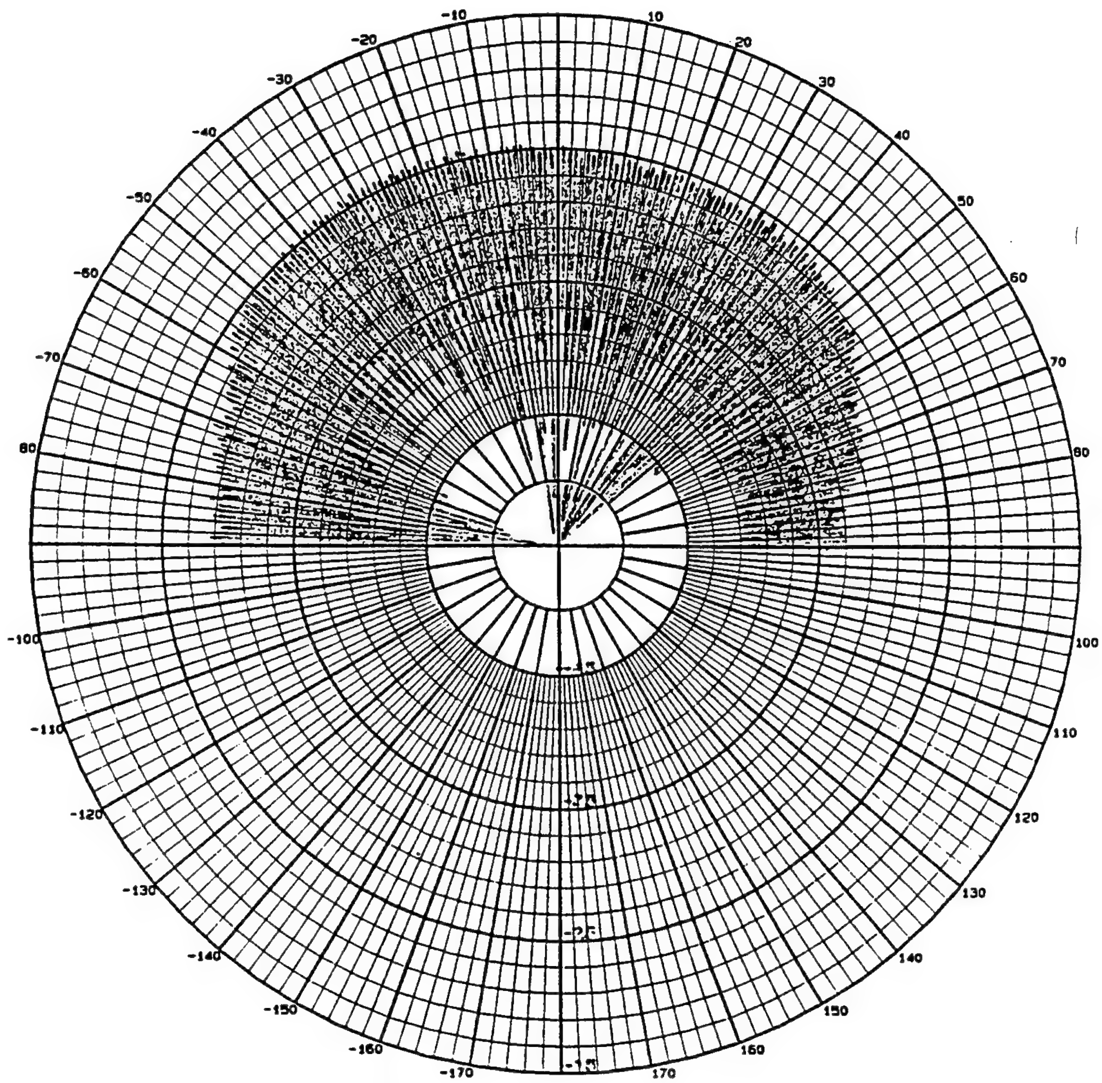

Az Vs. azamp

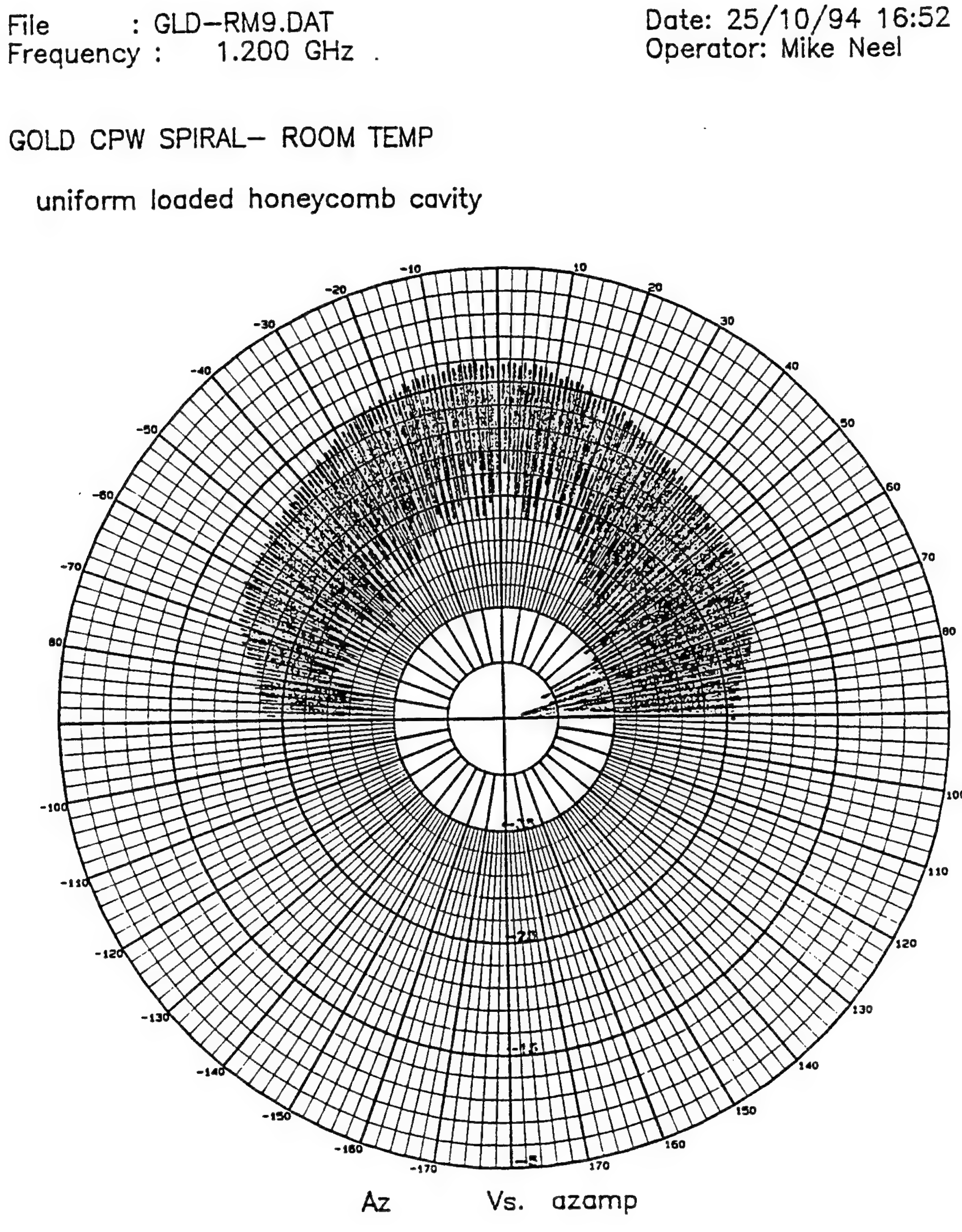
File : GLD–RM9.DAT
Frequency : 1.200 GHz .
Date: 25/10/94 16:52
Operator: Mike Neel
GOLD CPW SPIRAL– ROOM TEMP
uniform loaded honeycomb cavity
-10
10
-20
20
-30
30
-40
40
-50
50
-60
60
-70
70
80
80
-100
100
-110
110
-120
120
-130
130
-140
140
-150
150
-160
160
-170
170
Az Vs. azamp

File : GLD–RM9.DAT
Frequency : 1.400 GHz

Date: 25/10/94 16:52
Operator: Mike Neel

GOLD CPW SPIRAL– ROOM TEMP

uniform loaded honeycomb cavity

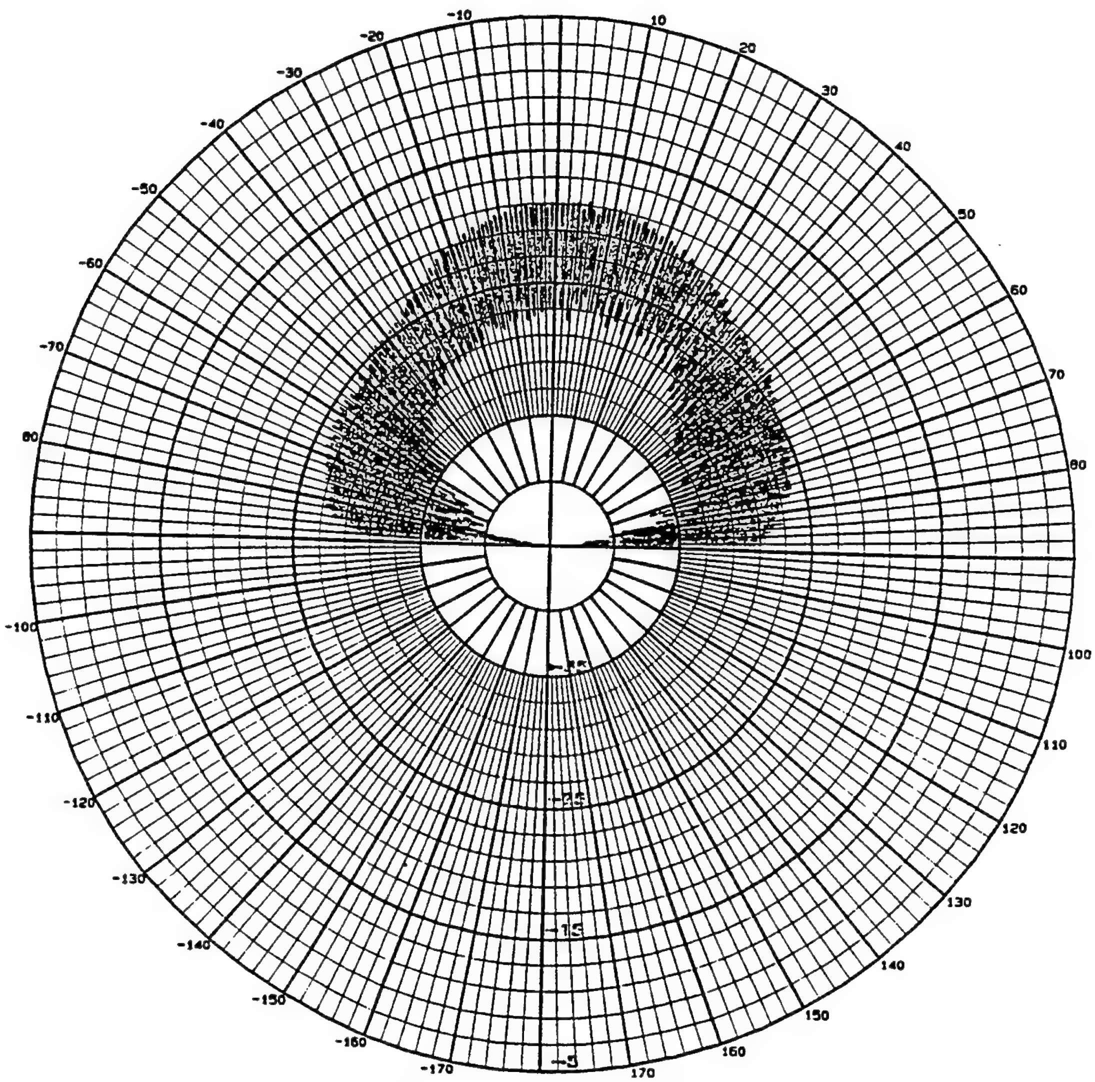

Az Vs. azamp

File : GLD–RM9.DAT
Frequency : 1.600 GHz

Date: 25/10/94 16:52
Operator: Mike Neel

GOLD CPW SPIRAL– ROOM TEMP

uniform loaded honeycomb cavity

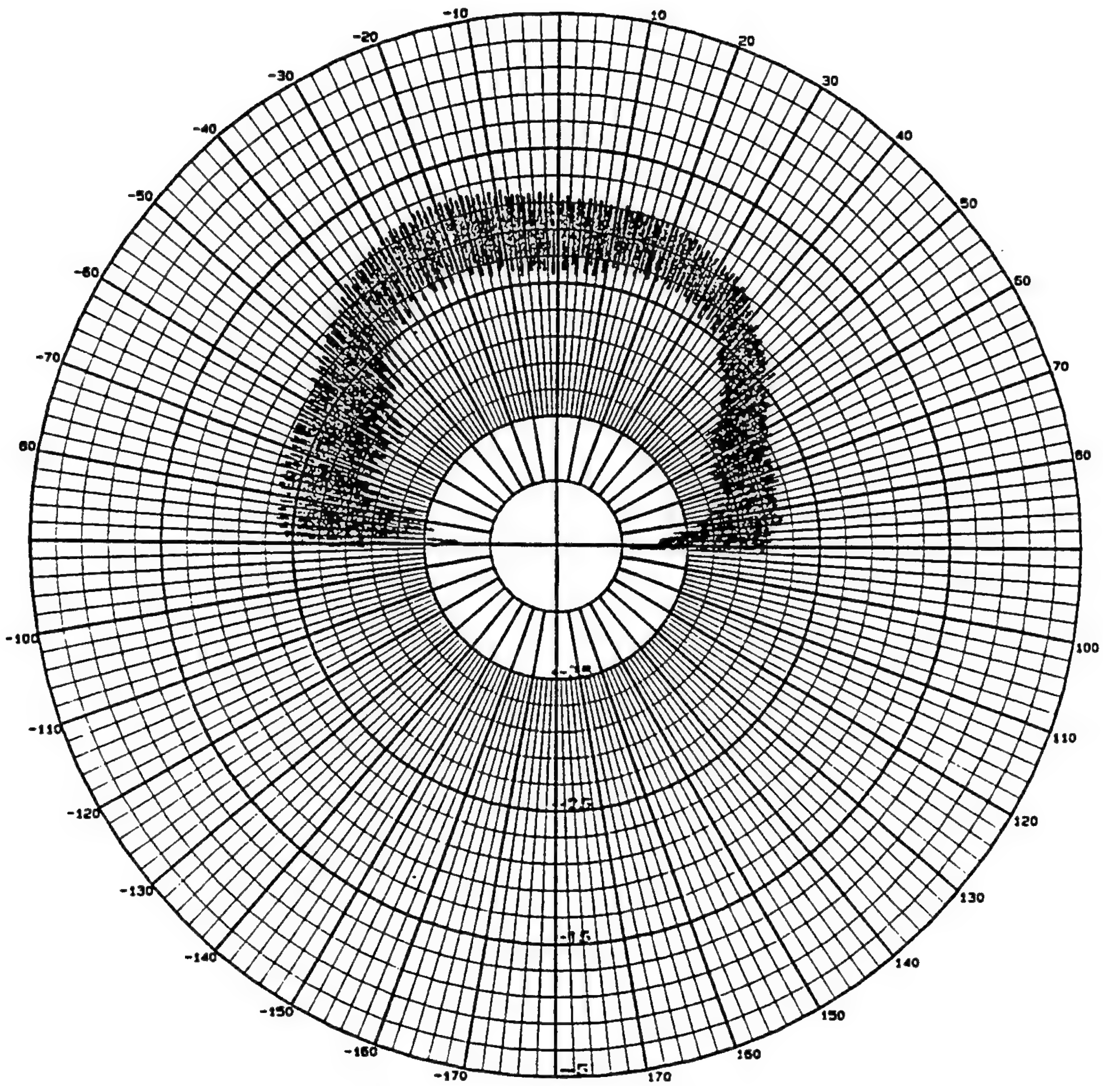

Az Vs. azamp

File : GLD–RM9.DAT
Frequency : 1.800 GHz

Date: 25/10/94 16:52
Operator: Mike Neel

GOLD CPW SPIRAL– ROOM TEMP

uniform loaded honeycomb cavity

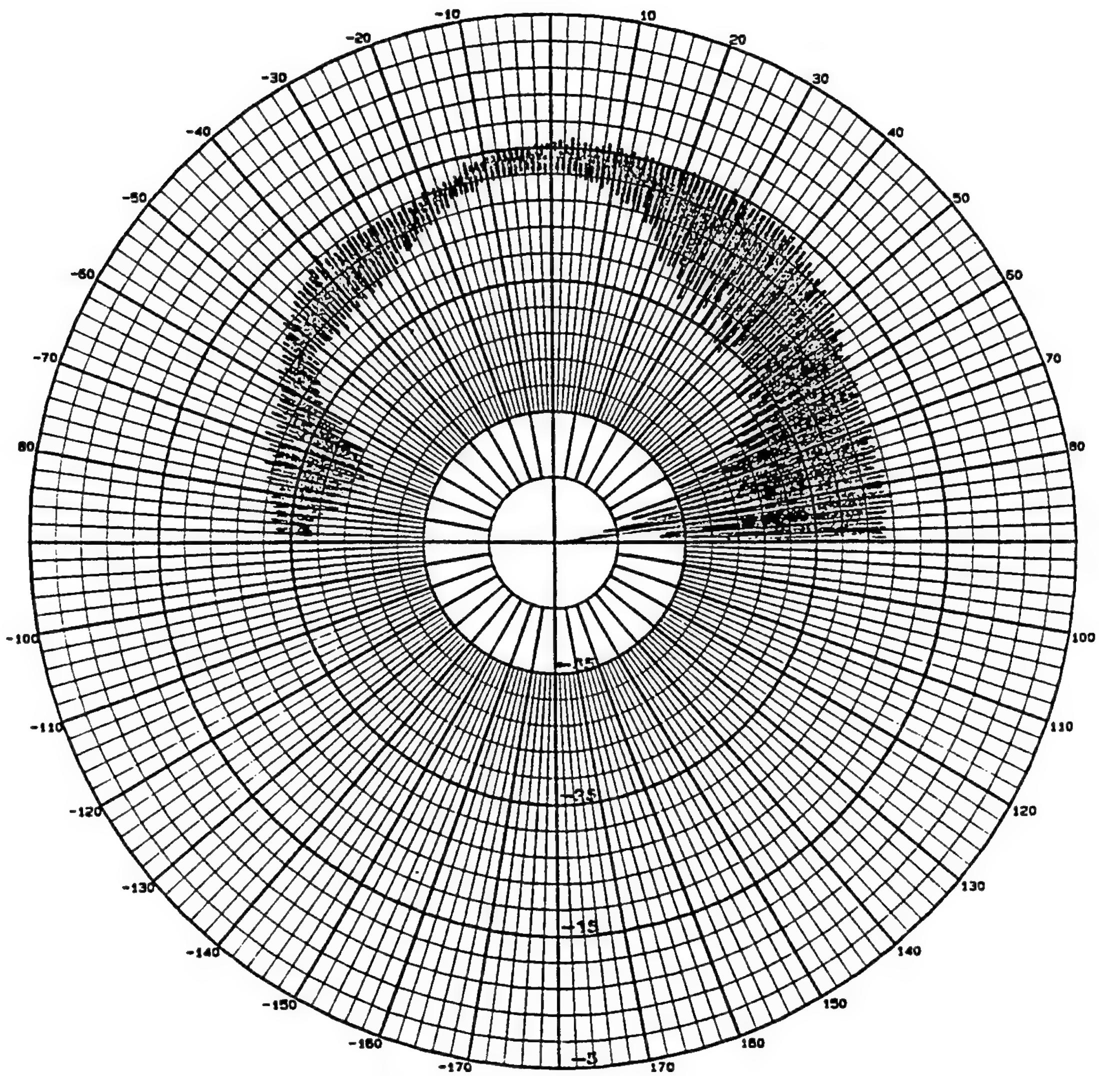

Az Vs. azamp

File : GLD–RM9.DAT
Frequency : 2.000 GHz

Date: 25/10/94 16:52
Operator: Mike Neel

GOLD CPW SPIRAL– ROOM TEMP

uniform loaded honeycomb cavity

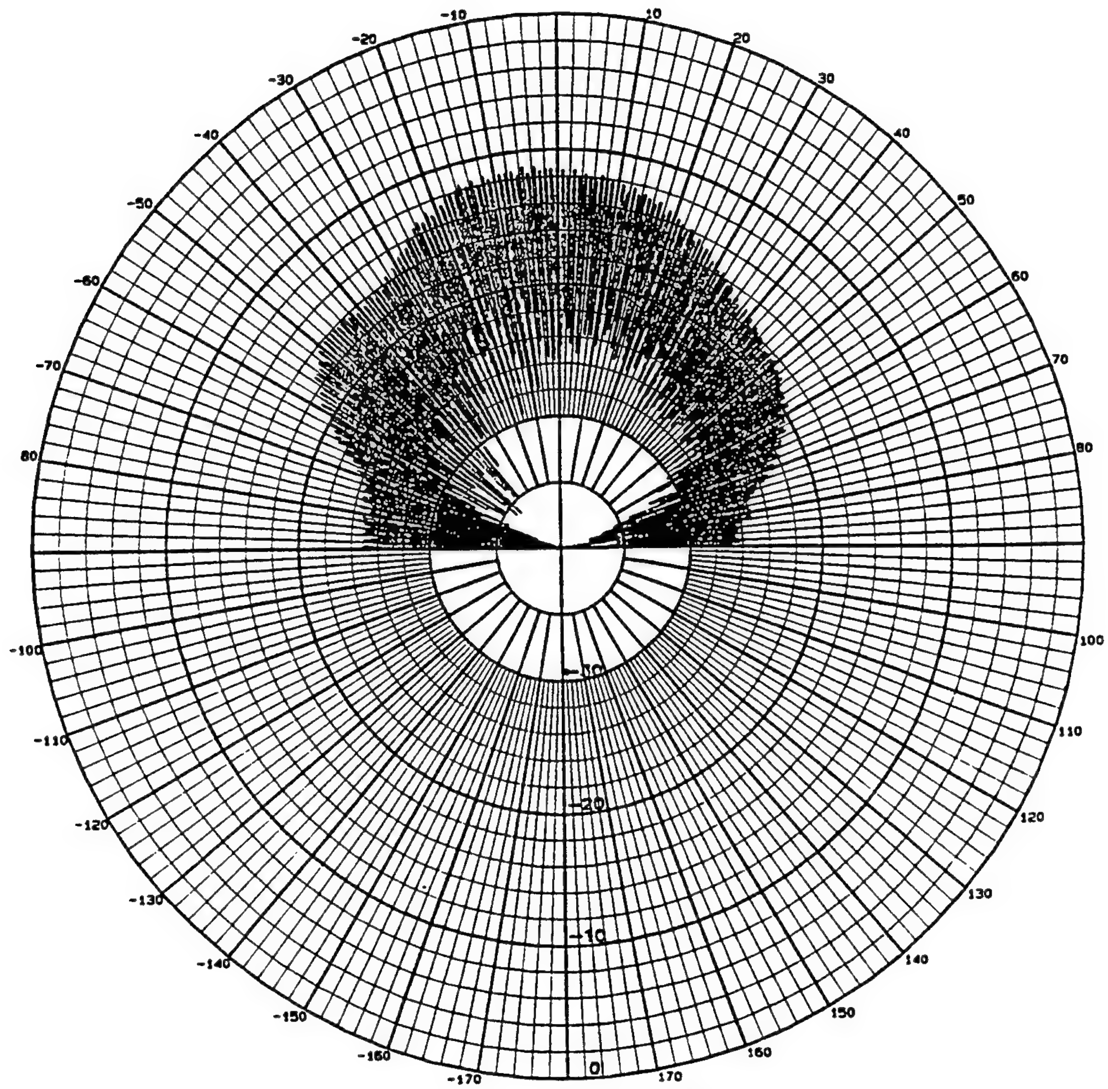

Az Vs. azamp

File : HTS−1.DAT
Frequency : 0.500 GHz

Date: 18/07/95 11:07
Operator: Mike Neel

HTS CPW FED SPIRAL

ABSORBER LOADED CAVITY

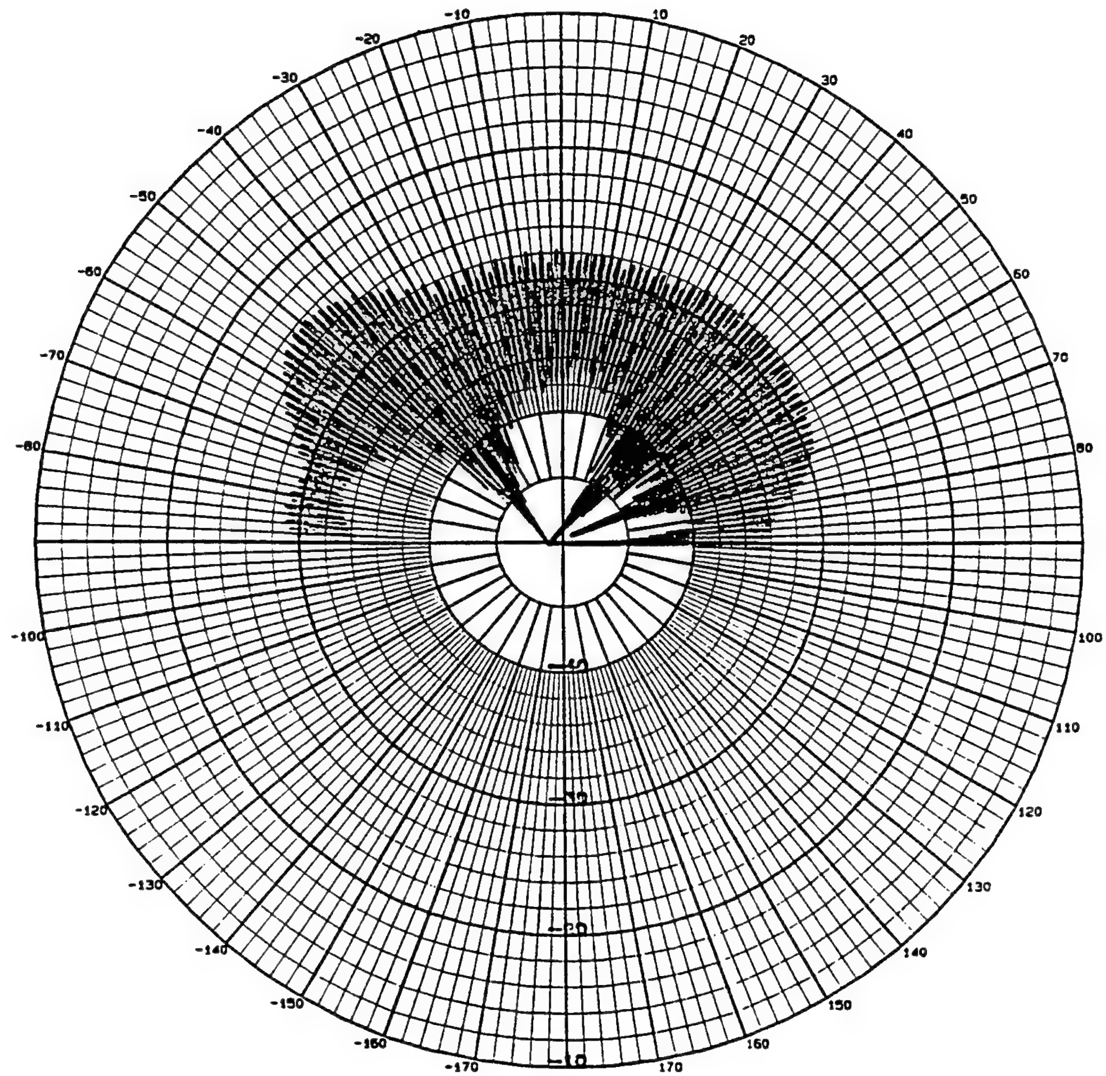

Az Vs. azamp

File : HTS−1.DAT
Frequency : 0.600 GHz

Date: 18/07/95 11:07
Operator: Mike Neel

HTS CPW FED SPIRAL

ABSORBER LOADED CAVITY

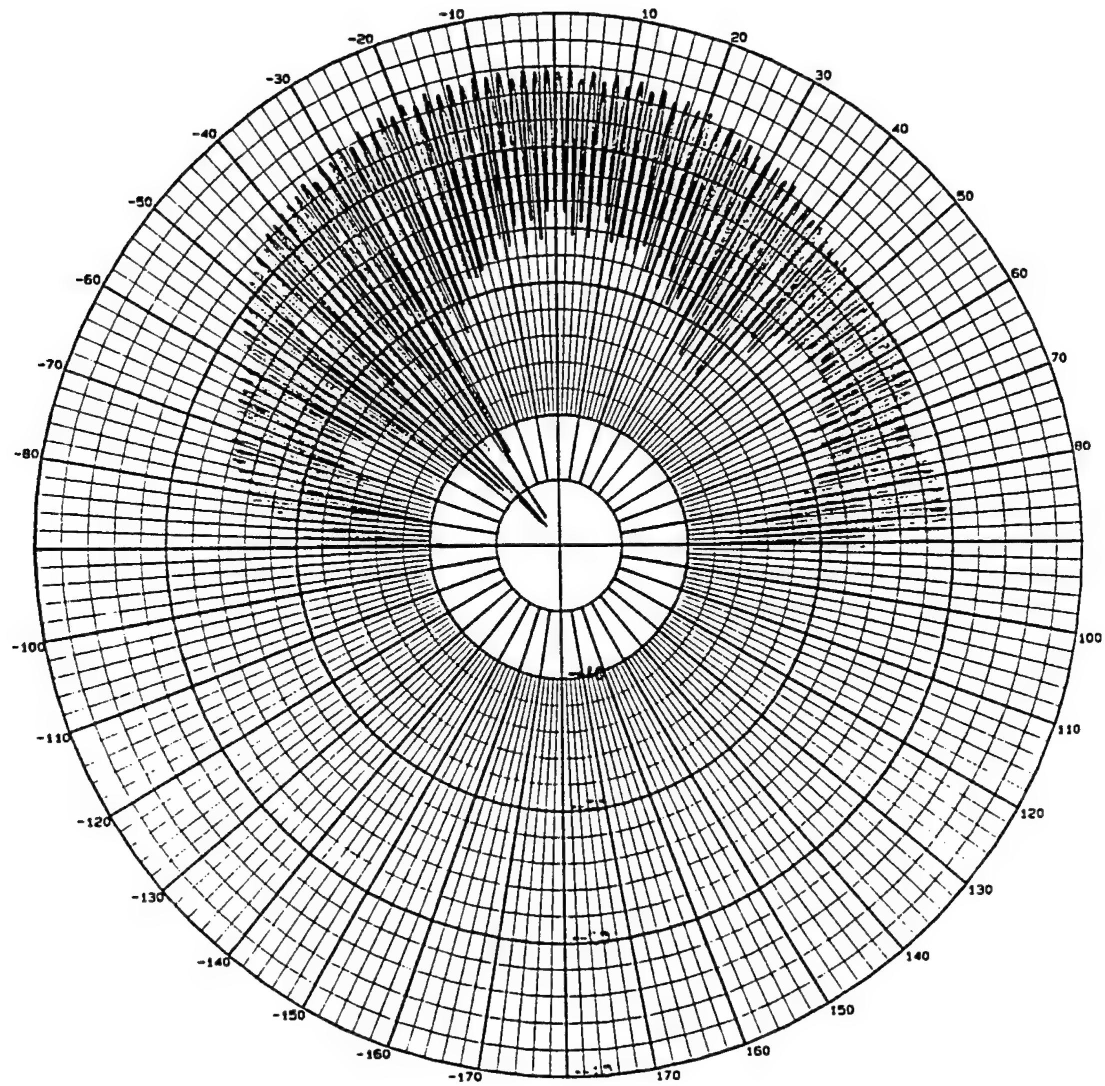

Az Vs. azamp

File : HTS−1.DAT
Frequency : 0.700 GHz

Date: 18/07/95 11:07
Operator: Mike Neel

HTS CPW FED SPIRAL

ABSORBER LOADED CAVITY

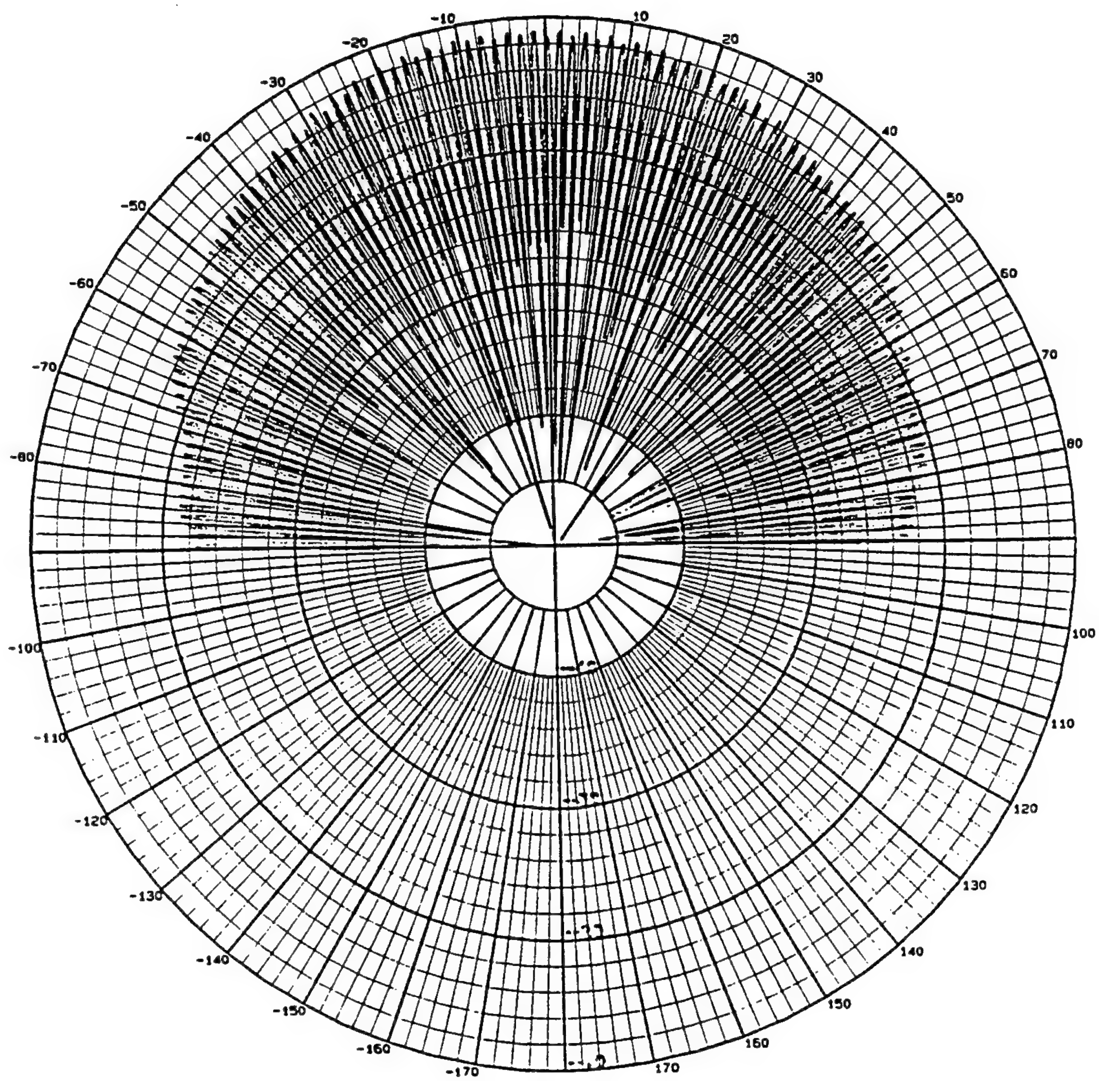

Az Vs. azamp

File : HTS−1.DAT
Frequency : 0.800 GHz

Date: 18/07/95 11:07
Operator: Mike Neel

HTS CPW FED SPIRAL

ABSORBER LOADED CAVITY

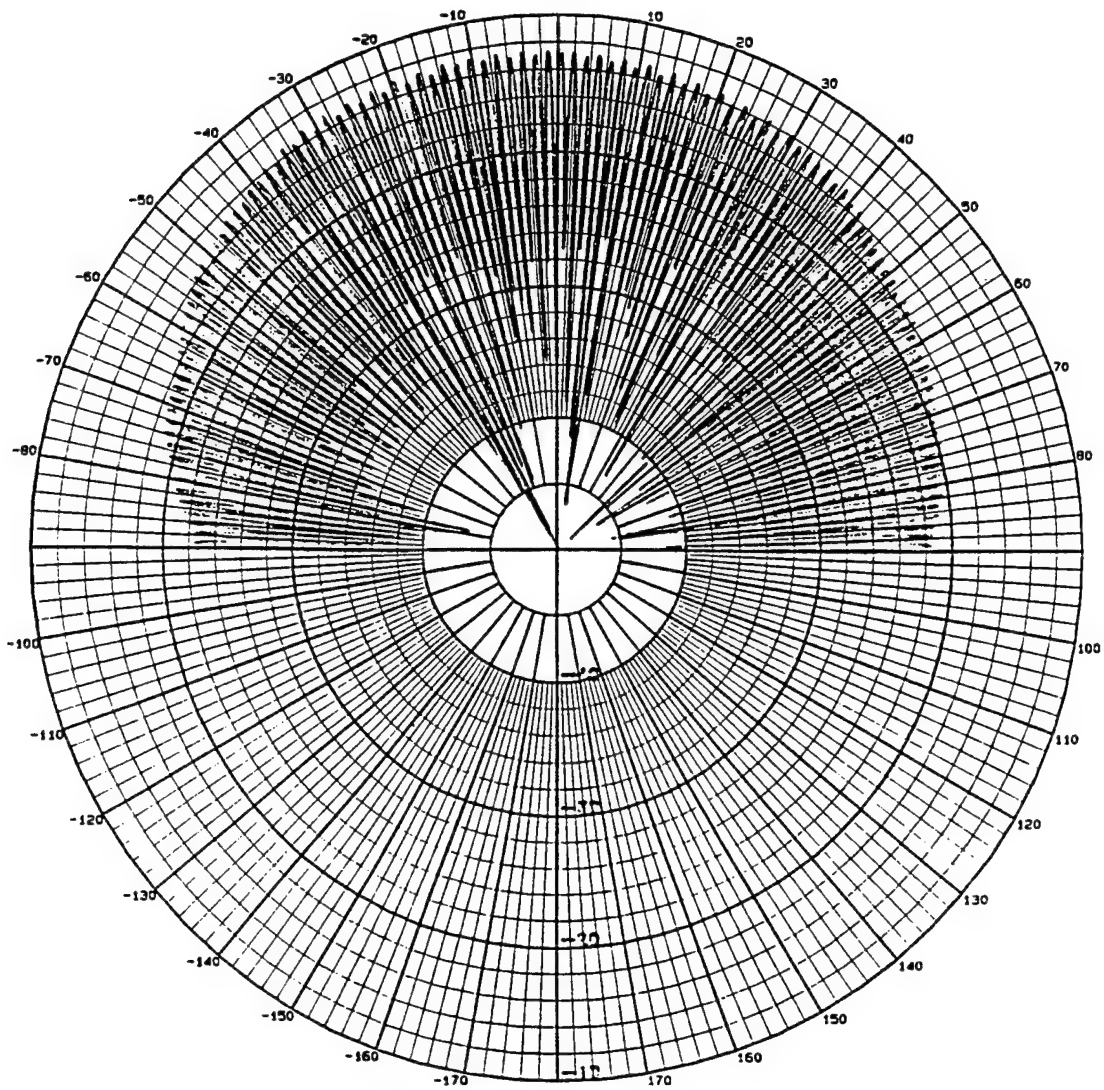

Az Vs. azamp

File : HTS−1.DAT
Frequency : 0.900 GHz

Date: 18/07/95 11:07
Operator: Mike Neel

HTS CPW FED SPIRAL

ABSORBER LOADED CAVITY

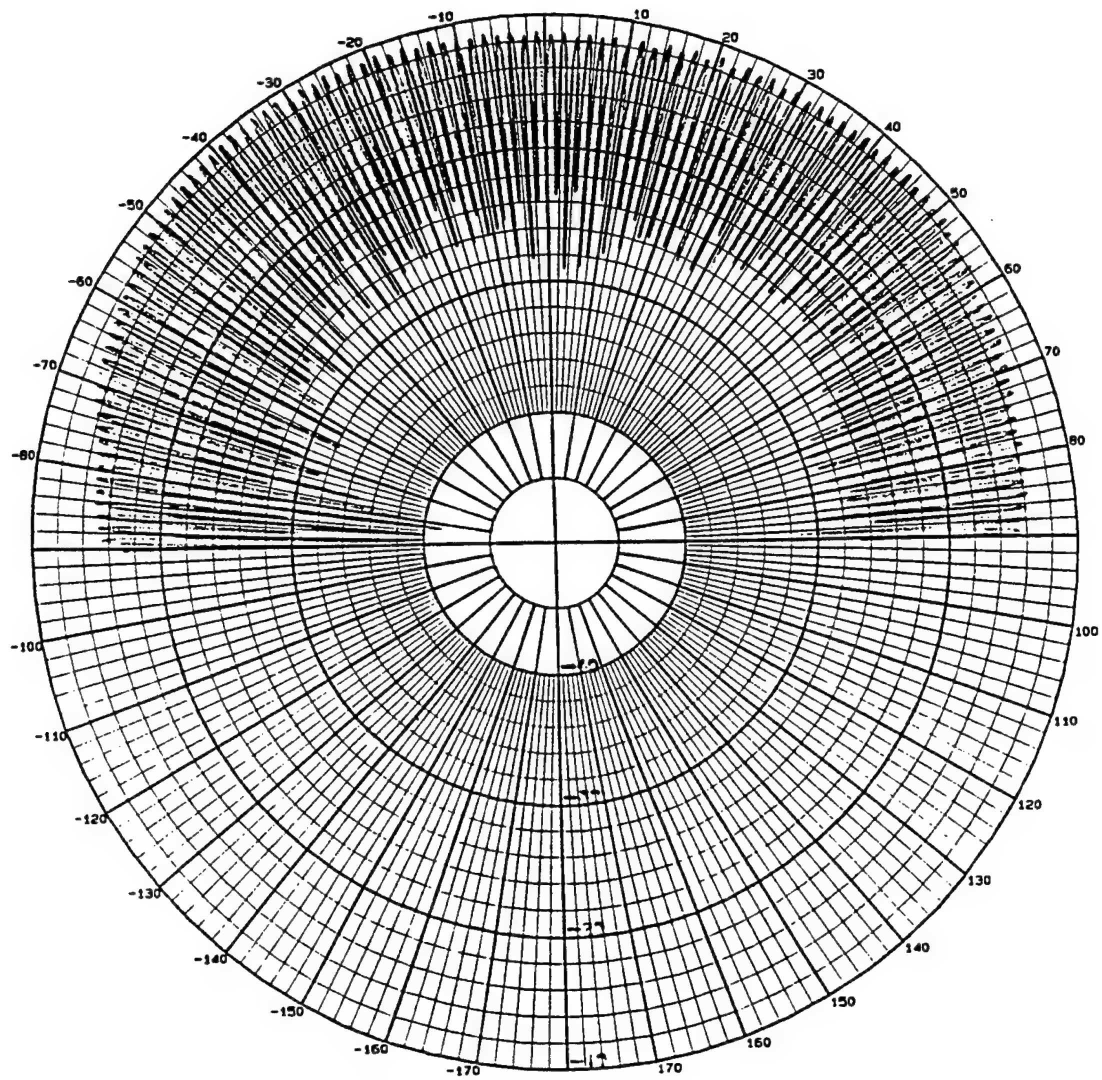

Az Vs. azamp

File : HTS−1.DAT
Frequency : 1.000 GHz

Date: 18/07/95 11:07
Operator: Mike Neel

HTS CPW FED SPIRAL

ABSORBER LOADED CAVITY

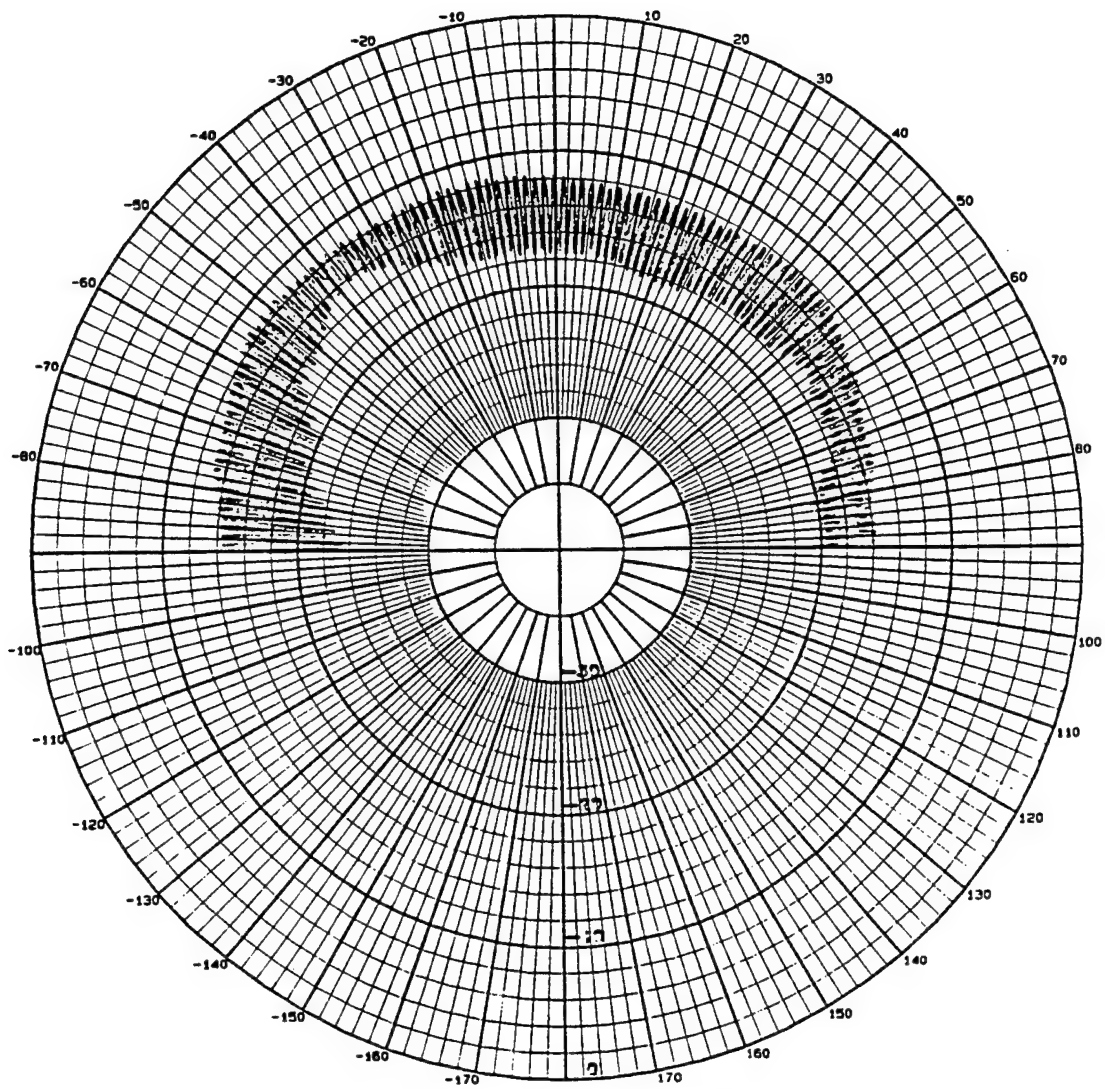

Az Vs. azamp

File : HTS−1.DAT
Frequency : 1.200 GHz

Date: 18/07/95 11:07
Operator: Mike Neel

HTS CPW FED SPIRAL

ABSORBER LOADED CAVITY

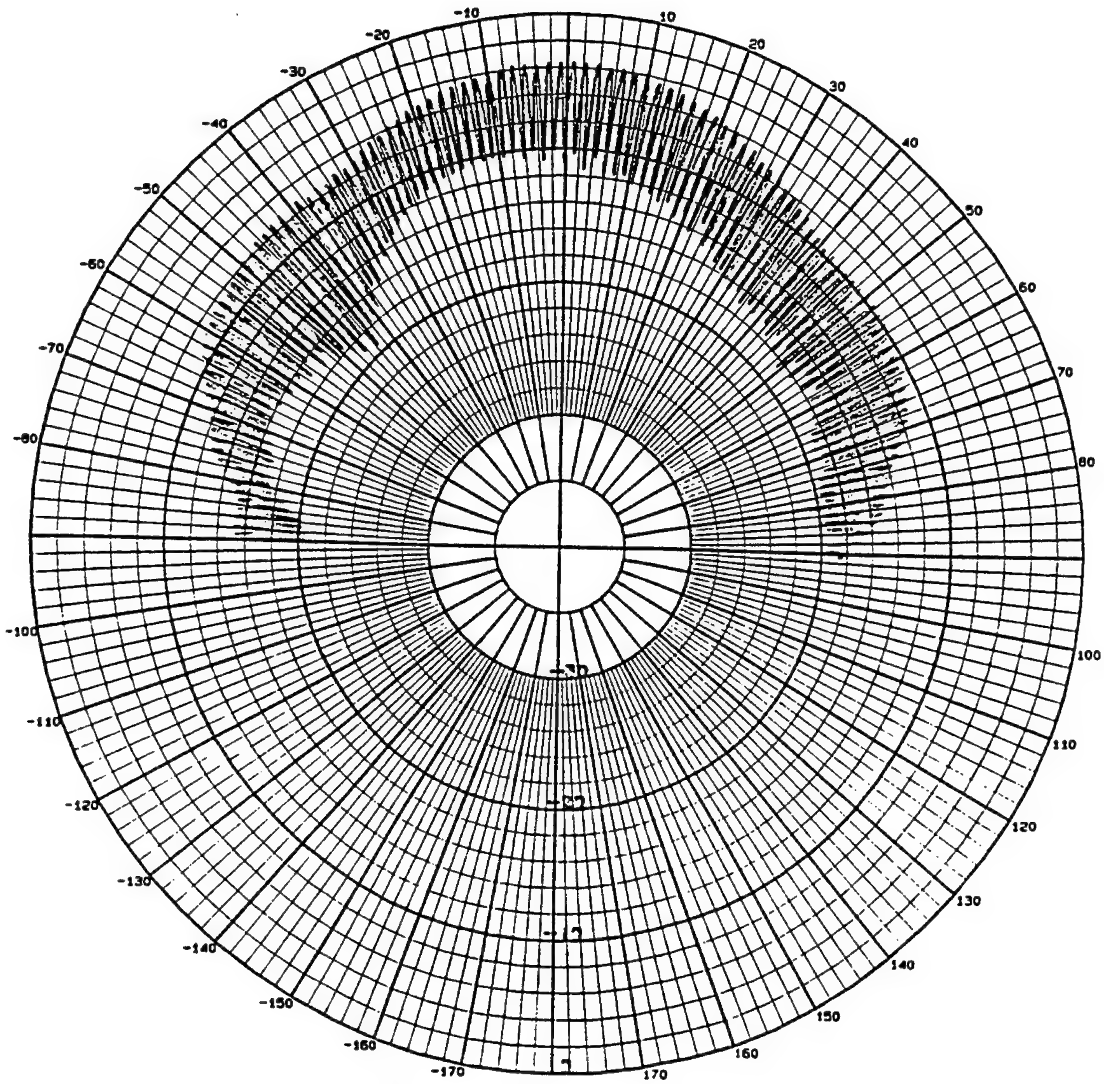

Az Vs. azamp

File : HTS–1.DAT
Frequency : 1.400 GHz

Date: 18/07/95 11:07
Operator: Mike Neel

HTS CPW FED SPIRAL

ABSORBER LOADED CAVITY

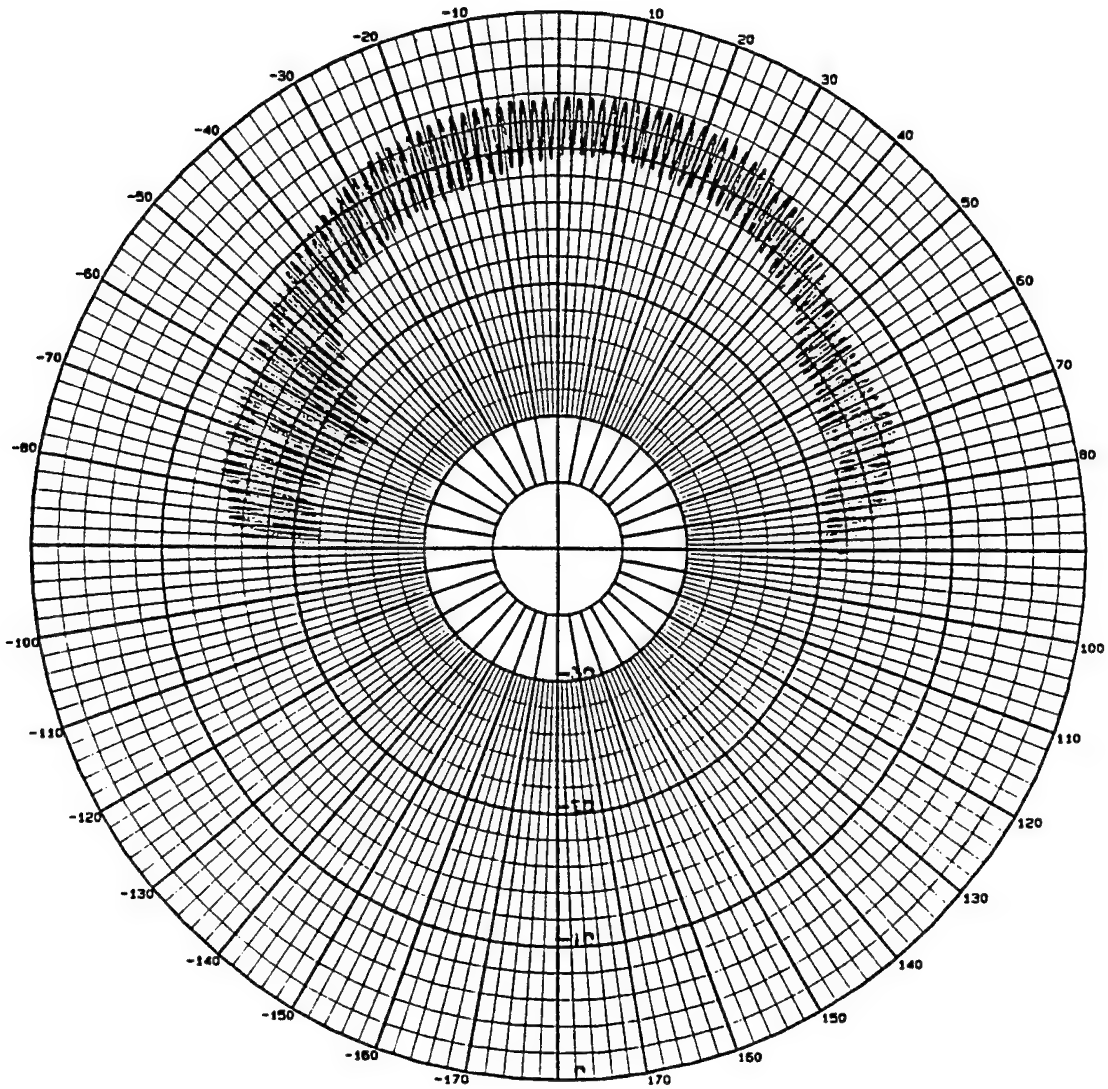

Az Vs. azamp

File : HTS−1.DAT
Frequency : 1.600 GHz

Date: 18/07/95 11:07
Operator: Mike Neel

HTS CPW FED SPIRAL

ABSORBER LOADED CAVITY

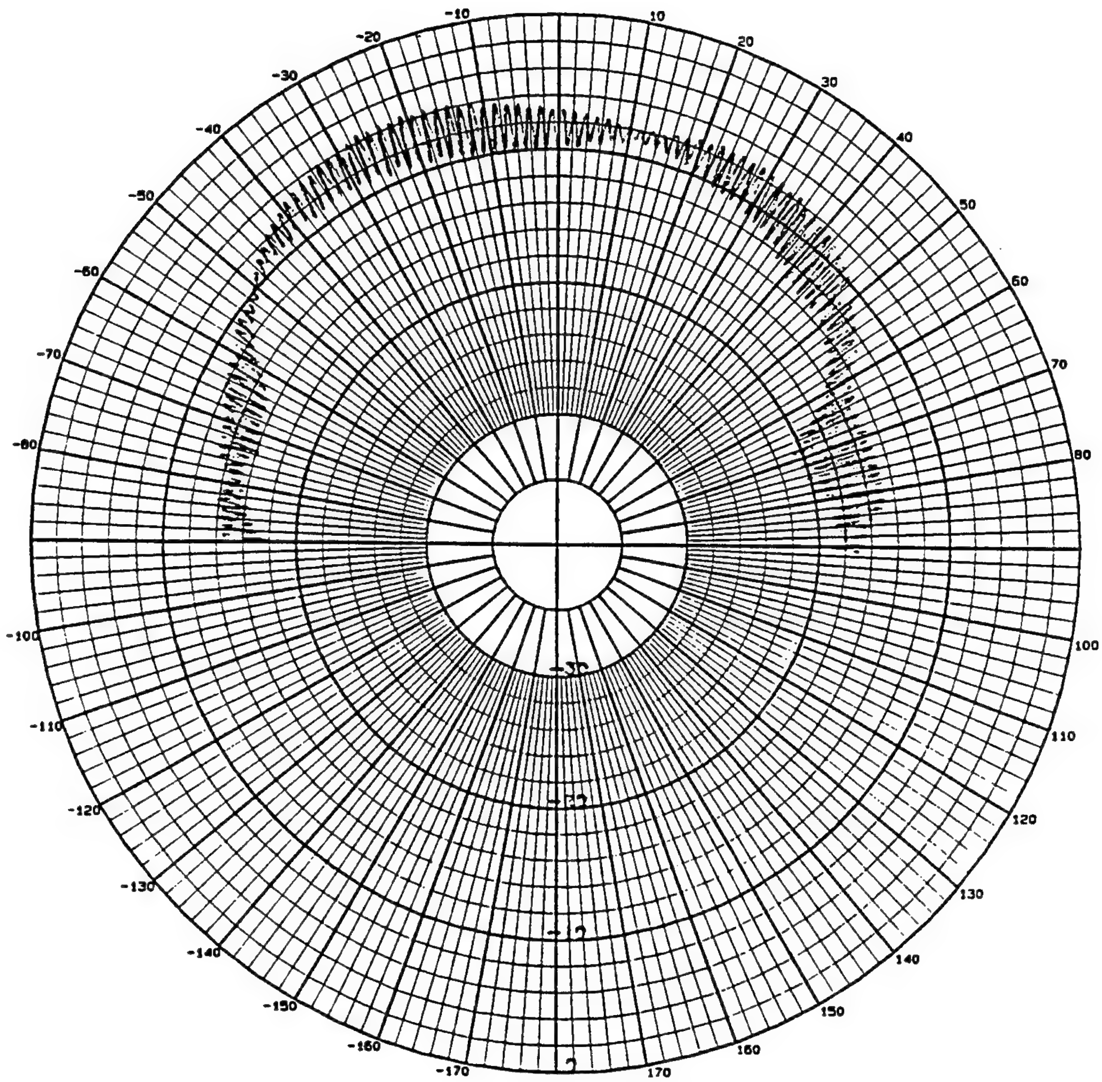

Az Vs. azamp

File : HTS−1.DAT
Frequency : 1.800 GHz

Date: 18/07/95 11:07
Operator: Mike Neel

HTS CPW FED SPIRAL

ABSORBER LOADED CAVITY

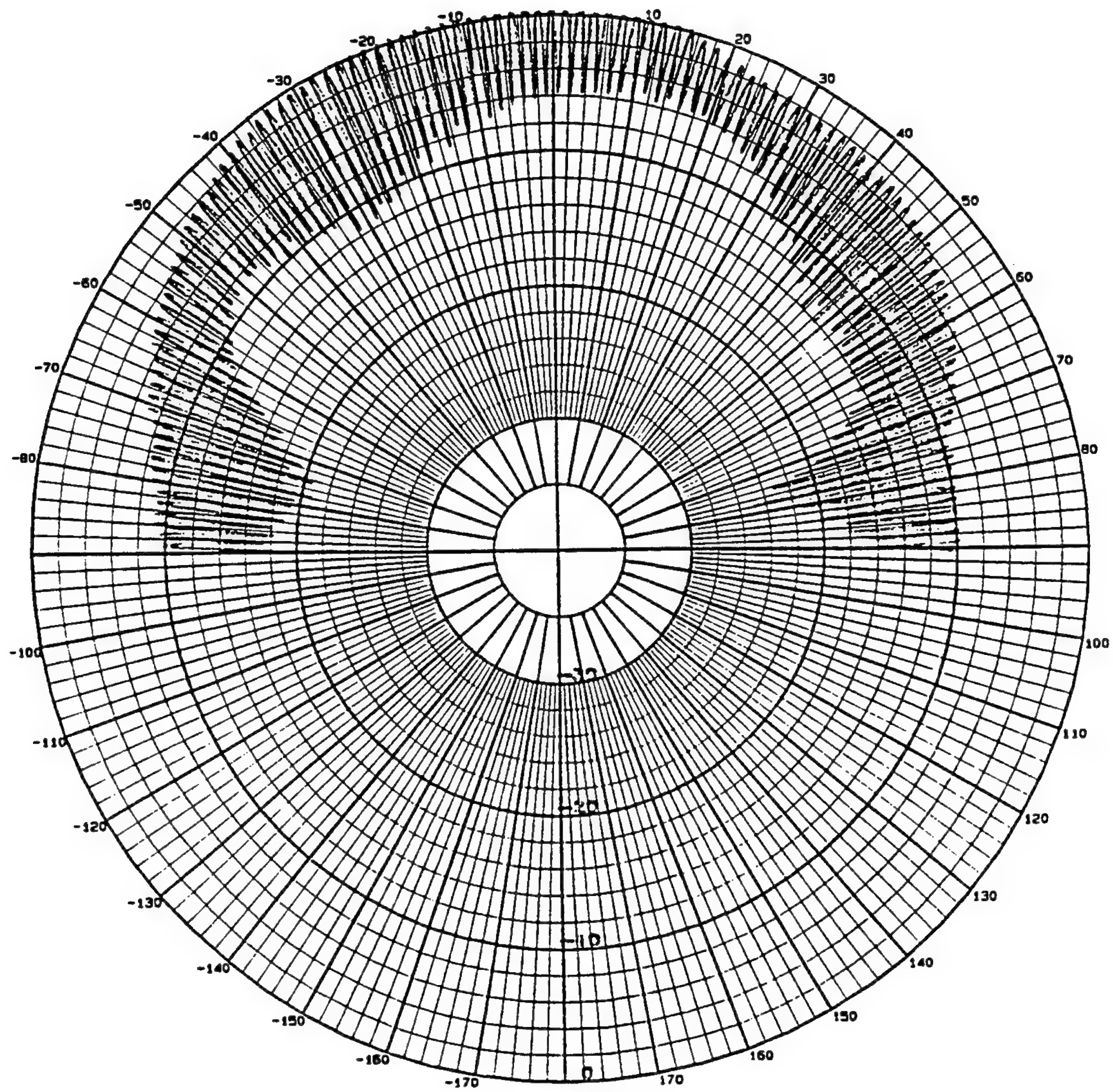

Az Vs. azamp

File : HTS−1.DAT
Frequency : 2.000 GHz

Date: 18/07/95 11:07
Operator: Mike Neel

HTS CPW FED SPIRAL

ABSORBER LOADED CAVITY

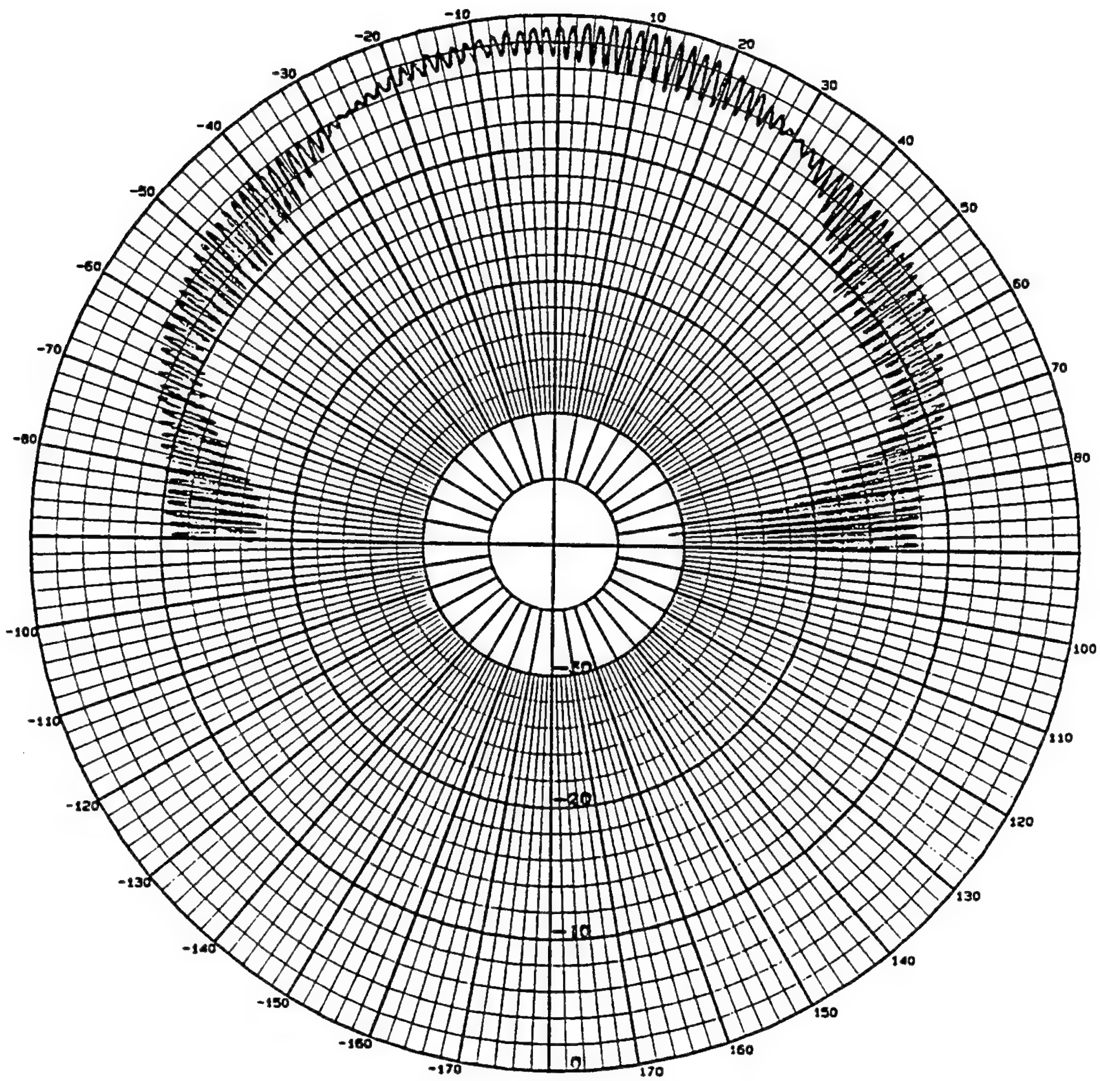

Az Vs. azamp

File : AEL–1.DAT
Frequency : 0.500 GHz

Date: 18/07/95 11:47
Operator: Mike Neel

AEL SN 1 SPIRAL

ABSORBER LOADED CAVITY

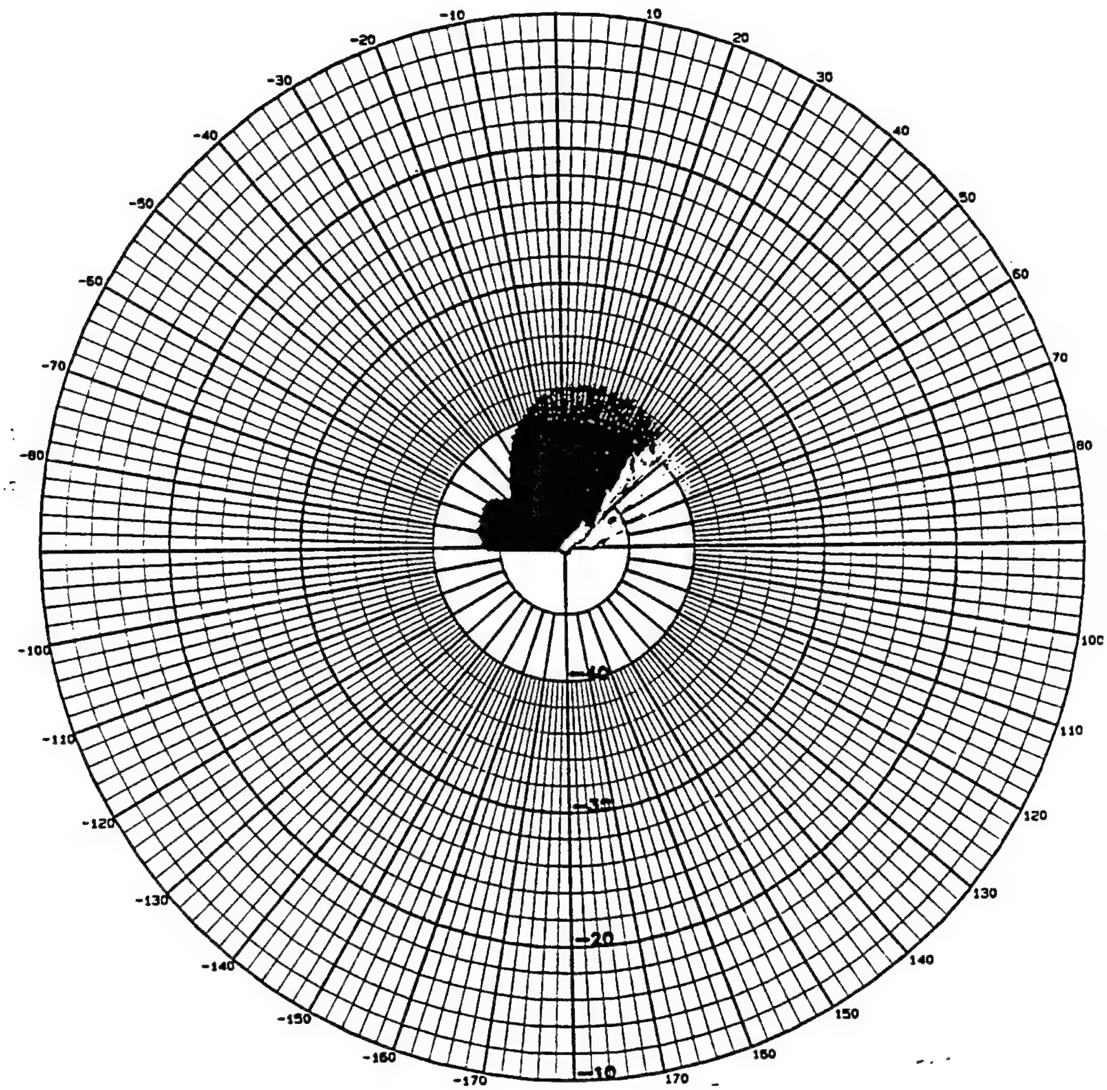

Az Vs. azamp

File : AEL−1.DAT
Frequency : 0.600 GHz

Date: 18/07/95 11:47
Operator: Mike Neel

AEL SN 1 SPIRAL

ABSORBER LOADED CAVITY

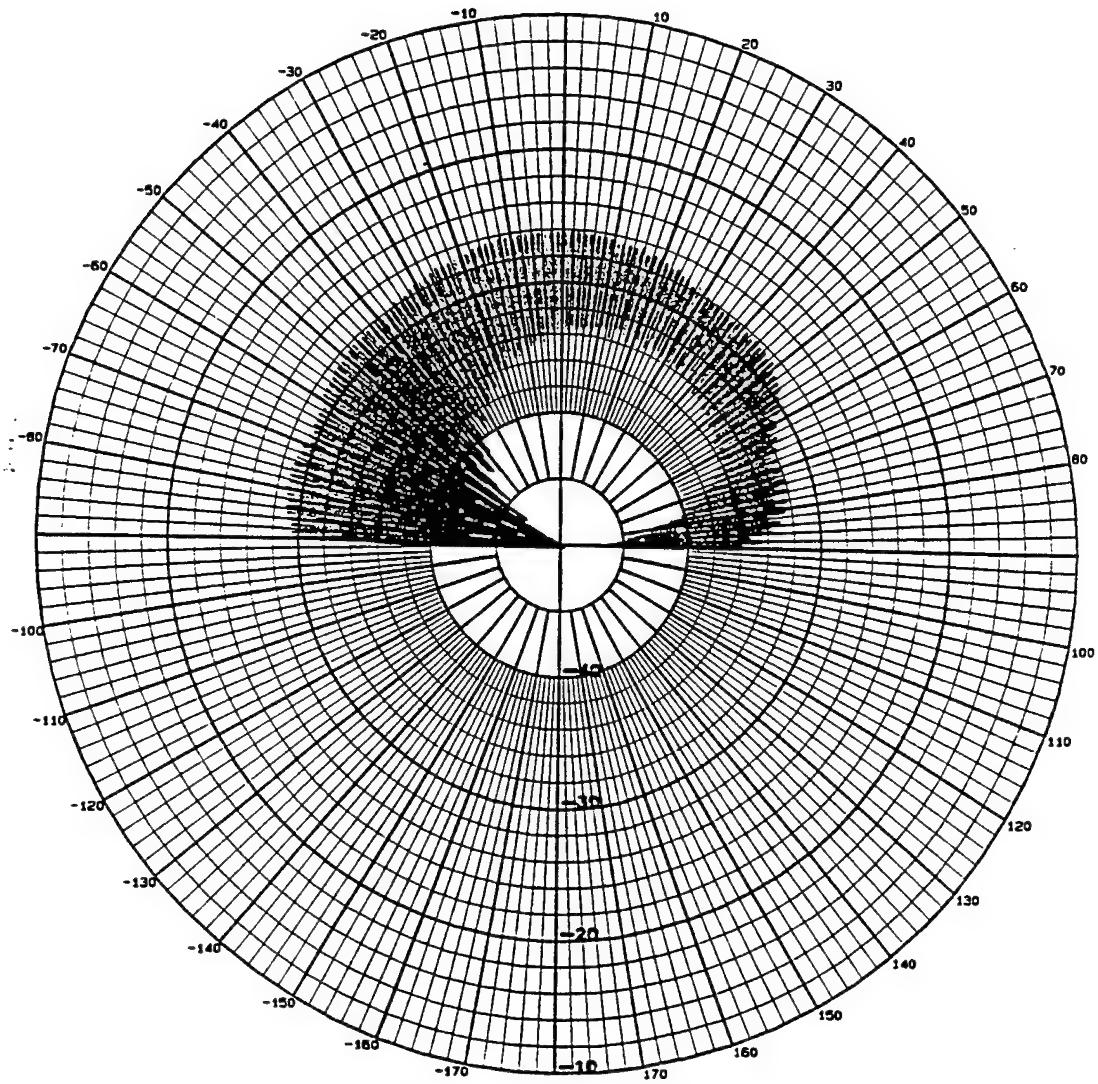

Az Vs. azamp

File : AEL-1.DAT
Frequency : 0.700 GHz

Date: 18/07/95 11:47
Operator: Mike Neel

AEL SN 1 SPIRAL

ABSORBER LOADED CAVITY

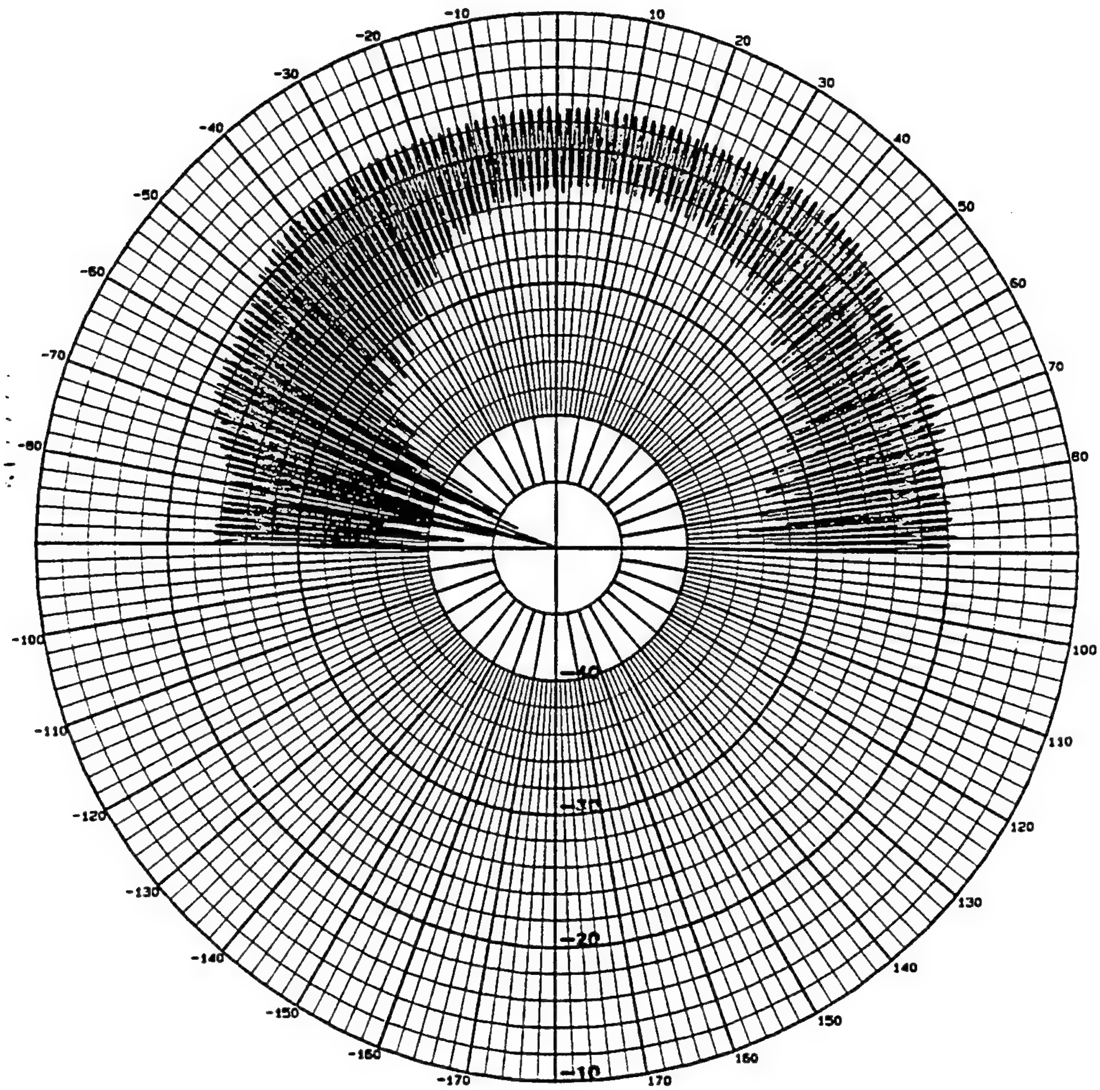

Az Vs. azamp

File : AEL-1.DAT
Frequency : 0.800 GHz

Date: 18/07/95 11:47
Operator: Mike Neel

AEL SN 1 SPIRAL

ABSORBER LOADED CAVITY

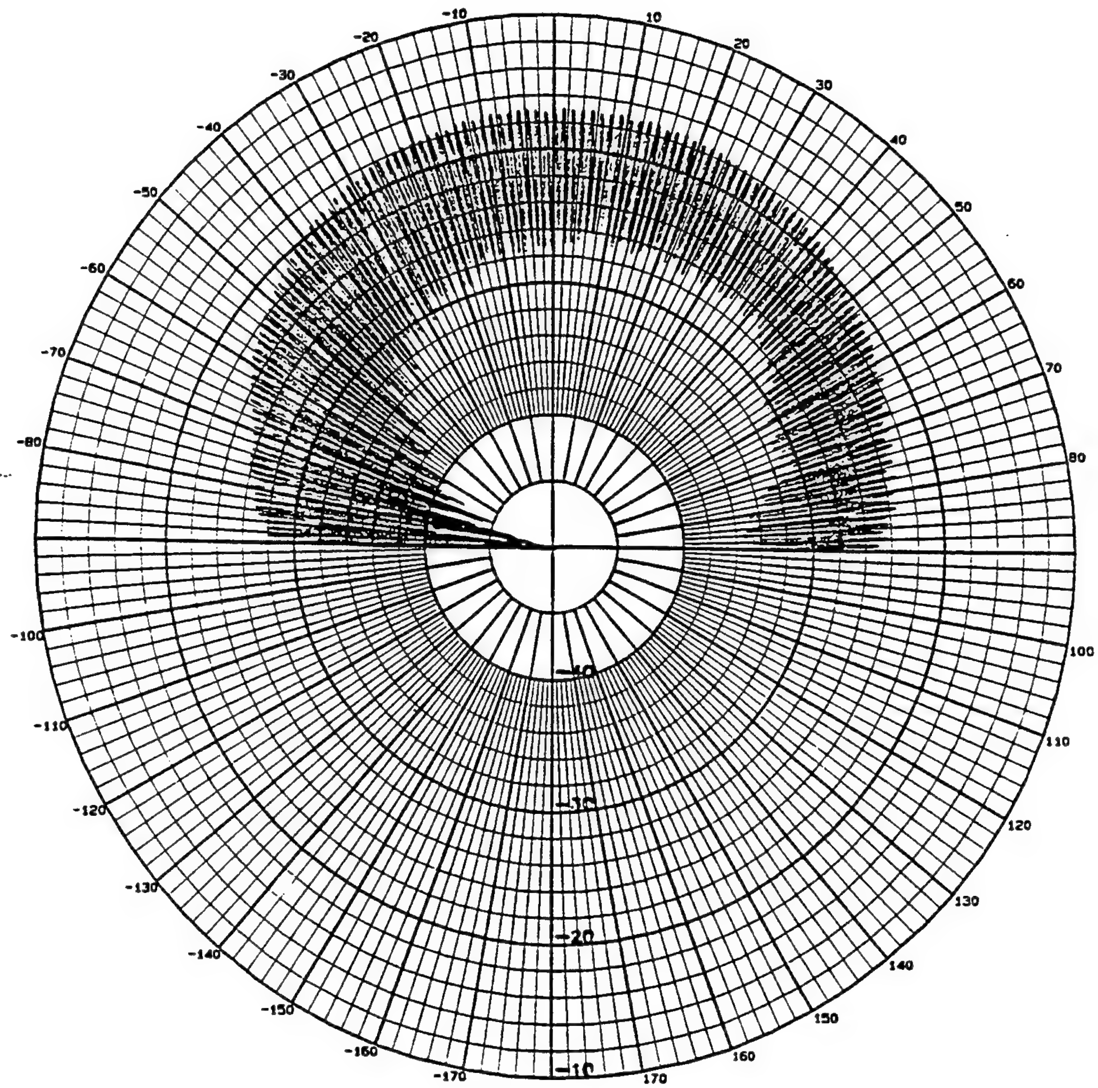

Az Vs. azamp

File : AEL−1.DAT
Frequency : 0.900 GHz

Date: 18/07/95 11:47
Operator: Mike Neel

AEL SN 1 SPIRAL

ABSORBER LOADED CAVITY

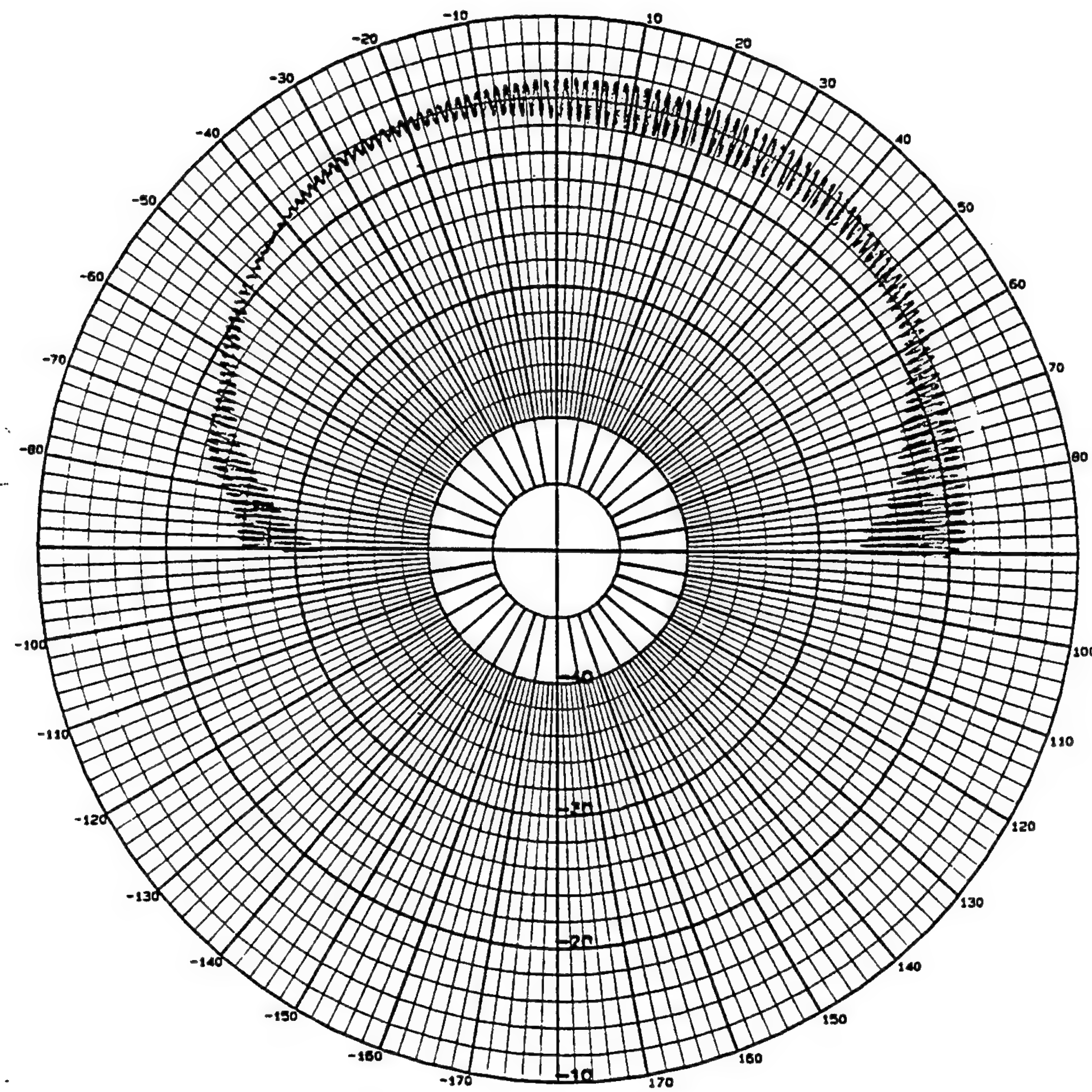

Az Vs. azamp

File : AEL–1.DAT
Frequency : 1.000 GHz

Date: 18/07/95 11:47
Operator: Mike Neel

AEL SN 1 SPIRAL

ABSORBER LOADED CAVITY

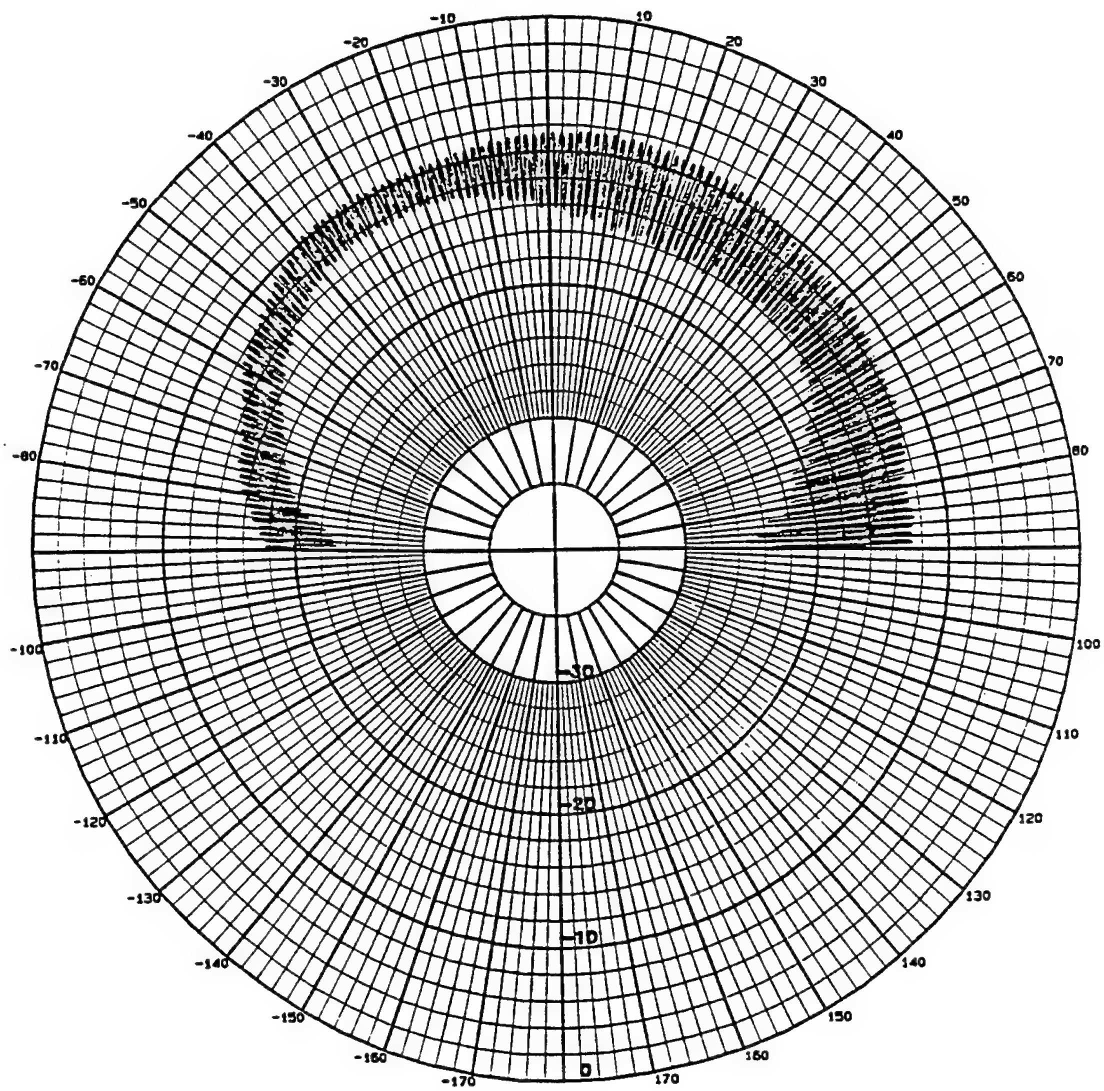

Az Vs. azamp

File : AEL–1.DAT
Frequency : 1.200 GHz

Date: 18/07/95 11:47
Operator: Mike Neel

AEL SN 1 SPIRAL

ABSORBER LOADED CAVITY

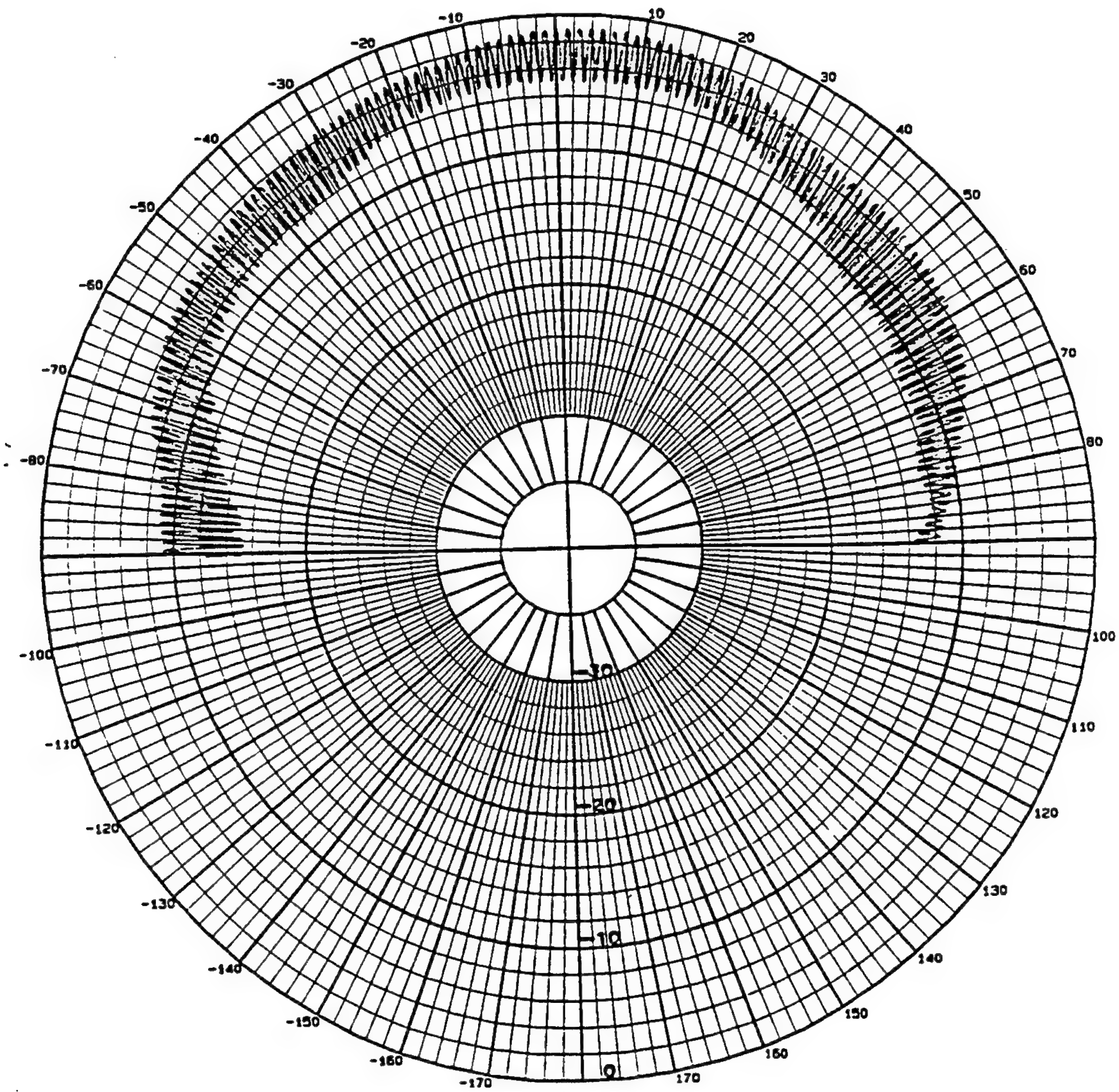

Az Vs. azamp

File : AEL–1.DAT
Frequency : 1.400 GHz

Date: 18/07/95 11:47
Operator: Mike Neel

AEL SN 1 SPIRAL

ABSORBER LOADED CAVITY

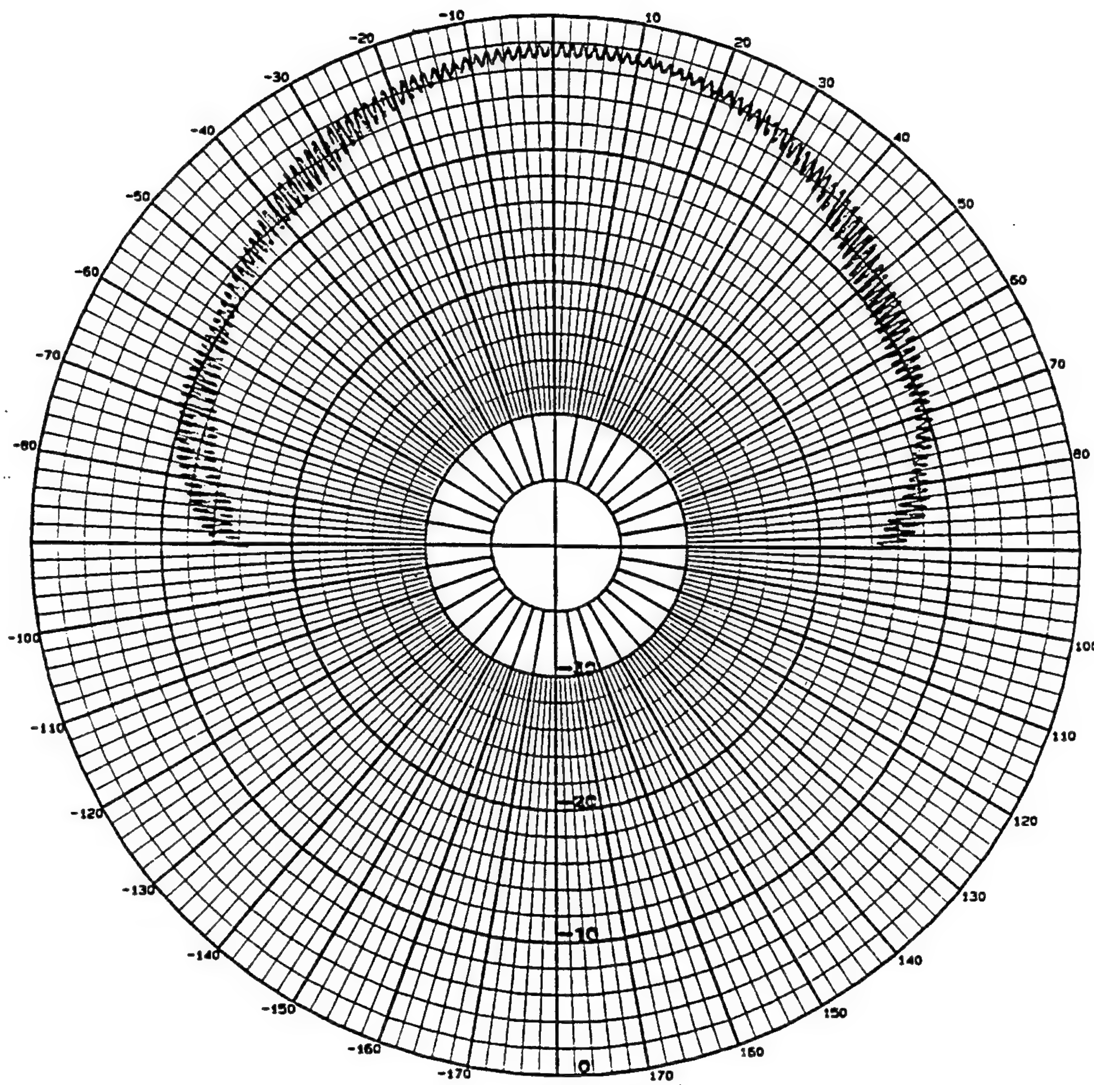

Az Vs. azamp

File : AEL-1.DAT
Frequency : 1.600 GHz

Date: 18/07/95 11:47
Operator: Mike Neel

AEL SN 1 SPIRAL

ABSORBER LOADED CAVITY

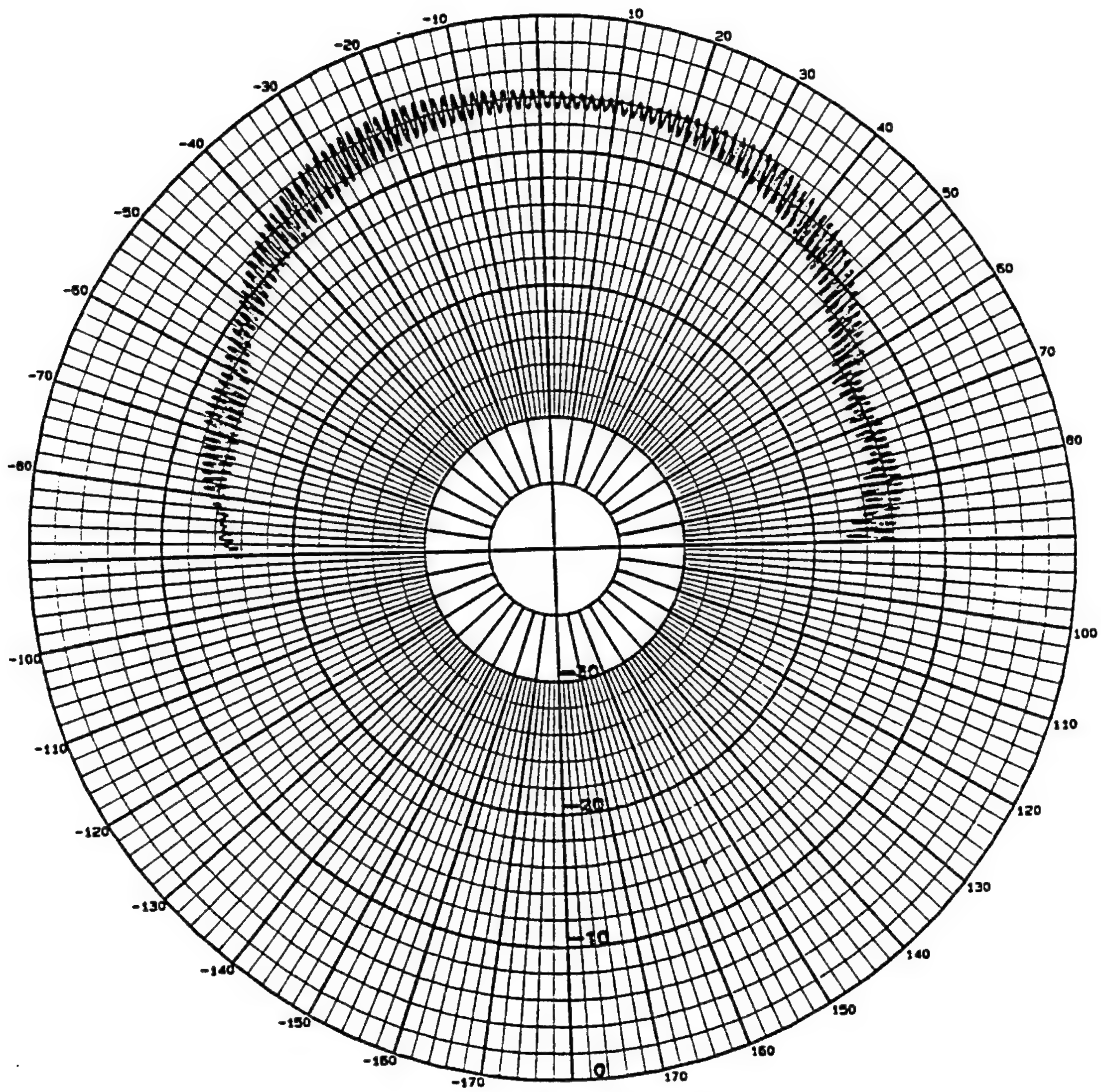

Az Vs. azamp

File : AEL−1.DAT
Frequency : 1.800 GHz

Date: 18/07/95 11:47
Operator: Mike Neel

AEL SN 1 SPIRAL

ABSORBER LOADED CAVITY

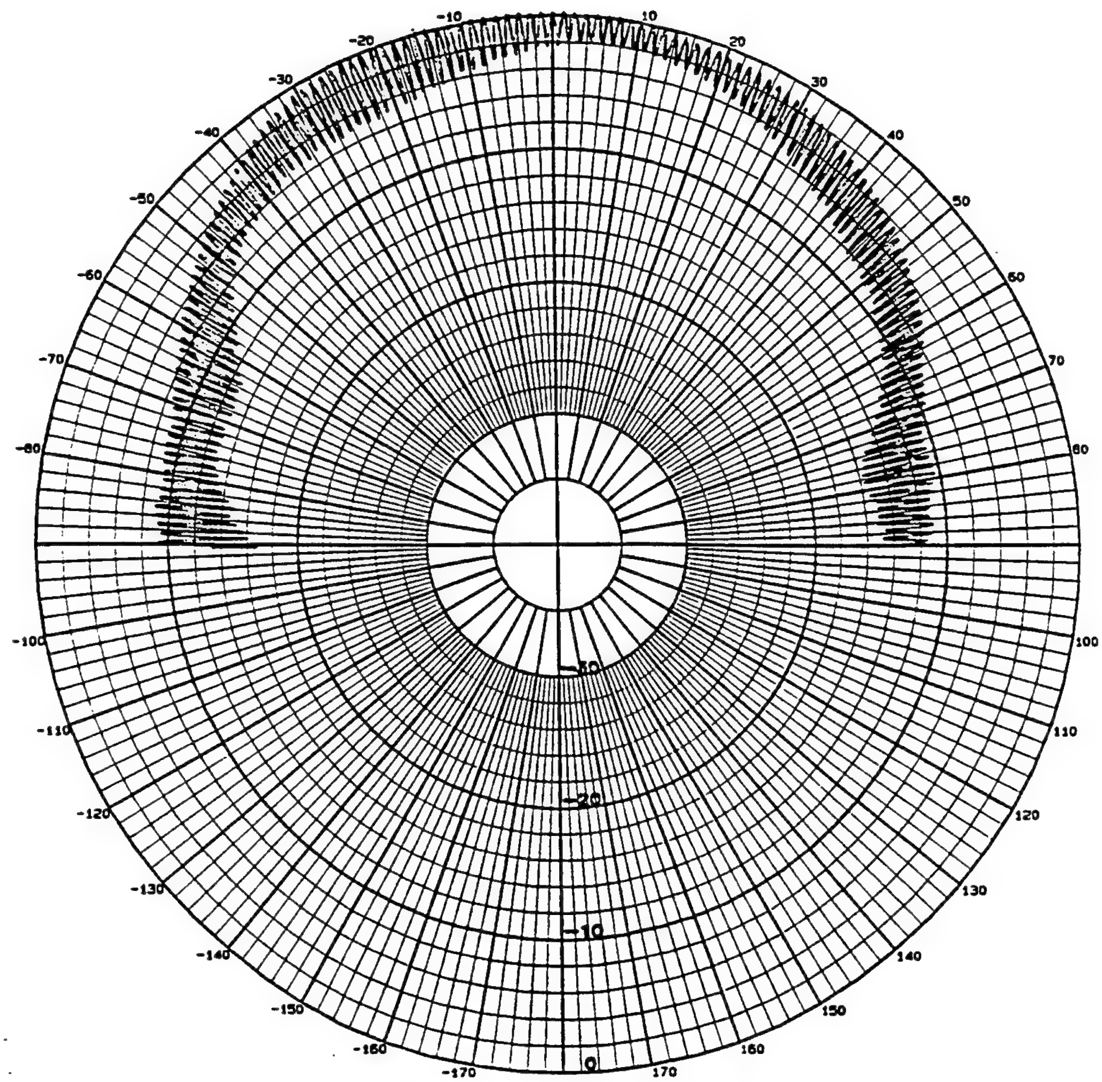

Az Vs. azamp

Date: 18/07/95 11:47
Operator: Mike Neel

ile : AEL–1.DAT
requency : 2.000 GHz

EL SN 1 SPIRAL

BSORBER LOADED CAVITY

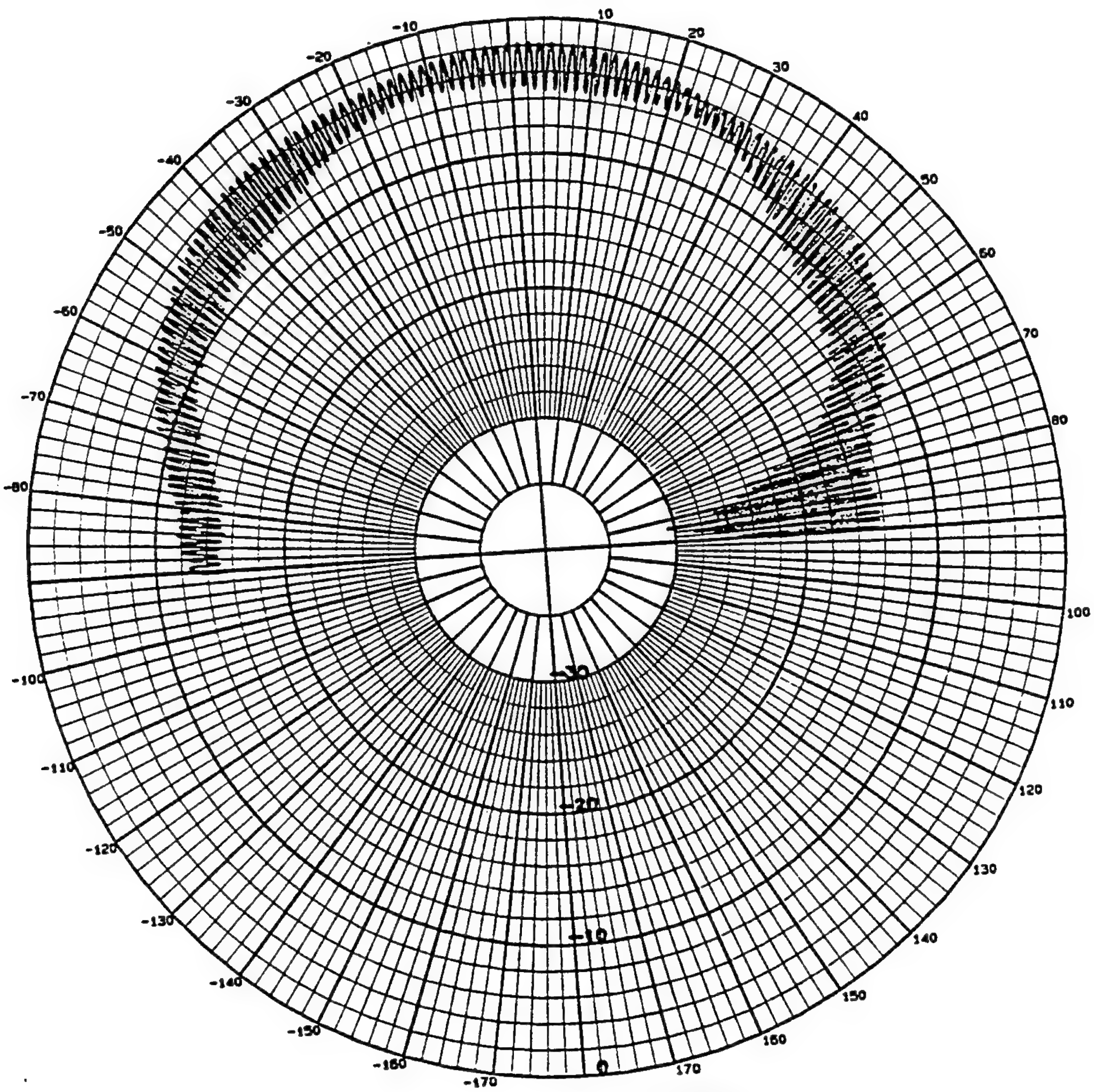

Az. Vs. azamp

Appendix F

inch

HTS 1.5"-CAVITY SPIRAL TEST DATA

The data in this section illustrates the antenna chamber patterns taken on the Microstrip Mode Spiral design with a 1.5-inch deep cavity, with no absorber inside.

File : HTS-4.DAT
Frequency : 0.500 GHz

Date: 18/07/95 15:23
Operator: Mike Neel

HTS CPW FED SPIRAL

1.5" DEEP EMPTY CAVITY

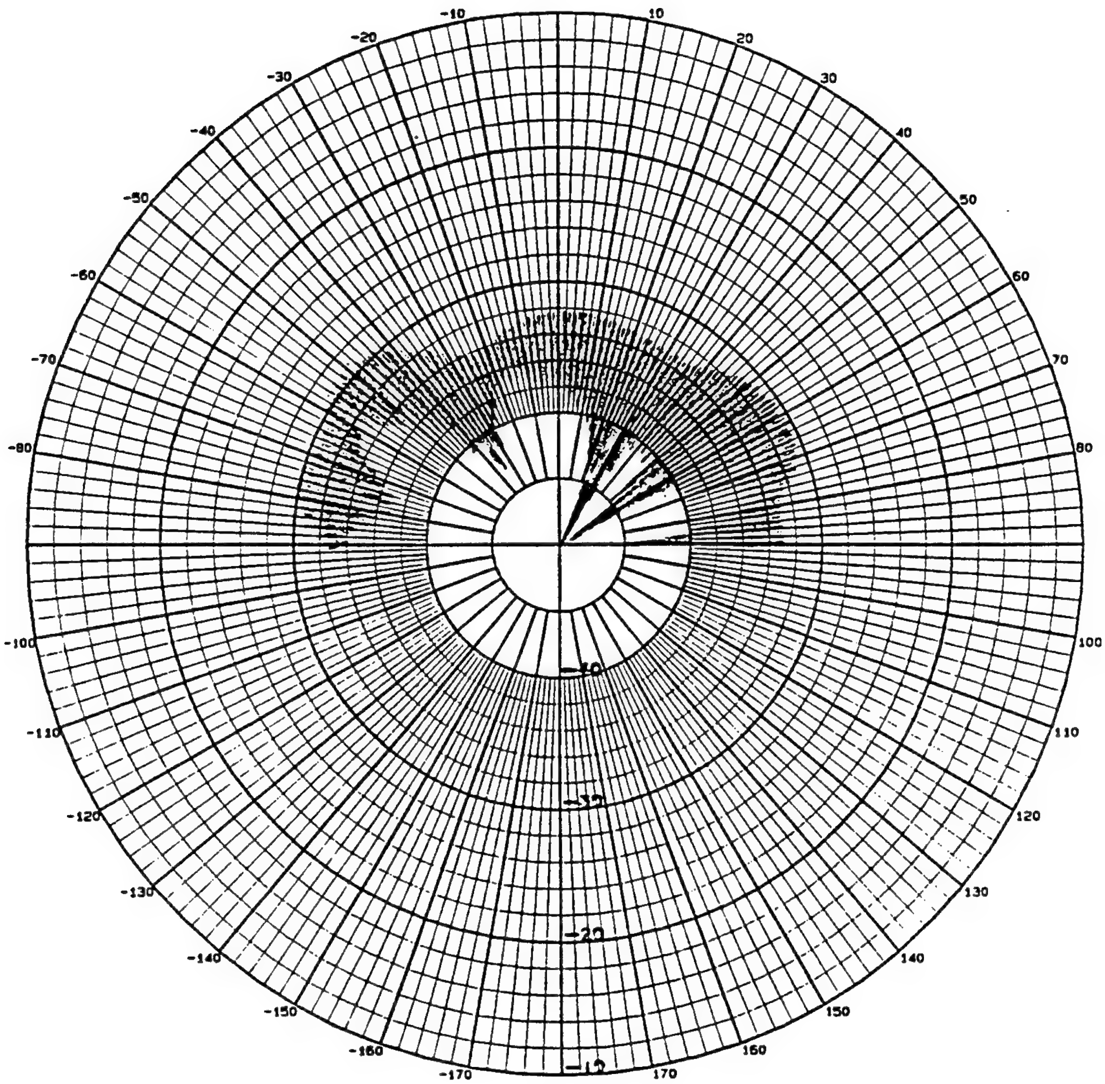

Az Vs. azamp

File : HTS−4.DAT
Frequency : 0.600 GHz

Date: 18/07/95 15:23
Operator: Mike Neel

HTS CPW FED SPIRAL

1.5" DEEP EMPTY CAVITY

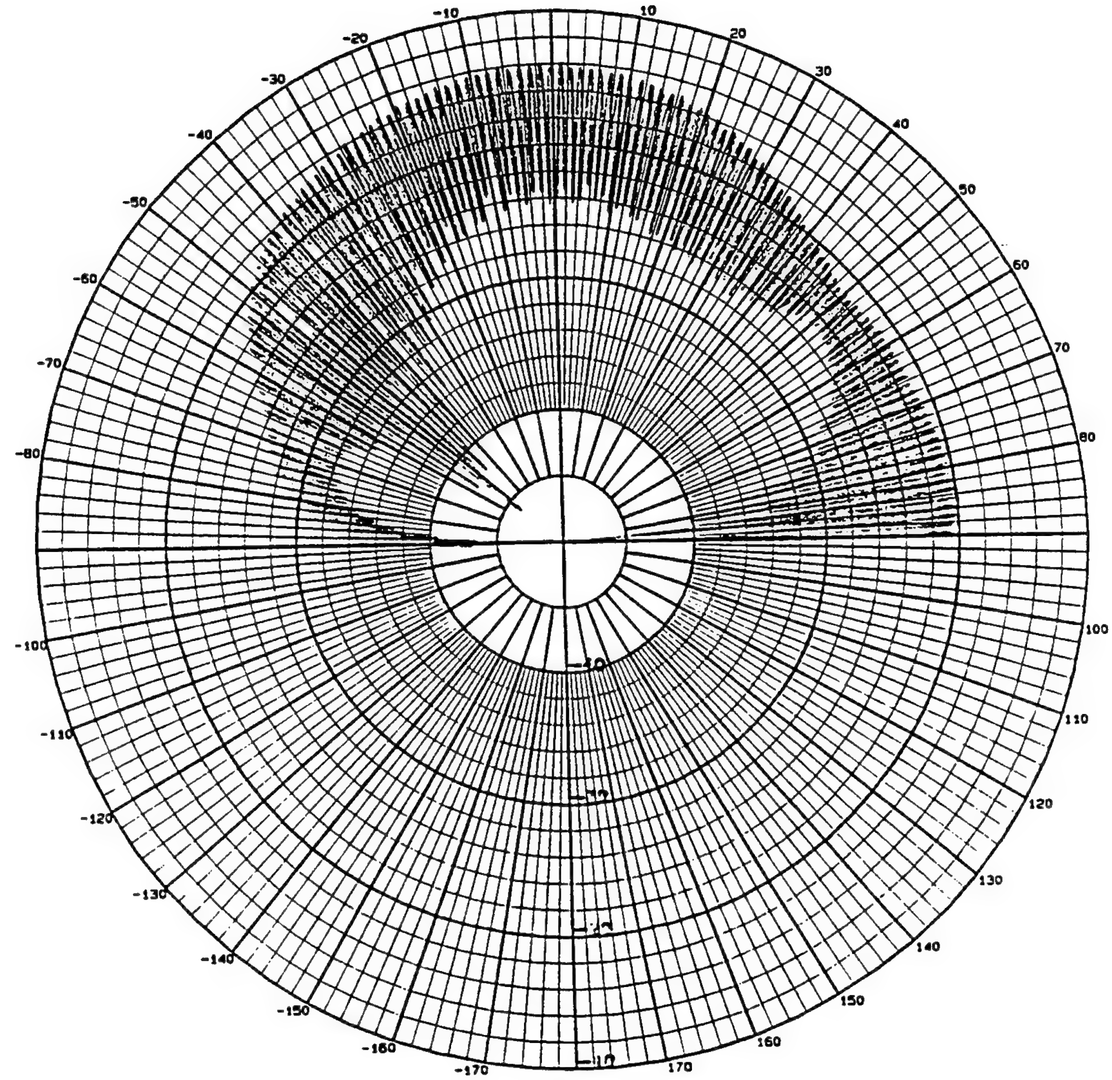

Az Vs. azamp

File : HTS–4.DAT
Frequency : 0.700 GHz

Date: 18/07/95 15:23
Operator: Mike Neel

HTS CPW FED SPIRAL

1.5" DEEP EMPTY CAVITY

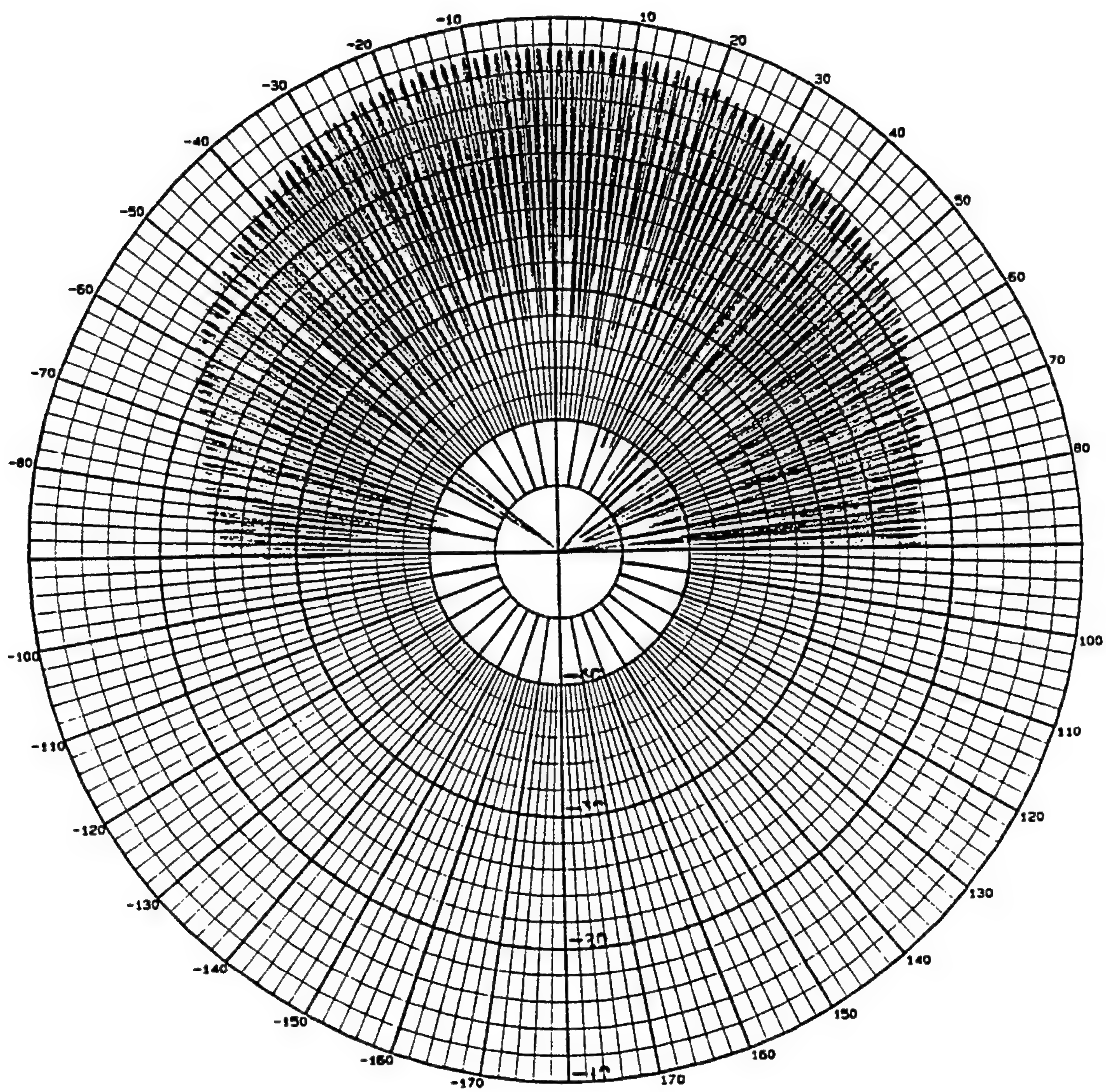

Az Vs. azamp

File : HTS−4.DAT
Frequency : 0.800 GHz

Date: 18/07/95 15:23
Operator: Mike Neel

HTS CPW FED SPIRAL

1.5" DEEP EMPTY CAVITY

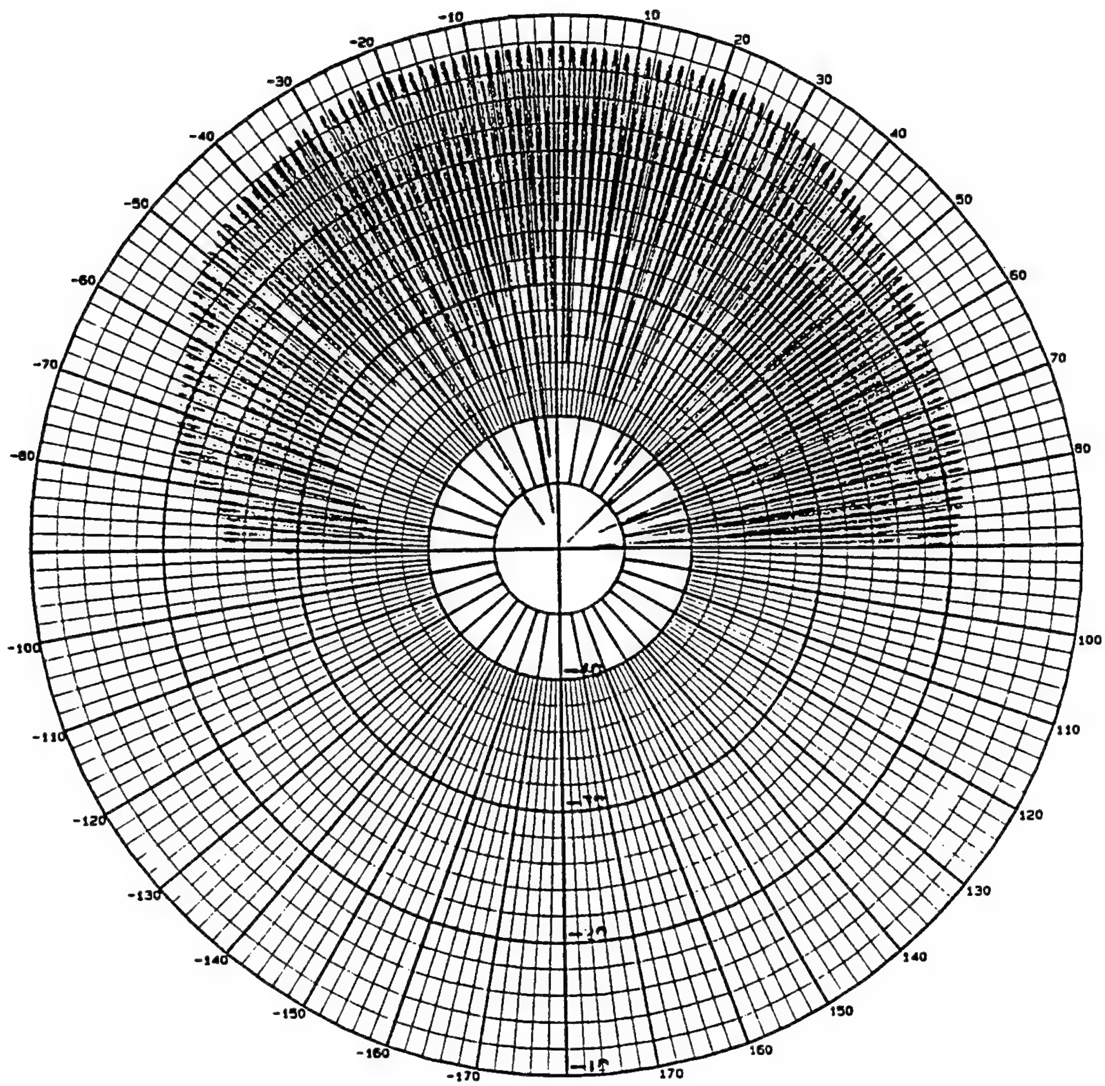

Az Vs. azamp

File : HTS–4.DAT
Frequency : 0.900 GHz

Date: 18/07/95 15:23
Operator: Mike Neel

HTS CPW FED SPIRAL

1.5" DEEP EMPTY CAVITY

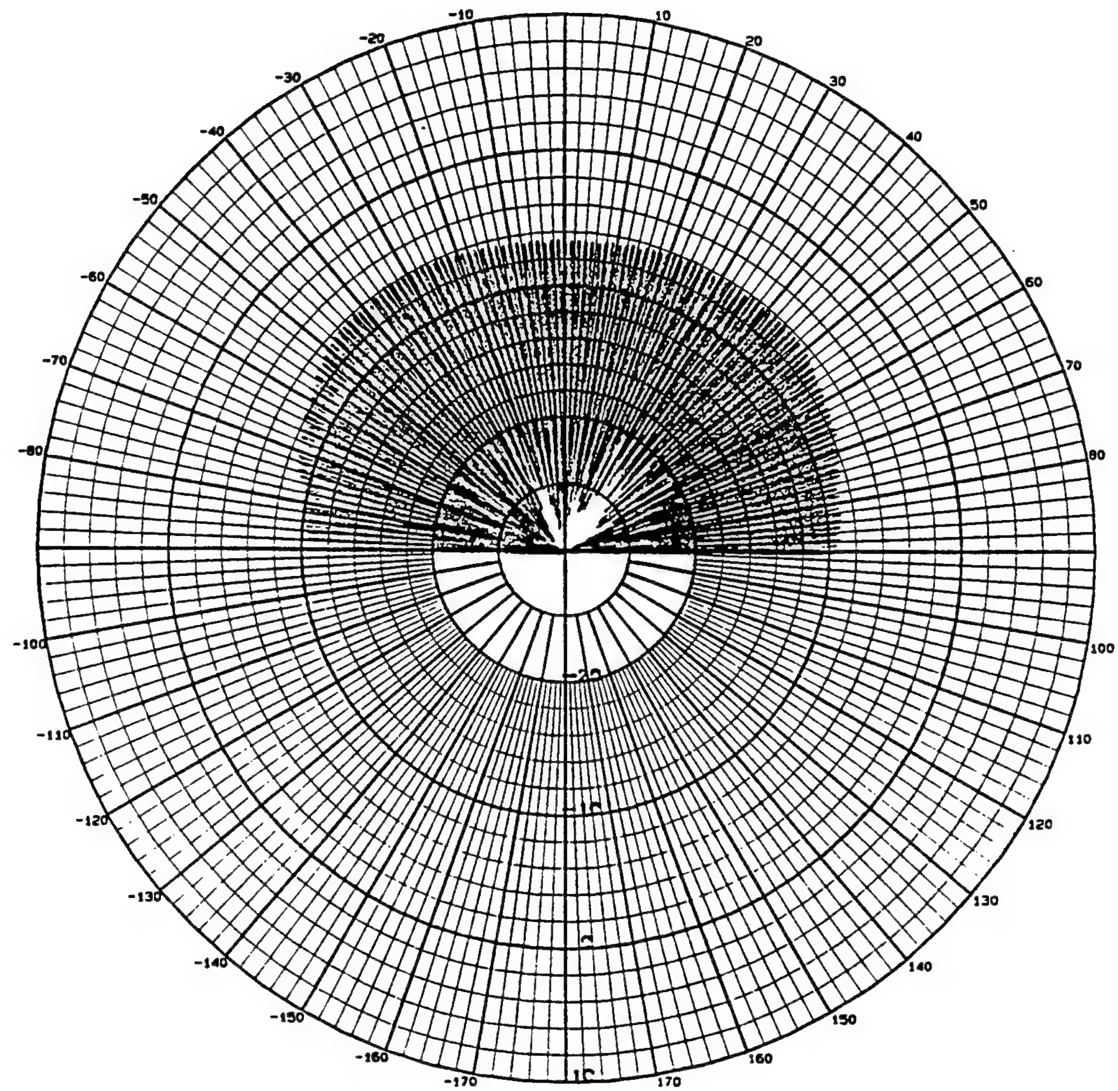

Az Vs. azamp

File : HTS–4.DAT
Frequency : 1.000 GHz

Date: 18/07/95 15:23
Operator: Mike Neel

HTS CPW FED SPIRAL

1.5" DEEP EMPTY CAVITY

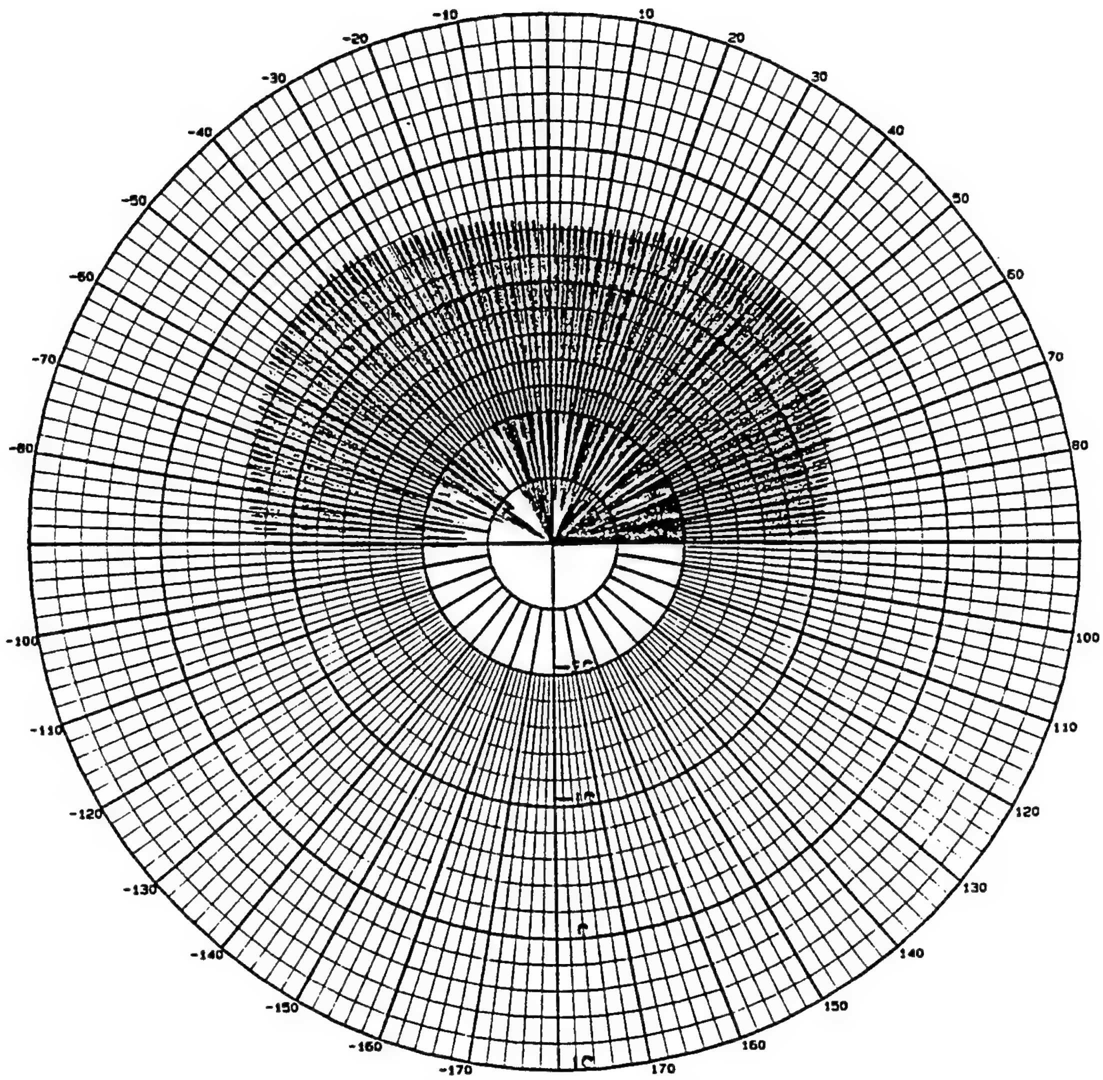

Az Vs. azamp

File : HTS−4.DAT
Frequency : 1.200 GHz

Date: 18/07/95 15:23
Operator: Mike Neel

HTS CPW FED SPIRAL

1.5" DEEP EMPTY CAVITY

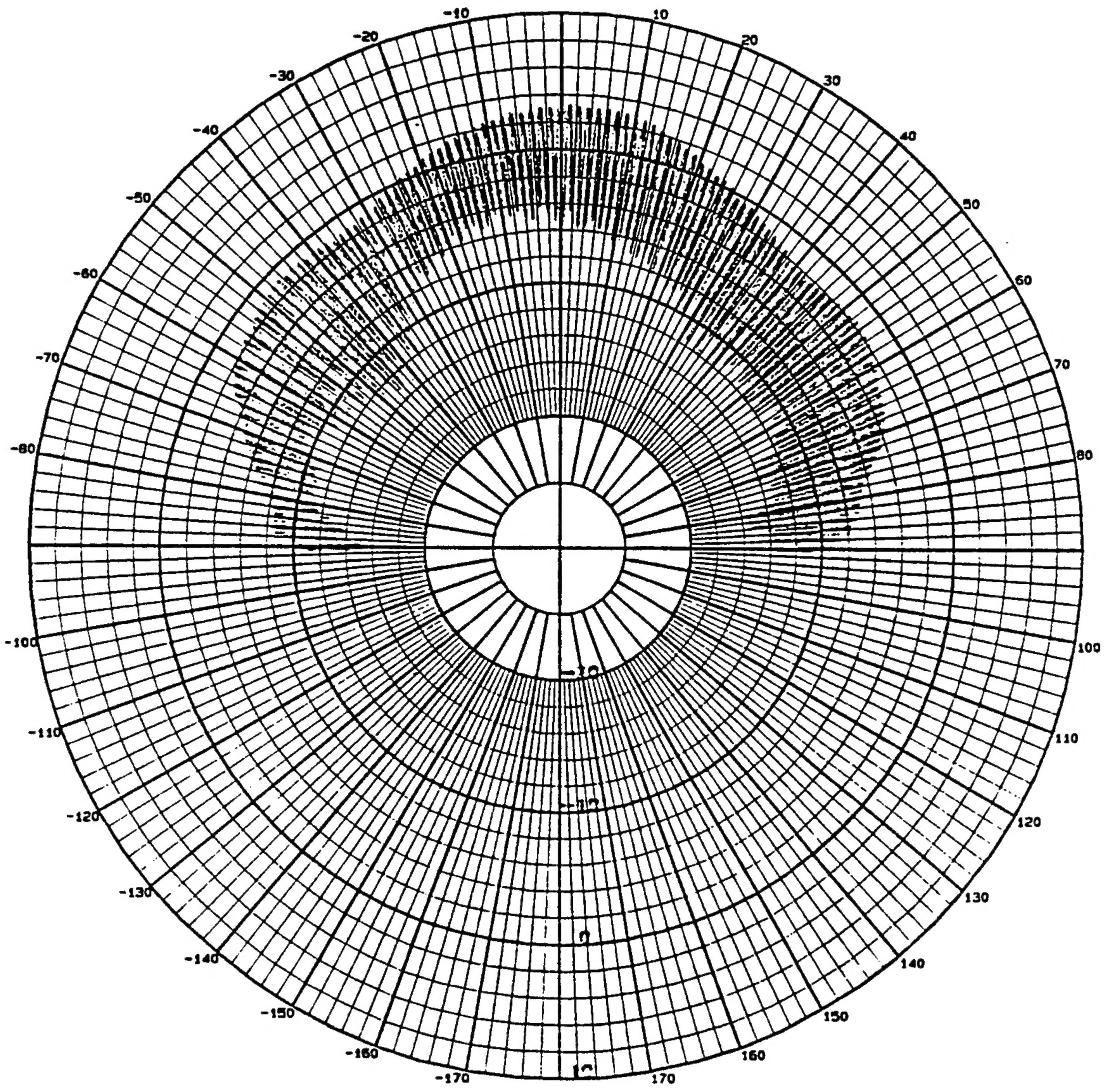

Az Vs. azamp

File : HTS–4.DAT
Frequency : 1.400 GHz

Date: 18/07/95 15:23
Operator: Mike Neel

HTS CPW FED SPIRAL

1.5" DEEP EMPTY CAVITY

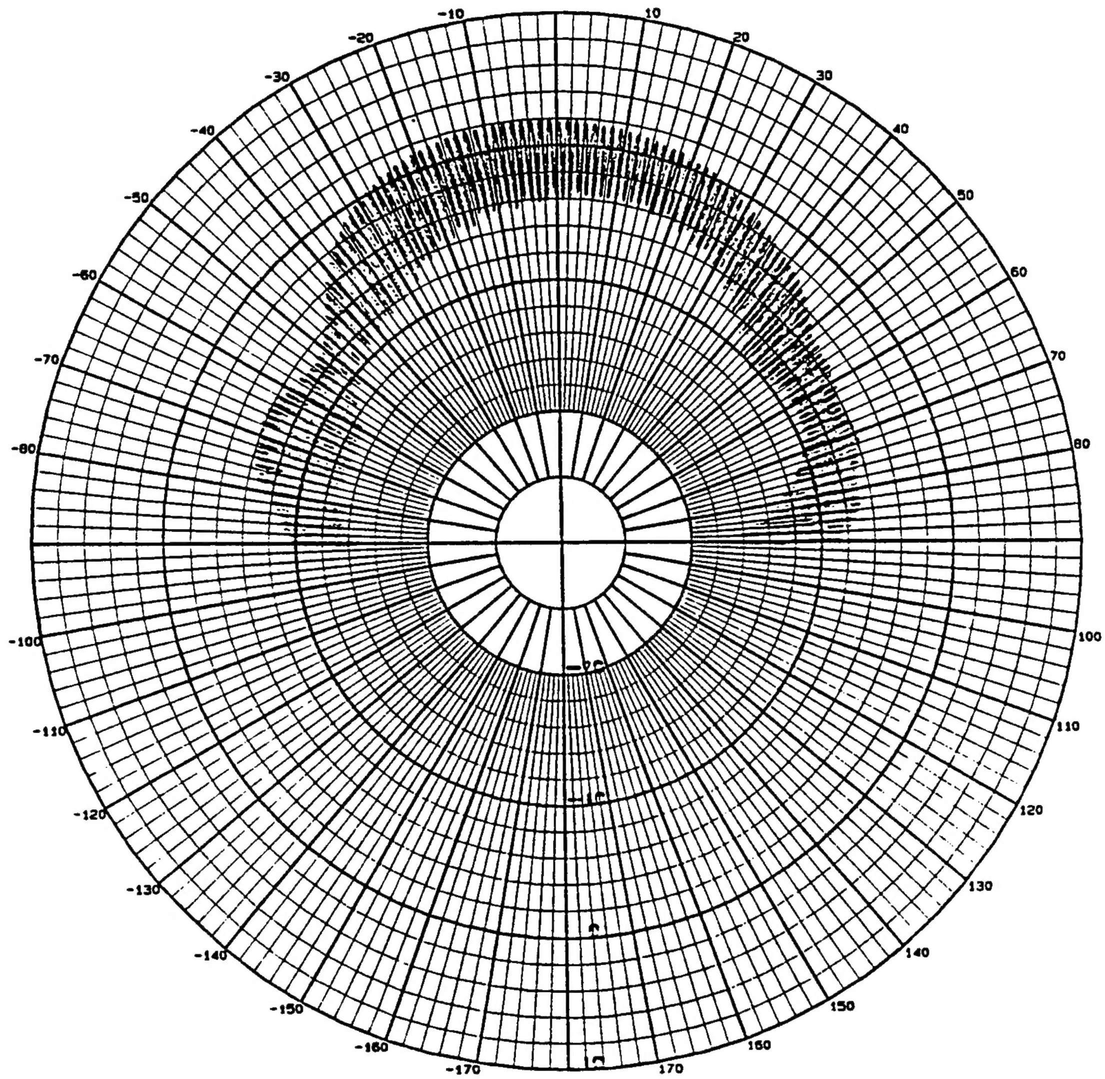

Az Vs. azamp

File : HTS–4.DAT
Frequency : 1.600 GHz

Date: 18/07/95 15:23
Operator: Mike Neel

HTS CPW FED SPIRAL

1.5" DEEP EMPTY CAVITY

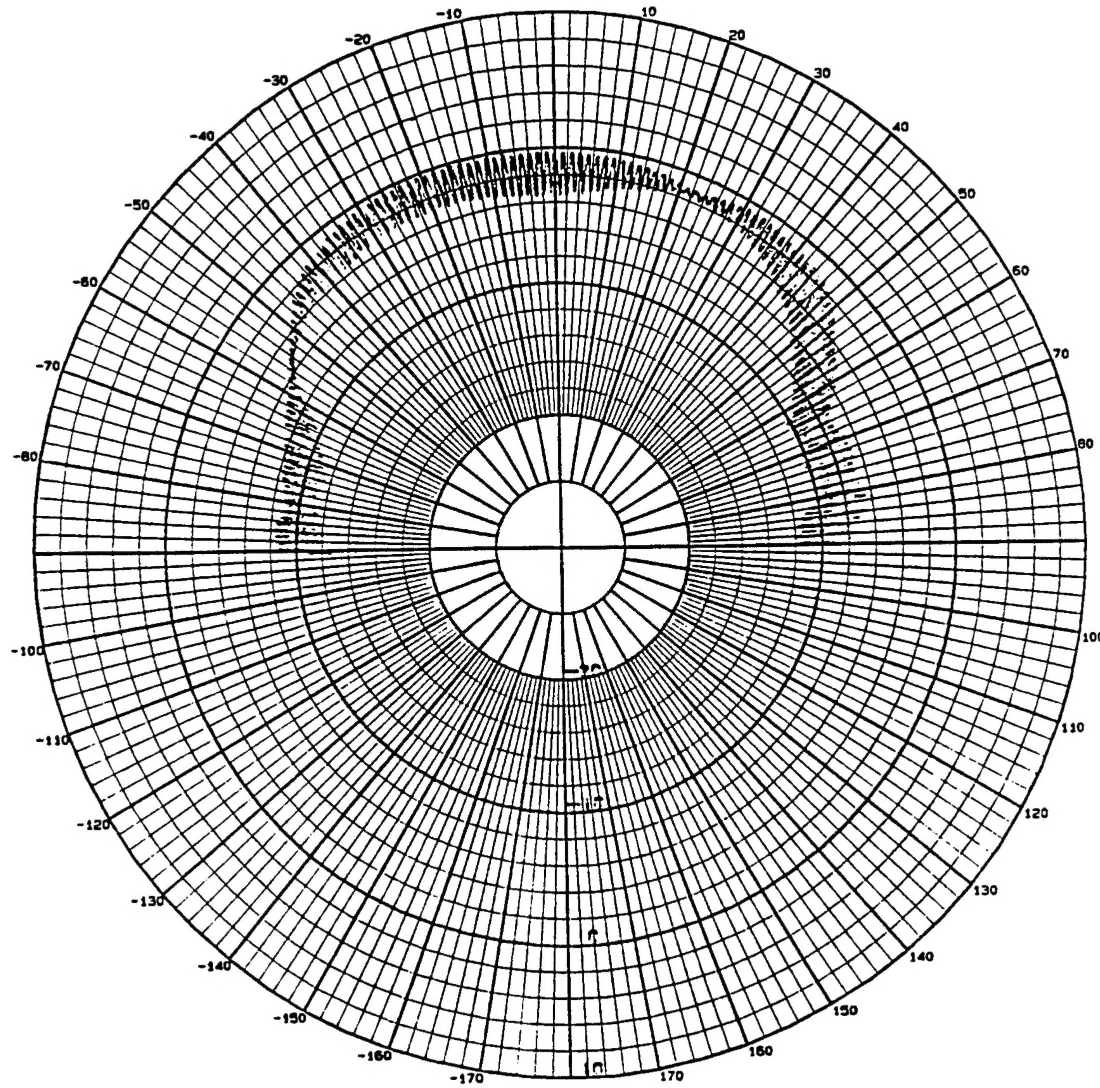

Az Vs. azamp

INITIAL DISTRIBUTION

1 Office of Naval Research, Arlington (Code 312, Dr. D. Van Vechten)
2 Naval Research Laboratory
    Code 6300, Dr. D. Gubser (1)
    Code 6850, Dr. M. Nissenoff (1)
2 Army Electronic Command, Fort Monmouth
    AMSEL-RD-IEW-TAS-M, S. Sahba (1)
    IEWD Directorate, Advanced Concepts Branch (1)
1 Air Force Wright Laboratories, Dynamics Directorate, Wright-Patterson Air Force Base
    (WL/AAWW-1, P. Ryan)
2 Advanced Research Projects Agency, Arlington, VA
    Dr. F. Patten (1)
    Dr. S. Wolf (1)
2 Defense Technical Information Center, Alexandria, VA
4 AEL Defense Corporation, Lansdale, PA
    F. Euchler (1)
    D. Martin (1)
    J. Schuchardt (1)
    G. Sun (1)
1 Center for Naval Analyses, Alexandria, VA (Technical Library)
2 Dupont, Central Research and Development Experimental Station, Wilmington, DE
    Dr. D. Laubacher (1)
    Dr. A. Lauder (1)
1 R. C. Hansen, Inc., Tarzana, CA (Dr. R. C. Hansen)
1 Superconductor Technologies, Santa Barbara, CA (J. Madden)
1 University of Houston, Department of Electrical Engineering, Houston, TX (Dr. J. Williams)
1 WEO Corporation, Marietta, GA (Dr. J. J. H. Wang)

ON-SITE DISTRIBUTION

4 Code 4BL000D (3 plus Archives copy)
1 Code 4B1200D, P. Overfelt
3 Code 4B1L00D
    D. Banks (1)
    D. Bowling (1)
    A. Martin (1)
2 Code 455560D
    W. Katzenstein (1)
    J. Otto (1)
1 Code 472000D, K. Higgins
7 Code 472200D
    C. Hauser (1)
    T. Hoppus (1)
    B. Joy (1)
    J. McCammon (1)
    R. Skatvold (1)
    D. Stapleton (1)
    D. Wagner (1)
2 Code 472230D
    D. Paolino (1)
    F. Schieffen (1)
15 Code 472310D, M. Neel